Long-term management and discounting of groundwater resources with a case study of Kuki'o, Hawai'i

by

Thomas Ka'eo Duarte

B.S.E., Princeton University (1995)

Submitted to the Department of Civil and Environmental Engineering
in partial fulfillment of the requirements for the degree of

Doctor of Philosophy

at the

MASSACHUSETTS INSTITUTE OF TECHNOLOGY

MASSACHUSETTS INSTITUTE OF TECHNOLOGY
SEP 1 9 2002
LIBRARIES
BARKER

September 2002

© 2002 Massachusetts Institute of Technology. All rights reserved.

The author hereby grants to Massachusetts Institute of Technology permission to reproduce and
to distribute copies of this thesis document in whole or in part.

Signature of Author . . . .
Department of Civil and Environmental Engineering
16 August 2002

Certified by 8/16/2002
Charles F. Harvey
Assistant Professor of Civil and Environmental Engineering
Thesis Supervisor

Accepted by . . . . . .
Oral Buyukozturk
Chairperson, Department Committee on Graduate Students

Long-term management and discounting of groundwater resources with a case study of Kuki'o, Hawai'i

by

Thomas Ka'eo Duarte

Submitted to the Department of Civil and Environmental Engineering
on 16 August 2002, in partial fulfillment of the
requirements for the degree of
Doctor of Philosophy

Abstract

Long-term management strategies for groundwater resources are examined with theoretical examples and with a case study of Kuki'o, Hawai'i.

In Part I a groundwater mining and a dryland salinization optimal management problem are solved analytically, and used to examine the implications of how one values the future through discounting. Exponential and hyperbolic discounting functions are tested with the full range of discount rates and time-scales for the hydrologic system. While the optimal management strategies change depending on the form of the discounting function, they are relatively insensitive to the discount rate itself. For all solutions an initial Dirac delta of pumping brings the system from initial conditions to the optimal trajectory. Following this initial spike of pumping, the exponential pumping solutions are constant over all time. The hyperbolic pumping solutions are more complex, time-dependent functions and they asymptotically approach the no-discounting solution at late times.

In Part II a hydrologic-economic model is constructed for a dual coastal and high-level aquifer system at Kuki'o, Hawai'i. The high-level aquifer is modeled as a leaky bucket, while the coastal aquifer is modeled using a sharp-interface formulation of the basal lens. Salinization of pumping wells due to saltwater upconing is superimposed upon the sharp-interface model using an empirical equation based on data from the area. Energy costs, coastal and high-level capital costs, and various forms of the demand curve are incorporated. It is found that it is always optimal to first use the coastal aquifer then turn to the high-level aquifer when the coastal wells become too saline. The optimal trajectories are most sensitive to the form of the demand curve and to leakage from the high-level to coastal aquifer. It is determined that the long-term sustainable yield of the region is roughly 12×10^3 m^3/yr, which is 3 times what the near-future demand is anticipated to be. However, this economically optimal strategy completely mines the high-level aquifer, salinizes the coastal aquifer to 1/3 of seawater and lowers groundwater flux to the ocean by 75%.

Thesis Supervisor: Charles F. Harvey
Title: Assistant Professor of Civil and Environmental Engineering

Acknowledgements:

Much thanks to my advisor Charles Harvey for his guidance from start to finish. His integrity, patience, and humor through the years has been much appreciated.

Dr. Eric Adams was very helpful with the fluid dynamics, and Professor Franklin Fisher an enormous help with the economics.

A big mahalo to Steve Bowles and the crew at Waimea Water Services for all their help with the Kuki'o project.

To my Boston 'ohana who kept me going when Hawai'i seemed so, so far away...with special aloha to Rhea for being there for so much of my time at MIT.

To my Hawai'i 'ohana for just being what you are. You kept me rooted even after 10 years away.

To my parents for supporting me no matter what. It's pau!

Finally, I dedicate this to my kupuna, both alive and in spirit. Mahalo for making me what I am. The journey has just begun. I ask for you continued guidance.

Contents

List of Figures

List of Tables

Part I

Long-term sustainability and discounting of groundwater resources

Chapter 1

Introduction

Meeting the needs of the present without compromising the ability of future generations to meet their own needs. That is the definition of sustainable development as put forth in the 1987 Bruntland report [53]. The concept of sustainability has become a buzz word in development and environmental circles, and easily finds it way into policy papers and management plans. However, incorporating the concept of sustainability into reasonable quantitative frameworks for optimization and evaluation is by no means easy. It is an active area of research for economists, environmentalists, engineers, and scientists.

Sustainable management of freshwater resources is a priority in many areas of the world. Growing populations are taxing surface and groundwater resources. The ability to obtain drinking water is only part of the problem. A major concern now is the availability of water for food production.

Groundwater aquifers are one of the hardest natural resources to manage. The time for natural recharge to replenish aquifers may be very long, and the time to flush contaminants from aquifers longer. Decisions made today may have ramifications for water quantity and quality many decades into the future. In many of the world's most important food producing regions, such as India, Pakistan and the western United States, groundwater is already being pumped faster than nature is recharging [39]. Water contamination by natural and man-made pollutants is also a growing problem. Salinization, either by evaporative or seawater intrusion processes, threatens many coastal and island communities where population centers are often located. There are already many regions of the world where salinization has forced the closing

of wells and an end to irrigation.

It has become apparent that current economic frameworks used for environmental valuation and assessment may be inappropriate for some natural systems; especially if one is concerned with the very long-term. Economic forces are driving resource degradation, and therefore we need to develop an economic environment in which unsustainable development is unattractive.

Heal [19] suggests three axioms to characterize sustainable management of natural resources:

1. A treatment of the present and the future that places a positive value on the very long run.

2. Recognition of the ways in which environmental assets contribute to economic well-being.

3. Recognition of the constraints implied by the dynamics of environmental assets.

The first axiom is basically giving due consideration to the future via proper discounting. This means making decisions today which are consistent with one's temporal preferences. The second is saying that we must re-evaluate how we value our environmental assets. Their impact on our well-being should be a function of the existing state of the natural phenomenon as well as the value of consumption. The last axiom recognizes the need to attempt to correctly model the dynamics and inherent constraints of our natural resources. This paper is primarily concerned with the first and third axioms. We construct models of hydrologic systems that account for water and solute mass balance, and consider how the management of these systems depends on the discounting function.

Chapter 2

Background on Discounting

Discounting of future costs and benefits becomes necessary when attempting to measure the long-term effects of our actions today...which is exactly what sustainable planning and management hopes to do. However, developing appropriate quantitative guidelines for doing so is difficult. A primary problem is that we simply don't know what the future holds. How will our descendents think about and value the earth's resources? What will market interest rates look like? Will new technologies solve our environmental woes? The environmental planner must make a decision today despite all this uncertainty. Even if one is able to model this uncertainty, there still is the problem of how to value the future given the uncertainty.

There are numerous ideas, both philosophical and mathematical, regarding the matter. After a short historical background, five discounting formulations are presented.

(1) No Discounting

(2) Constant Exponential Discounting

(3) The Green Golden Rule

(4) Chichilnisky's Criterion

(5) Hyperbolic Discounting

Though the literature on discounting in economics and in natural resources management is exhaustive, most of it relates to discounted utilitarianism. Some general books on economics, optimization, and discounting are listed in the bibliography [12, 13, 27, 54, 33]. Good overviews are given in **Choice over Time**, edited by Loewenstein and Elder [33], and in **Discounting and Intergenerational Equity**, edited by Portney and Weyant [38].

2.1 Historical Background

Much of the philosophy behind intertemporal choice has been in discussion since the early 1800s. In it's early stages, the discussions and published work on the subject were put forth by economists such as Rae, Senior, and Jevons who possessed a firm grasp of psychology. John Rae wrote extensively of the key determinants that effect our willingness to "defer gratification" [42]. Trying to answer the question of why interest should be paid on capital, Senior developed his "abstinence theory", which essentially viewed interest as compensation to the holder for enduring the pain of not consuming [48]. Jevons instead looked at the "pleasure of anticipation" of future benefits, and he made many observations about de-valuing the future that have been verified empirically by psychologists and economists in recent years [26].

Subsequent work by economists such as Bohm-Bawerk and Fisher led to an increasingly less psychological treatment of intertemporal choice. Bohm-Bawerk [4] shed light on the systematic tendency to underestimate future wants, and Fisher [15] helped to formalize Bohm-Bawerk's work by being the first to apply indifference curves to intertemporal choice in the 1930s. Soon after, the discounted utility (DU) model was formulated by Samuelson in 1937 [46]. Though Samuelson himself noted the relative arbitrariness of the DU model's assumptions, the practical simplicity of the new model made it the primary framework for making intertemporal decisions.

The DU model of intertemporal choice in decision making has encountered relatively little scrutiny until the last decade or so. Partly in response to green politics and an increasing interest in large scale management models over long timescales, scholars are once again scrutinizing the *de facto* rule of the DU model with a constant discount rate. It is not an issue of whether the DU model is wrong, it is whether or not the framework is appropriate in all situations, and, if not, what is.

A recent workshop sponsored by Resources for the Future, which generated the book **Discounting and Intergenerational Equity** [38], suggests the current state of affairs among experts in the field:

1. Most all experts agree it is essential to discount the future at some positive rate.

2. For projects with time horizons of about 40 years or less a discount rate should be used

which "reflects the opportunity cost of capital" [38]. This suggests a descriptive outlook on discounting, and amounts to commonly cited discount rates (i.e. the prevailing market rate).

3. For periods longer than 40 years "discomfort sets in", experts vary in their suggestions, and more prescriptive approaches are entertained. Many suggest using different discount rates depending on the future period over which you are calculating net present values. Citing empirical studies and recent uncertainty analyses, some economists suggest using progressively lower discount rates the further into the future one is making a decision.

4. Most radical of all, a few economists are questioning the utility of standard welfare economic approaches and feel decision making for far future, far reaching environmental issues should be treated like making decisions for allocating foreign aid.

Some experts argue for modified use of exponential discounting. This usually involves having different discount rates for the "near" and "far" future. For example, Rabl [41] recommends "the conventional social discount rate for the short term (about 30 years) and the growth rate of the economy for the long term". Along these same lines, the most touted alternative discounting method today is hyperbolic discounting. It is supported by a variety of empirical, philisophical, and mathematical evidence; which is presented later in this chapter.

One could also argue that instead of modifying the discounting factor, the objective function or constraint set should be modified to account for long-term goals. For example, in management of a semi-arid groundwater aquifer, instead of using a more "stock preserving" discount function, add a constraint that doesn't let water levels drop below a pre-determined critical level. Accounting for future goals through model constraints is an important aspect of any water management model, but it is a method that is fairly problem specific. A primary goal of this paper is to examine the implicit characteristics of the discounting function. Despite the obvious power of intelligent model constraints, the modeler must still choose a discount function that properly describes future valuation.

2.2 No Discounting

No discounting means that we place exactly as much value on the utility of an event happening today as we do on that same utility being delivered at any given time in the future. Given a utility function[1], u, for a renewable resource which is a function of consumption, c, and stock, s, the optimization problem takes the form, with appropriate constraints and initial conditions:

$$V = max \int_0^\infty u(c_t, s_t)dt \tag{2.1}$$

where V may be taken as the maximized net system utility.

Though some environmentalists have argued for no discounting, especially in regards to global warming [9, 6], it is not a very realistic formulation for primarily one reason: the vast majority of the world's people and policy makers just don't think that way. It is an environmentally idealistic formulation that may be a future outlook to strive for, but it is impractical for the realities of modern society. For that reason, zero discounting is only used for comparative purposes in this study. However, it should be noted that the environmental outlook of some cultures, primarily those of indigenous peoples, does approach the temporal outlook implied by no discounting.

2.3 Constant Exponential Discounting

Also referred to as utilitarian discounting or the discounted utility model (DU), this is by far the most prevalent method used to evaluate optimal development trajectories. The stream of benefits are discounted using an exponential discounting function with a constant discount rate. Throughout this study *exponential discounting* or *DU* implies exponential discounting with a constant discount rate. Framed in the context of the same utility function and constraint set as outlined above, this maximization problem takes the form:

$$V = max \int_0^\infty e^{-rt} u(c_t, s_t)dt \tag{2.2}$$

[1] Assumed to satisfy the appropriate axioms and conditions of additivity. See, for example, Pollack [37]

where r is the constant **discount rate.** The expression e^{-rt} is the **discount factor** or discounting function. Denoting the discounting function by $\mathcal{D}(t)$, the discount rate using *any* $\mathcal{D}(t)$ is given by:

$$r(t) = \frac{\mathcal{D}'(t)}{\mathcal{D}(t)} \tag{2.3}$$

For an exponential discounting function with constant r, this obviously leads to a constant value for the discount rate, $r(t) \Rightarrow r \neq f(t)$. This is the only function that produces a constant discount rate.

This method of discounting has the advantages of (1) intertemporal independence and (2) stationarity[2]. Independence implies that if two optimal trajectories, $X = (x_1 ... x_n)$ and $Y = (y_1 ... y_n)$, yield the same utility at some point in time, then a decision between them only depends on the remaining $(n-1)$ points. In other words, decisions concerning current preferences are independent of prior consumption. If you are indifferent between apples and oranges, preferential independence means you don't care if you ate oranges every day versus eating one of each on alternating days.

Stationarity means that if the first outcome for X and Y are the same, then dropping x_1 and y_1 and shifting the remaining outcomes by that time period will not affect the overall outcome. This implies a neutral attitude towards time delay. If you prefer \$100 today versus \$110 in a week, you will also prefer \$100 in ten years versus \$110 in ten years plus one week. This property of stationarity means that you value the future consistently in the same way. Other discounting formulations, such as the hyperbolic discounting function, do not have this property. Many argue that making a decision when you already know you will change your mind is illogical, but there are reasonable sets of temporal preferences that will lead naturally to such behavior [17][18].

These two properties naturally lead to the exponential discounting function: "Stationarity and intertemporal independence (along with other technical axioms) imply that any representation of preferences over temporal prospects can be monotonically transformed into a discounted-utility representation" [33].

However, various temporal choice studies by scientists, economists, and psychologists indi-

[2]There are other technical axioms involved that can be found in, for example, Koopmans (1960) and Pollak (1967) [31, 37]

cate that humans don't behave according to the exponential model [51, 10, 33]. This model is also controversial, especially among environmentalists, because the far future is discounted away severely with an exponential discount function. As illustrated by Heal [22], if one discounts present world GNP over 200 years at 5 percent per annum, it's worth only a few thousand dollars.

A fundamental problem that this paper focuses on is the incompatibility between economic and some hydrologic time scales. Utilitarian discounting works well for most modern business decisions because the time frame is short. A couple of decades is a long time for economists, but is relatively short for hydrologists. In groundwater resources the time scales for depletion, pollution, or replenishement are often on the order of decades to centuries.

Though many economists and environmentalists have argued against the DU model [43, 16, 19], it is still the most accepted method in the field of intertemporal economics. Heal [20] argues that, "discounted utilitarianism dominates our approach more for a lack of convincing alternatives than because of the conviction it inspires". Heal may have a point, but I think he goes too far given the obvious usefulness of exponential discounting in many arenas of society.

It is not that this model is wrong in and of itself, but whether it describes society's preferences in meeting the long-term goals of some of today's large-scale, environmental management projects. The issues are "when isn't it appropriate?", "why?", and "how do we respond?". The primary decisions of concern are long-term decisions concerning goods that are non-renewable or have long times scales of renewal. Environmental decisions such as groundwater management, contamination clean-up, climate change, and biodiversity are prime examples.

2.4 Green Golden Rule

An approach which seeks to rank optimal paths by their long-run payoff is the so-called "Green Golden Rule" (GGR). Introduced by Beltratti, Chichilnisky and Heal [7], it is "the configuration of the economy which gives the maximum indefinitely maintainable benefit level". In essence, this method ranks paths by which one gives the most benefit in the very long run. As noted by Heal [22], the GGR actually goes too far in this respect. The GGR maximization problem

takes the form:

$$V = max \lim_{t \to \infty} u(c_t, s_t) \tag{2.4}$$

This is an extreme, boundary-point model which may be used primarily for comparative purposes.

2.5 Chichilnisky Criterion

An interesting compromise to exponential discounting and the GGR is the approach introduced by Chichilnisky [8]. In essence, she combines the two methods through a set of axioms for ranking alternative development paths. This method places most value on the short term and at infinite time, but is also sensitive to outcomes on the long time scales we are concerned with – decades to centuries. Chichilnisky's criterion takes the form:

$$V = max[\theta \int_0^\infty e^{-rt} u(c_t, s_t) dt + (1 - \theta) lim_{t \to \infty} u(c_t, s_t)]. \tag{2.5}$$

The proof for this method is dependent on infinity; which is generally too strong a condition to conform with reality. However, when applied to renewable resources, Chichilnisky's criterion reduces to the discounted utilitarian approach with a declining discount rate; in other words, hyperbolic-type discounting [21].

2.6 Hyperbolic Discounting

A key characteristic of these methods is that the discount rate falls to zero in the long-term, and therefore the discount factor decreases to zero much more slowly than in exponential discounting. This places a lot more weight on the future than discounted utilitarianism. This type of formulation is called "slow-discounting" by Harvey [17, 18]; who provides some mathematical and philosophical arguements for this type of discounting. Reflecting the hyberbolic rather than exponential curves generated, I will always refer to this type of framework as hyperbolic discounting. However, please note that there are other ways to have a discount factor with a non-constant discount rate. It just turns out that this is a manageable and practical function that has much supporting evidence in its favor.

The empirical evidence comes from the diverse fields of economics, ecology, biology, and psychology. Lumley [34] infers discount rates from Philippine farmers, Poulos and Whittington [40] consider life-saving programs in LDCs, and Thaler [51] directly studies how people discount sums of money. There are many more examples [25, 29, 49, 23, 58], and they all indicate that humans tend to discount the future hyperbolically. Loewenstein and Prelec[33] discuss some of the primary conflicts between exponential discounting and the way people actually discount events. It may be argued that these data don't necessarily mean policy makers should make decisions based on the recorded behavior of others, but the very fact that there is evidence that human's act more hyperbolically than exponentially calls for investigation of this function.

Many authors have sought to rectify the inconsistency's between exponential discounting and empirical studies. The previously discussed Chichilnisky criterion for one [8]. Loewenstein and Prelec [33] enumerate the anomalies cited above and propose a form of hyperbolic discounting as a model that accounts for them. Harvey [17, 18] constructs his own rational model of behavior and puts forth hyperbolic discounting as the resultant method in that context.

A smaller group of scholars have recently attacked the issue by looking at uncertainty in the discount rate. These works generally start with the constant exponential discounting model, add uncertainty to the discount rate, and show that the discount rate that emerges declines over time. For instance, Sozou [50] argues that the value of a future reward should be discounted in a fashion that incorporates the hazard that the reward will not be realized. If there is uncertainty in this underlying hazard rate he shows that this may lead to a hyperbolic "time-preference function". Weitzman [55] shows that if we are uncertain about future discount rates "this provides a strong generic rationale for using certainty-equivalent social discount rates that decline over time". In a more recent paper Weitzman [56] looks at a gamma distribution of discount rates collected from a survey of economists, and demonstrates the resulting "sliding-scale" discount rate that declines with time. Azfar [1] takes a similar approach, using hazard rates, and proves essentially the same thing as Weitzman.

Economics and human behavior aside, hyperbolic discounting's characteristic of placing more weight on the future may be reason enough to consider using it as a prescriptive model for some applications. For instance, in optimization models where the resource is necessary for life and is only renewed on long timescales, hyperbolic discounting's implicit tendency to hold

on to more stock in the future may be a desirable trait. In a way this is like accounting for uncertainty in the future by holding on to stock, irregardless of what future generations may choose to do with that stock (hence a possible violation of stationarity).

Two different formulations from this family of functions are looked at in this study. The first is a two parameter model. This model has been used by numerous researchers, such as Loewenstein and Prelec [33], and arises naturally in Weitzman's gamma discounting formulation [56].

$$V = max \int_0^\infty \left(\frac{1}{1+bt}\right)^a u(c_t, s_t)dt \tag{2.6}$$

A simpler version, which requires only one parameter, is derived by choosing a constant value for **a** in the two-parameter model. This study considers the case where $a = 2$.

$$V = max \int_0^\infty \left(\frac{1}{1+bt}\right)^2 u(c_t, s_t)dt \tag{2.7}$$

2.7 Application of Discounting in this Study

The GGR can be shown to be the same as no discounting [7]. Furthermore, the optimal trajectory derived using Chichilnisky's criterion will asymptotically approach the GGR. Therefore, solving the exponential or hyperbolic function with the discount rate set to zero yields the GGR solution.

In addition, it can be shown that, for renewable resources, Chichilnisky's criterion reduces to exponential discounting with a discount rate that declines to zero with time [8]. Hyperbolic discounting is the most well known and understood framework which satisfies this stipulation. Therefore, by solving the hyperbolic formulation one automatically satisfies Chichilnisky's criterion.

In effect, it is only necessary to solve the optimization problems with exponential discounting and hyperbolic discounting.

2.8 Application to Water Resources

Though many economists support their arguments with simple, generalized models, few apply their discounting formulations to a specific physical system in nature. On the other hand, in the

water resource management literature many physically specific and complex management models incorporate economics, but only simple exponential discounting functions, [35, 52, 30, 44]. To the best of my knowledge no one has optimized groundwater resources using an alternative discounting model such as hyperbolic discounting.

Given the long time scales of system response and the fact that it is better understood and easier to model than subjects such as climate change or biodiversity depletion, optimal groundwater management is a good "real life" test case for examining the characteristics of far-future discounting methodologies.

Chapter 3

Groundwater Pumping Problem

This section deals with finding the optimal pumping rate from a simple groundwater aquifer model. The formulation is 1-dimensional. However, the problem could easily be made 3-dimensional without affecting the nature of the problem or the solution.

3.1 Problem Description

The objective is to maximize utility of groundwater extraction for agriculture, recreation, industry or some other use. The benefit of using the water is proportional to pumping rate, while the cost of using the water is proportional to the product of the hydraulic lift, s, and the pumping rate, q. Cost increases as the aquifer is depleted. Net instantaneous benefit is then benefit minus cost.

$$f(q, s, t) = q(t)[\alpha - \beta s(t)] \tag{3.1}$$

where f is net benefit per unit time, α $[\frac{\$}{m}]$ is the marginal value of a unit of q, and β $[\frac{\$}{m^2}]$ reflects the marginal cost of pumping an increment of water.

It should be noted that having benefit increase linearly with pumping is an assumption that is probably only plausible for low to medium pumping rates; depending on the system's physics and economics. In reality, at very high pumping rates other factors are limiting and the marginal value of more water goes to zero and may even be negative. A non-linear benefit function will be considered later in a numerical model. For the simple case considered here the constraints keep pumping within reasonable limits.

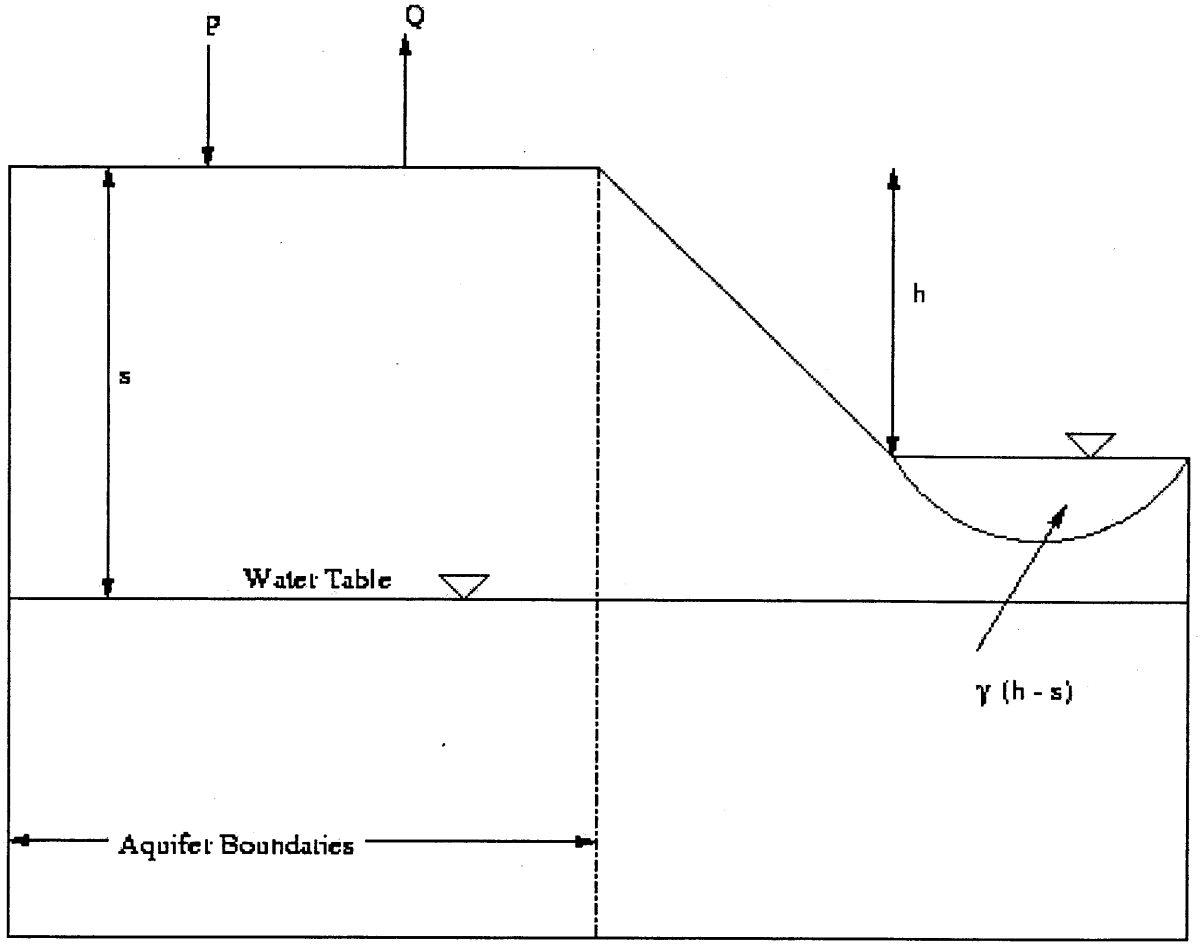

Figure 3-1: Schematic for groundwater mining problem.

The corresponding maximization problem is:

$$V = max \int_0^\infty \mathcal{D}(t)q(t)[\alpha - \beta s(t)]dt \tag{3.2}$$

where V is net present value of the stream of benefits [\$], and $\mathcal{D}(t)$ is the discount function[1]. The decision variables q and s are related by a state equation which describes the physical system; Figure 3-1. This is the aquifer mass balance equation:

$$\frac{ds}{dt} = q - p + \gamma(h - s) \tag{3.3}$$

where h represents a depth below a datum in a neighboring water body (i.e. lake or river), p is net recharge $[\frac{m}{t}]$, and γ $[\frac{1}{t}]$ is a constant describing leakage in or out of the system. Note that if the water table is pumped down below the depth of the neighboring water body, $s > h$, then water flows into the aquifer. Solving for q:

$$q = s' + p + \gamma(s - h) \tag{3.4}$$

The initial condition for the aquifer is steady-state with no pumping,

$$s_{t=0} = h - \frac{p}{\gamma}.$$

3.2 Solution Method

To solve the maximization problems we use the Euler-Lagrange method of calculus of variations to find closed form solutions.

The Euler-Lagrange method may be summarized for our purposes as follows. Define V to be the maximized integral of a functional, $F(x', x, t)$, where x is the decision variable and ($'$) denotes differentiation with respect to time.

$$V = max \int_{t_o}^{t_1} F(x', x, t)dt \tag{3.5}$$

[1]The utility function is assumed to satisfy the necessary technical axioms such as additivity; see Pollack [37].

with initial conditions

$$\begin{aligned} x(t_o) &= x_o \\ x(t_1) &= x_1. \end{aligned}$$

For a curve $x = x^\star(t)$ to satisfy this maximization problem, it must satisfy the Euler-Lagrange equation of optimization,

$$\frac{\partial F}{\partial x} - \frac{d}{dt}\left(\frac{\partial F}{\partial x'}\right) = 0 \tag{3.6}$$

and the appropriate initial and boundary conditions.

To facilitate the comparison of different discounting schemes, one may define $F(x', x, t)$ as the product of a discount function, $\mathcal{D}(t)$, and a net benefit equation P(x',x,t) which describes the physical system and its stated benefits and costs. V may now be considered the maximized *net present value* of system utility.

$$V = max \int_{t_o}^{t_1} \mathcal{D}(t) P(x', x, t) dt \tag{3.7}$$

Expanding out the necessary terms for the Euler-Langrange equation (3.6),

$$\frac{\partial(\mathcal{D}P)}{\partial x} = \mathcal{D}\frac{\partial P}{\partial x} \tag{3.8}$$

$$\frac{\partial(\mathcal{D}P)}{\partial x'} = \mathcal{D}\frac{\partial P}{\partial x'} \tag{3.9}$$

$$\frac{d}{dt}\left(\frac{\partial(\mathcal{D}P)}{\partial x'}\right) = \mathcal{D}'\frac{\partial P}{\partial x'} + \mathcal{D}\frac{d}{dt}\left(\frac{\partial P}{\partial x'}\right) \tag{3.10}$$

Substituting into the Euler-Lagrange equation, we have a differential equation which may be solved for the optimal curve $x = x^\star(t)$, subject to the appropriate initial and boundary conditions.

$$\mathcal{D}\left[\frac{\partial P}{\partial x} - \frac{d}{dt}\left(\frac{\partial P}{\partial x'}\right)\right] = \mathcal{D}'\frac{\partial P}{\partial x'} \tag{3.11}$$

$$\frac{\partial P}{\partial x} - \frac{d}{dt}\left(\frac{\partial P}{\partial x'}\right) = \frac{\mathcal{D}'}{\mathcal{D}}\frac{\partial P}{\partial x'} \tag{3.12}$$

Note that $\frac{\mathcal{D}'}{\mathcal{D}} = r(t)$, the discount rate.

3.3 Solution

Before solving, it is useful to non-dimensionalize the problem. The objective function and state equation may be non-dimensionalized using h as a characteristic length scale, α as a scaling factor for dollars, and γ as a characteristic time scale.

The non-dimensional groups are $\rho = \frac{r}{\gamma}$, $s^* = \frac{s}{h}$, $\beta^* = \frac{\beta h}{\alpha}$, $p^* = \frac{p}{h\gamma}$, $\tau = t\gamma$, $q^* = \frac{q}{h\gamma}$, and $V^* = \frac{V}{h\alpha}$. The group $\rho = \frac{r}{\gamma}$ is the ratio of the rate of discounting over the rate of leakage out of the system. This parameter is termed a *time-scale factor*; since it reflects time scales of discounting over time scales of leakage out of the system[2]. The group $\beta^* = \frac{\beta h}{\alpha}$ is the ratio of the cost of a unit of water over the value of that unit of water for use. This proportion is referred to as a *cost-benefit factor*; since it reflects the ratio of costs to benefits. The group $p^* = \frac{p}{h\gamma}$ is the ratio of the flux of water into the system over the flux of water out of the system. This proportion is called the *recharge factor*; since it reflects the ratio of recharge and leakage in the system.

Making the appropriate tranformations, the mass balance equation becomes:

$$q^* = s^{*\prime} + p^* + s^* - 1 \tag{3.13}$$

$$V^* = max \int_0^\infty \mathcal{D}(\tau) q^* [1 - \beta^* s^*] d\tau \tag{3.14}$$

Substituting q^* into the objective function, the benefit equation is defined as,

$$P(s^{*\prime}, s^*, \tau) = [s^{*\prime} + s^* + p^* - 1][1 - \beta^* s^*] \tag{3.15}$$

$$P = s^{*\prime} - \beta^* s^{*\prime} s^* - \beta^* s^{*2} + \beta^* s^* - p^* \beta^* s^* + s^* + p^* + 1 \tag{3.16}$$

We now have a non-dimensional maximization problem of the form

$$V^* = max \int_0^\infty \mathcal{D}(\tau) P(s^{*\prime}, s^*, \tau) d\tau \tag{3.17}$$

[2]The same applies for the discounting parameter b^* used in the hyperbolic solutions.

The corresponding terms needed to evaluate the Euler-Lagrange equation are:

$$\frac{\partial P}{\partial s^*} = 1 - \beta^* s^{*\prime} - p^* \beta^* - 2\beta^* s^* + \beta^* \tag{3.18}$$

$$\frac{\partial P}{\partial s^{*\prime}} = 1 - \beta^* s^* \tag{3.19}$$

$$\frac{d}{d\tau}\left(\frac{\partial P}{\partial s^{*\prime}}\right) = -\beta^* s^{*\prime} \tag{3.20}$$

Substituting into Equation 3.12, canceling terms and simplifying,

$$\frac{\mathcal{D}'}{\mathcal{D}} = \frac{1 - \beta^*(p^* + 2s^* - 1)}{1 - \beta^* s^*}. \tag{3.21}$$

Notice that, for this physical system, this solution applies no matter the discounting function used. If the discount rate, $\frac{\mathcal{D}'}{\mathcal{D}}$, is constant the solution for s^* will also be constant in time.

Also note that this solution is inconsistent at t = 0 unless the aquifer initial conditions happen to already be at the optimal solution level. There must be a Dirac delta of pumping at time $t = \epsilon$ to bring s^* from initial conditions to the optimal solution trajectory. This initial slug of pumping must bring the aquifer from the initial aquifer depth ($s_{t=0} = h - \frac{p}{\gamma}$), to the optimal depth s^* given by Equation 3.21. This is true for these analytical solutions, but obviously not true for real systems. In actuality it would take a period of time to come to the optimal trajectory from initial conditions.

3.4 Exponential Discounting

We first consider the constant exponential discounting case where $\mathcal{D}(t) = e^{-rt}$; $\mathcal{D}(\tau) = e^{-\rho\tau}$ in non-dimensional form. Substituting into the Euler-Lagrange equation, we immediately see that time disappears from the solution. Solving for s^* and then q^*:

$$s^* = \frac{1 + \rho + \beta^*(1 - p^*)}{\beta^*(2 + \rho)} \tag{3.22}$$

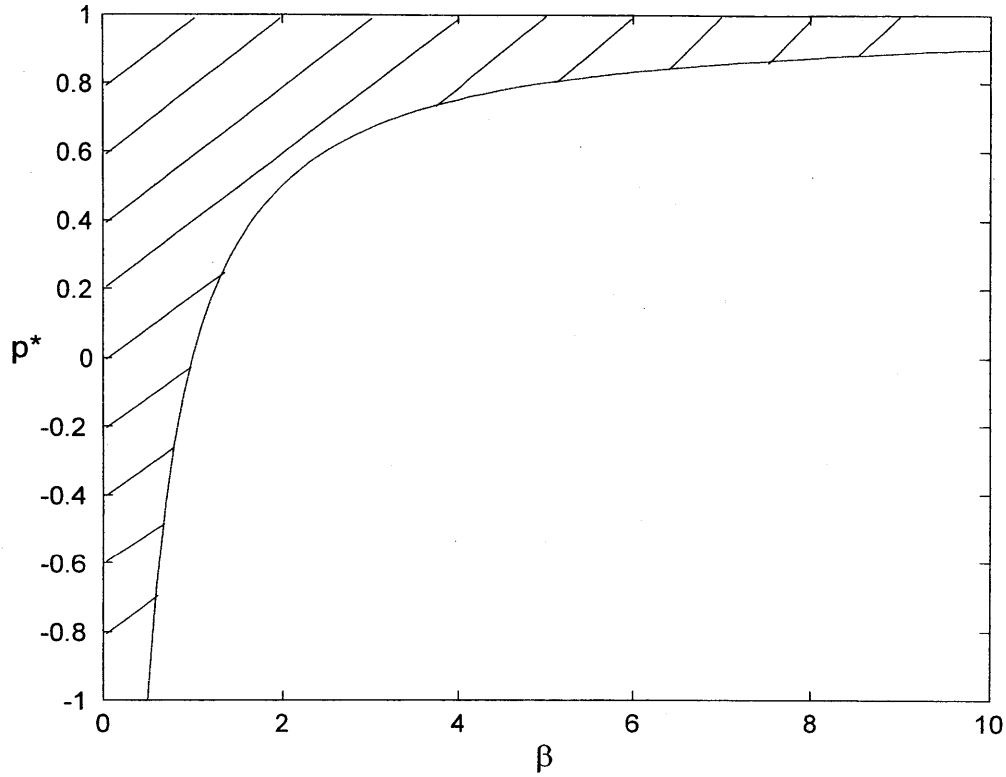

Figure 3-2: Feasible region for recharge and cost factor. Feasible region is the hatched region.

$$q^* = \frac{(1+\rho)[1-\beta^*(1-p^*)]}{\beta^*(2+\rho)} \tag{3.23}$$

Though no inequality constraints were used in the analysis, two physically reasonable bounds may now be imposed on the system. First, the water table must always be below the ground surface. This condition is given by the steady-state form of Equation 3.13 with no pumping.

$$s^* = 1 - p^* \tag{3.24}$$

To insure that the water table is always underground the non-dimensional recharge parameter must be less than one, $p^* < 1$.

The second condition is that the injection of water, $q < 0$, is not desirable[3]. The solution

[3] We assume that injection can't "reverse" the cost of pumping and turn it into profit

for q^* (3.23) requires that

$$\beta^*(1-p^*) \leq 1 \tag{3.25}$$

for q^* to be positive. A plot of this curve, bounded above by the stipulation that $p^* < 1$ is shown in Figure 3-2. The feasible region is everywhere above the curve. These stipulations are met in all the analyses, and parameters were chosen accordingly.

Now we may solve for the maximum net present value by substituting s^* (3.22) and q^* (3.23) into the objective function:

$$V^* = \int_0^\infty e^{-\rho\tau} \frac{(1+\rho)(1-\beta^*(1-p^*))^2}{\beta^*(2+\rho)^2} d\tau \tag{3.26}$$

Integrating over the limits,

$$V^* = \frac{(1+\rho)(1-\beta^*(1-p^*))^2}{\rho\beta^*(2+\rho)^2} \tag{3.27}$$

Though we arrive at a closed form solution, as $\rho \to 0$ the long-term net profit approaches infinity. The reason is that the situation for $\rho = 0$ is the result for no discounting. This means that the infinite future is valued as much as the present and that some stock is held onto for all time.[4]

This integrated discounted net benefit does not include benefits from the initial Dirac delta of pumping. The instantaneous profit is found by assuming $q^* = \frac{ds^*}{d\tau}$ since the rate of change of water table dominates the fluid balance equation under such strongly transient conditions. Plugging into the objective function and integrating from 0 to ϵ, time when optimal trajectory takes over, we may solve for non-dimensional instantaneous profit V_i^*:

$$V_i^* = \int_0^\epsilon \frac{ds^*}{d\tau}[1-\beta^* s^*] d\tau \tag{3.28}$$

$$V_i^* = \int_{s_{ss}}^{s_{opt}} [1-\beta^* s^*] ds^* \tag{3.29}$$

$$V_i^* = [s_{opt} - \frac{\beta s_{opt}^2}{2}] - [s_{ss} - \frac{\beta s_{ss}^2}{2}] \tag{3.30}$$

[4]This result is only true because we are dealing with a renewable resource. If this was a non-renewable resource the exponential solution would exhaust all stock at some time dependent on the discount rate.

In the following analysis we assume the initial state is the steady-state water level ${s_{ss}}^* = 1-p^* = 0.5$ ($s_{ss} = 10m$). Now we just need to substitute in s_{opt} at time $t = \epsilon$ from our optimal trajectory. The exponential solutions yield 1.90 and the hyperbolic solutions described below yield 1.97 units of non-dimensional profit from this initial burst of pumping.

3.5 Hyperbolic Discounting

The general hyperbolic discounting weight is $\mathcal{D}(t) = (\frac{1}{1+bt})^a$, where **b** has units of $[\frac{1}{t}]$ like **r** in exponential discounting, and **a** is non-dimensional. Non-dimensionalizing, $\mathcal{D}(\tau) = (\frac{1}{1+\rho_h\tau})^a$ and $\mathcal{D}(\tau)' = -\frac{a\rho_h}{(1+\rho_h\tau)}(\frac{1}{1+\rho_h\tau})^a$; where $\rho_h = \frac{b}{\gamma}$. Substituting into the Euler-Lagrange equation and solving:

$$s^*(\tau) = \frac{1 + \frac{a\rho_h}{1+\rho_h\tau} + \beta^*(1-p^*)}{\beta^*(2 + \frac{a\rho_h}{1+\rho_h\tau})} \tag{3.31}$$

To obtain the optimal pumping trajectory one needs to compute s' first and then substitute into $q^* = s^{*\prime} + s^* + p^* - 1$.

$$\frac{ds^*}{d\tau} = -\frac{a{\rho_h}^2(1-\beta^*(1-p^*))}{\beta^*(2+2\rho_h\tau + a\rho_h)^2} \tag{3.32}$$

$$q^*(\tau) = \frac{(1-\beta^*(1-p^*))(2{\rho_h}^2\tau^2 + 3a{\rho_h}^2\tau + 4\rho_h\tau + a^2{\rho_h}^2 - a{\rho_h}^2 + 3a\rho_h + 2)}{\beta^*(2+2\rho_h\tau + a\rho_h)^2} \tag{3.33}$$

It is useful to examine the behavior of these functions as $\tau \to \infty$.

$$\lim_{\tau\to\infty} s^* = \frac{1+\beta^*(1-p^*)}{2\beta^*} \tag{3.34}$$

$$\lim_{\tau\to\infty} q^* = \frac{1-\beta^*(1-p^*)}{2\beta^*} \tag{3.35}$$

Notice that the limit as $t \to \infty$ is the same result as for no discounting. It can be shown that this point is the Green Golden Rule of sustainability[5].

The solutions for q^* and s^* may now be substituted back into the objective function to solve

[5]Since the hyperbolic formulation satisfies Chichilnisky's criterion for renewable resources, in the limit, Chichilnisky's criterion approaches the GGR as is necessary

for the maximum net present utilityV^*:

$$V^* = \int_0^\infty \left(\frac{1}{1+\rho_h\tau}\right)^a q^*[1-\beta^* s^*]d\tau \tag{3.36}$$

This integral may or may not converge to a finite solution depending on the value of **a** and the optimal paths of q^* and s^*. In reality however, the integral would be over finite time and the uncomfortable possibility of an infinite optimal solution value would not be an issue[6].

In this study we carry out all analyses with $\mathbf{a} = 2$. This insures a convergent solution. Substituting $\mathbf{a} = 2$ in the general hyperbolic solutions for q^*, s^*, and V^* :

$$s^*(\tau) = \frac{1 + \frac{2\rho_h}{1+\rho_h\tau} + \beta^*(1-p^*)}{\beta^*(2 + \frac{2\rho_h}{1+\rho_h\tau})} \tag{3.37}$$

$$q^*(\tau) = \frac{(1-\beta^*(1-p^*))({\rho_h}^2\tau^2 + 3{\rho_h}^2\tau + {\rho_h}^2 + 2\rho_h\tau + 3\rho_h + 1)}{2\beta^*(1+\rho_h\tau+\rho_h)^2} \tag{3.38}$$

$$V^* = \int_0^\infty \left(\frac{1}{1+\rho_h\tau}\right)^2 q^*[1-\beta^* s^*]d\tau \tag{3.39}$$

3.6 Results of the Control Model

The hyperbolic model with $\mathbf{a} = 2$ is compared to the exponential solution. Though varying **a** changes the exact values in the solution trajectories, the solution sets are qualitatively similar. These analytical results are aimed at a general comparison of the hyperbolic and exponential optimal solutions.

3.6.1 Parameters for the Control Model

The following table gives the parameter values used in the control model or base case. Both dimensional and dimensionless values are shown.

[6]The integral $\int_0^\infty (\frac{1}{1+bt})^a dt$ converges to a positive number for $a > 1$ but diverges for $a <= 1$. To avoid infinite optimal solutions, we only consider $a > 1$.

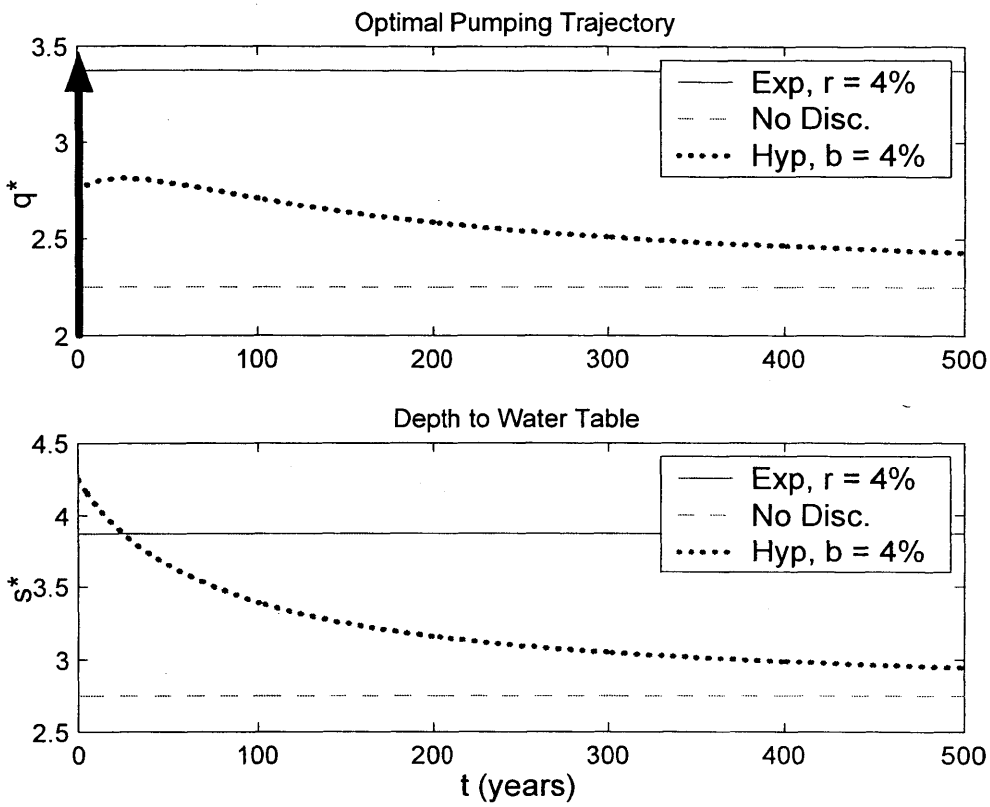

Figure 3-3: Optimal pumping rate and water table depth. The bold arrow at t = 0 represents the initial Dirac delta of pumping.

Parameter	Dimensional	Dimensionless
Head (h)	20 m	1
Profit Factor (α)	5 \$/m	1
Leakage Rate (γ)	0.02 /y	1
Discount Rate ($\rho = \frac{r}{\gamma}$)	0.04 /y	2
Cost Factor ($\beta^* = \frac{\beta h}{\alpha}$)	0.05 $\$/m^2$	0.2
Recharge Rate ($p^* = \frac{p}{h\gamma}$)	0.2 m/y	0.5

3.6.2 Summary of Results

Both solutions contain an initial, instantaneous withdrawal of water that brings the system from the steady-state initial head condition to the optimal trajectory. The initial drawdown for

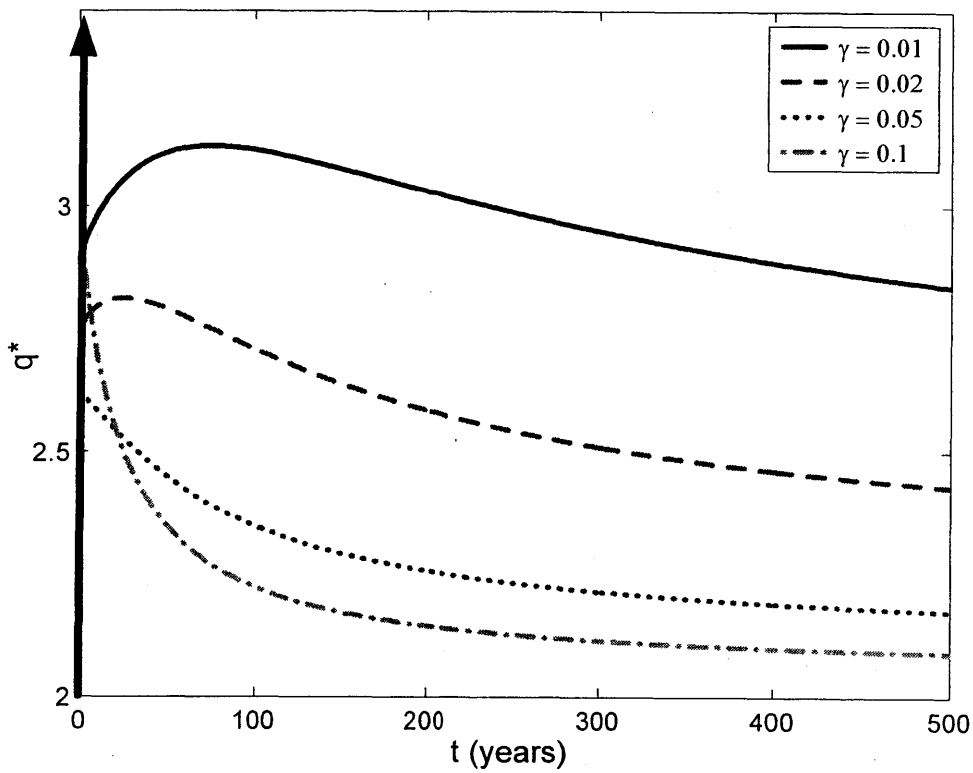

Figure 3-4: Optimal hyperbolic pumping trajectories for various aquifer leakage values; all other parameters the same as the Control.

both the exponential and hyperbolic cases will only be the same if they have the same discount rate, $\frac{D'}{D}$, at $t = 0$.

In reality, it would take time for the system to reach the optimal trajectory, and the initial rate of pumping would depend on the system physics and economics. Having a linear benefit function as we have in this simple example supposes that pumping a large amount at time $t = \epsilon$ is desirable and leads to this Dirac delta of pumping. A non-linear benefit function could get rid of this instantaneous slug of pumping and distribute the initial pumping over time. Alternatively, placing a limit on the pumping rate will also force the model to distribute initially high pumping over time.[7]

After the initial slug of pumping, the non-dimensional pumping rate for the exponential solution is constant at 3.38. Interestingly, the hyperbolic solution starts at 2.75, rises to 2.81 at about 26 years, then decreases asymptotically to the GGR solution of 2.25. As shown in Figure 3-4 the hyperbolic trajectory may have different characteristics depending on the γ value, and may not display the short term rise for systems with a large γ value.

The exponential solution for depth to the water table, s^*, is time invariant at a non-dimensional depth of 3.87, while the hyperbolic solution decreases smoothly over time from 4.25 to the GGR solution of 2.75 (Figure 3-3). As expected, for reasonable discount rates the exponential solution uses up the most "stock" of groundwater. The hyperbolic solution differs little from the exponential solution at small times, but preserves more and more stock into the future. These two solutions cross at around 26 years.

3.6.3 Sensitivity Analyses

Here the solutions' sensitivity to key non-dimensional parameters is tested. As a reminder, $\rho = \frac{r}{\gamma}$ is the ratio of the rate of discounting over the rate of leakage out of the system, $\beta^* = \frac{\beta h}{\alpha}$ is the ratio of the cost of a unit of water over the value of that unit of water for use, and $p^* = \frac{p}{h\gamma}$ is the ratio of the flux of water into the system over the flux of water out of the system.

Sensitivity to time-scale factor, $\rho = \frac{r}{\gamma}$: A higher ρ leads to an increase in pumping and hence to a greater depth to water table (decrease in stock). This follows because a higher discount rate means that one values the future less. Note that an increase in *dimensional*

[7] This is confirmed later with the numerical model.

discount rate or a decrease in leakage into the system has the same effect. A lower leakage rate means that less water is gained from the neighboring water source so the water table is lowered for a fixed r.

Sensitivity analyses indicate that the exponential solutions are sensitive to changes in ρ for $\rho < 20$, but insensitive to changes for larger ρ values. The hyperbolic solution is only sensitive for $\rho < 5$. An interesting result is that the no matter what positive non-dimensional discount rate ($\rho = \frac{r}{\gamma}$) is chosen in the exponential solution, the optimal pumping trajectory (Equation 3.23) can only change at most by a factor of 2. Shown below are the limit solutions for the extreme values for ρ.

For r $<< \gamma$:

$$\lim_{\rho \to 0} q^* = \frac{1 - \beta^*(1 - p^*)}{2\beta^*} \tag{3.40}$$

For r $>> \gamma$:

$$\lim_{\rho \to \infty} q^* = \frac{1 - \beta^*(1 - p^*)}{\beta^*} \tag{3.41}$$

On the other hand, the optimal hyperbolic pumping trajectory for the two extreme ρ_h values are, with $a = 2$[8] :

For b $<< \gamma$:

$$\lim_{\rho_h \to 0} q^* = \frac{1 - \beta^*(1 - p^*)}{2\beta^*} \tag{3.43}$$

For b $>> \gamma$:

$$\lim_{\rho_h \to \infty} q^* = \frac{(1 - \beta^*(1 - p^*))}{2\beta^*} \left(\frac{\tau^2 + 3\tau + 1}{\tau^2 + 2\tau + 1} \right) \tag{3.44}$$

For large discount rates and at $\tau = 0$ the solution for q^* (Equation 3.44) is equal to the the no-discounting solution. This equation also asymptotically approaches the no-discounting solution at very late times. However, over all time this solution for an infinite ρ_h changes at most by a factor of 1.25 at $\tau = 1$ (t $= \tau/\gamma = 50$ years) Figure 3-5.

[8]The general form is:

$$\lim_{\rho_h \to \infty} q^* = \frac{(1 - \beta^*(1 - p^*))(2\tau^2 + 3a\tau + a^2 - a)}{\beta^*(2\tau + a)^2} \tag{3.42}$$

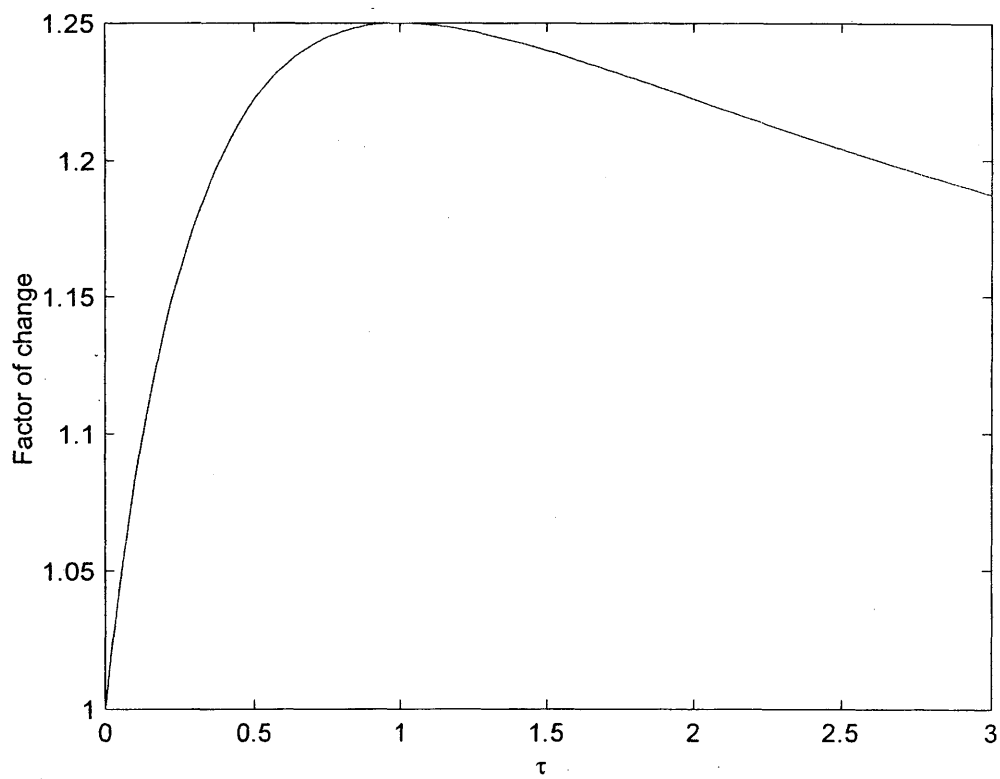

Figure 3-5: Factor of change in time for the hyperbolic groundwater mining problem as $t \to \infty$.

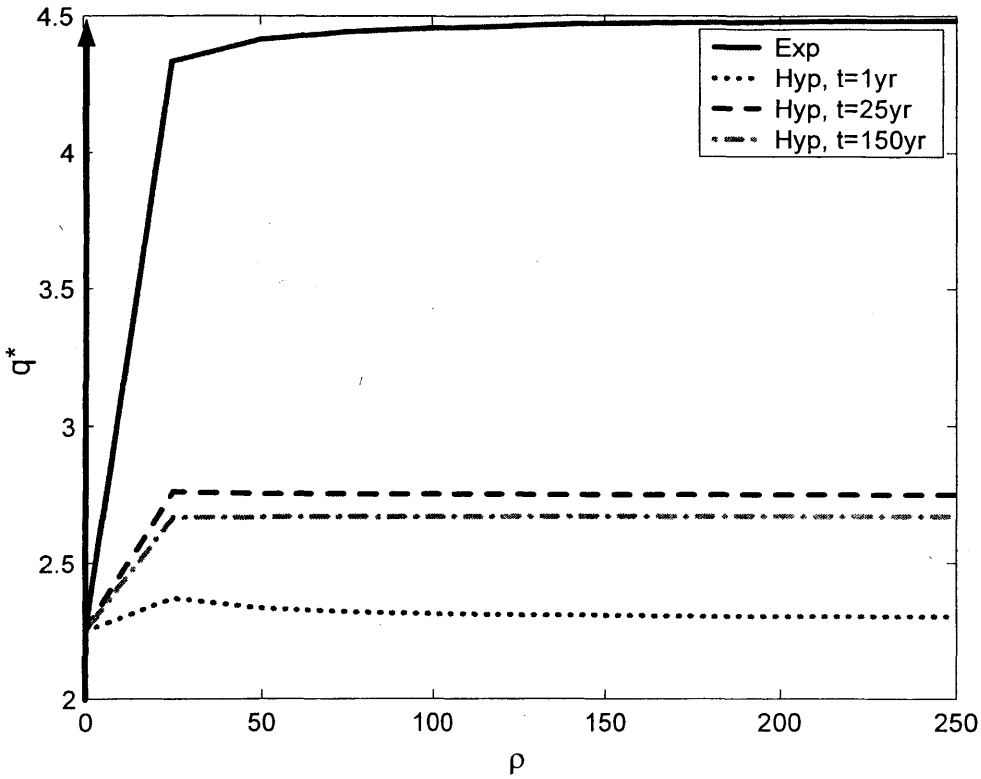

Figure 3-6: Plot of optimal pumping rate versus non-dimensional discount rate for the exponential solution, and for the hyperbolic solution at three different times.

For comparison, both discounting formulations are shown in Figure 3-6. As is obvious from this plot, and in support of the aforementioned statements, the exponential discounting solution is more sensitive to the discount rate than the hyperbolic discounting solution. This may have important implications for situations where the appropriate discount rate is ill-defined.

Sensitivity to cost-benefit factor, $\beta = \frac{\beta h}{\alpha}$: As expected, a higher β^* leads to higher water tables and a corresponding increase in stock. More cost per unit of water means less pumping when everything else is held constant. Pumping trajectories for both discounting formulations are very sensitive to β^* at low values, $\beta^* < 0.3$. As β^* becomes very small pumping increases in an exponential fashion and the water table depth increases significantly.

Sensitivity to recharge factor, $p^* = \frac{p}{h\alpha}$: An increase in recharge means that the water table will rise (increase in stock) if everything else is held constant. Both discounting models

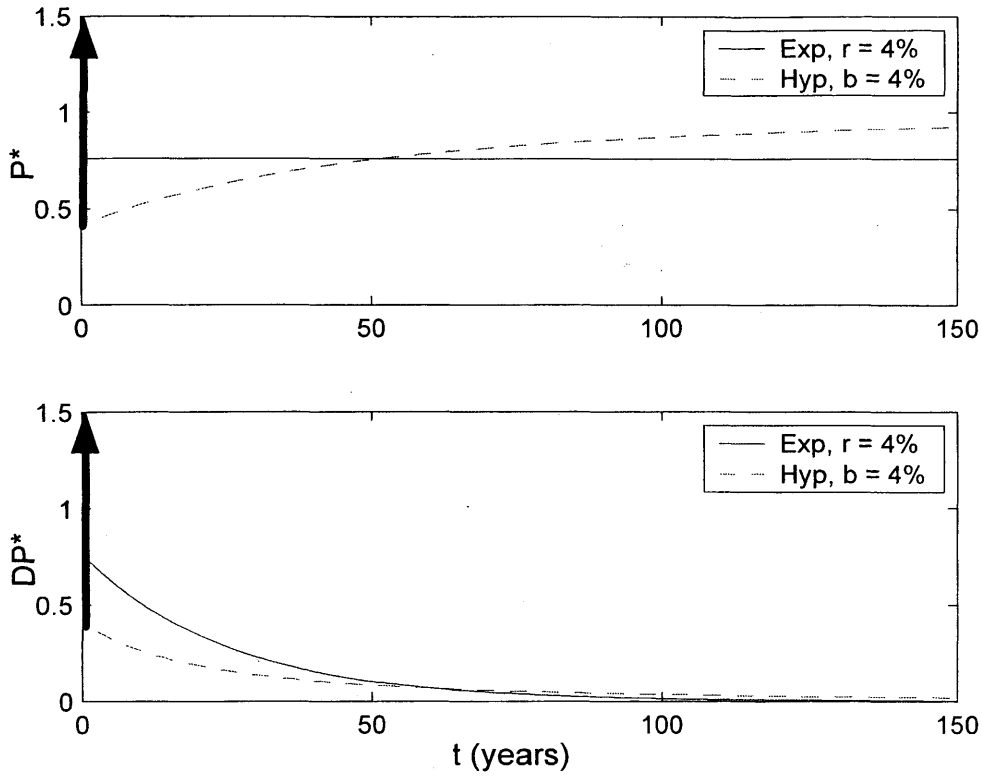

Figure 3-7: Non-discounted (top) and discounted (bottom) profit stream for exponential and hyperbolic models. Discounted plot shows discounted trajectory using each model's respective discounting function. The bold arrow represents the Dirac delta of profit at t = ϵ.

yield a positive linear relation between q^* and p^*.

3.6.4 Objective Function Results

After the initial spike of profit the rest of the optimal benefit trajectory may be plotted smoothly. It is first useful to plot the non-discounted function P^*, which is a non-dimensional rate of benefit; top part of Figure 3-7:

$$P^* = q^*[1 - \beta^* s^*] \tag{3.45}$$

The two discounted benefit curves, using each method's respective discounting weight, are shown in the bottom of Figure 3-7. The bold arrow at $t = 0$ represents the initial pumping spike.

For the first 50 years or so, the *near future*, the exponential optimal trajectory yields more benefit per unit time. Then at large times, the *far future*, the hyperbolic solution yields more benefit per unit time. Therefore, there is a period after 50 years and before the exponential trajectory goes to zero, over which the net monetary gains are higher for exponential discounting. Towards the latter half of this period, which may be called the *middle-future*, the hyperbolic trajectory begins to yield net gains which are larger. The implications of these results are discussed next.

3.6.5 Time Scale Issues

It seems that two issues are important when comparing the optimal trajectories produced using the two different discounting formulations.

(1) The projected futurity or time horizon of the project you are concerned with.
(2) The definition of *near, middle,* and *far future* in relation to the system being considered.

The first issue is an economic or political decision. The second is dependent upon the system's time rate of renewal versus the time scale of discounting; namely, the **time-scale factor**, $\rho = \frac{r}{\gamma}$. The lower the system time scale of response, γ, the larger the non-dimensional discount rate, and the sooner a hyperbolic-type trajectory may be beneficial. The intuition is this: a small γ implies a system that is renewable only on long time scales (approaching non-renewable). Therefore, it is to our benefit to be careful and insure benefits throughout the projects futurity. For a high γ, even if the system is severely depleted it can recover quickly, so the greater short-term profits of exponential discounting become more attractive.

In Figure 3-8 the non-discounted optimal benefit trajectories are plotted versus time for time scale factors $\rho = 0.5$, 1, 2, 3, and 5 (r = 1, 2, 4, 6, and 10%; $\gamma = 0.02$). The intersection of the hyperbolic and exponential profit curves for each discount rate represents the point at which the hyperbolic trajectory is yielding more non-discounted benefit per unit time. As stated above, for higher time scale factor this point of hyperbolic "takeover" takes place at an earlier time. I will refer to this point in time as the **Hyperbolic Takeover Time**, $HTT = f(\rho)$. A plot of HTT is shown in Figure 3-9. For average discount rates of 0.02 - 0.1, assuming the test

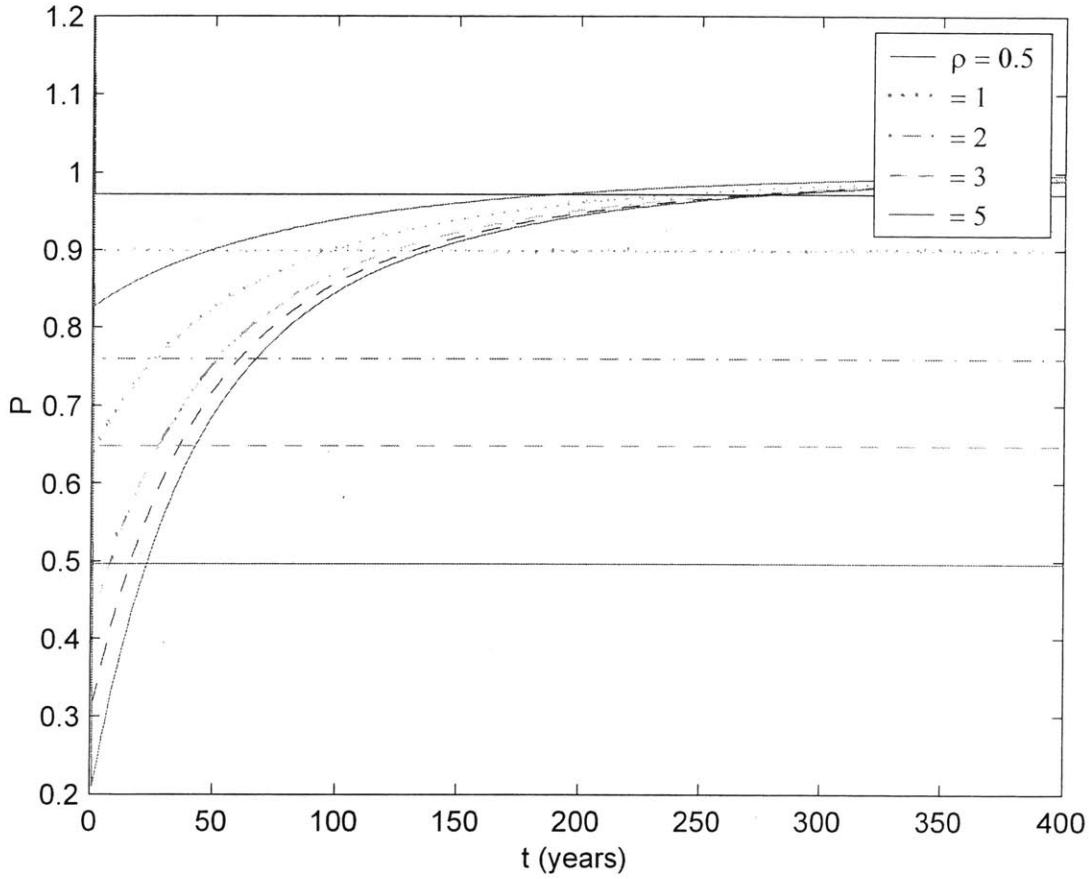

Figure 3-8: Non-discounted profit curves for various time scale factors.

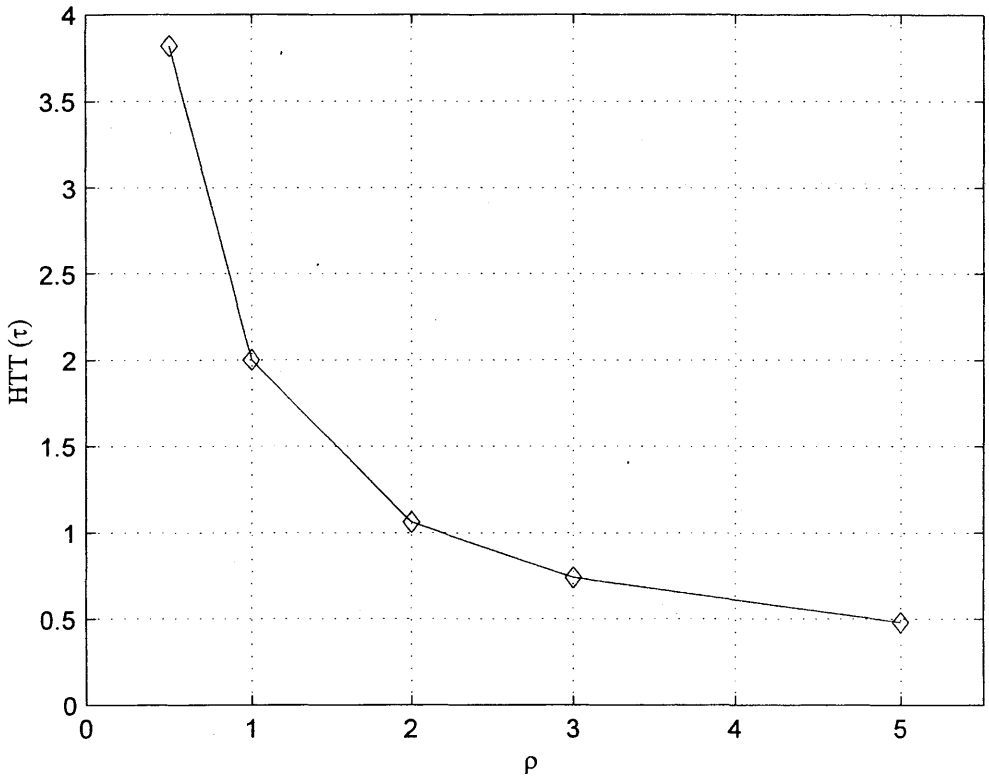

Figure 3-9: Plot of hyperbolic takeover time, HTT, for various time scale factors.

case value of $\gamma = 0.02$, the HTT is around 25-100 years; see table below. Of course, the HTT is *very* dependent on the characteristic time scale of the physical system being considered.

r (%)	HTT (years)
1	191
2	100
4	53
6	37
10	24

Therefore, in comparing hyperbolic discounting to exponential discounting, the following four steps are suggested:

(1) Determine the dominant time scale of the physical system. This should be the physical parameter which governs the system's rate of renewal and ability to return to equilibrium when perturbed.

(2) Define a non-dimensional time factor relating the time scale of the physical system to the discount rate.

(3) Construct a plot like that given in Figure 3-9.

(4) If the time frame of your project is lower than the HTT indicated, then using exponential discounting is probably fine. If the time frame of your project is longer, then hyperbolic discounting may make a notable difference on your optimal management strategy.

In summary, the plot of HTT is an attempt to visually characterize the approximate time scale over which hyperbolic discounting will noticeably affect your optimal solution relative to exponential discounting. It does **not** imply that hyperbolic discounting is preferable if the time frame of the management project is longer than your computed HTT.

Chapter 4

Salinization Problem

This section deals with finding the optimal withdrawal rate of irrigation water from a simple unconfined, groundwater aquifer such that dryland salinization will not set in. Pumping, q, is defined as $[\frac{m}{t}]$ and concentrations are dimensionless. The goal of this exercise is to explore any differences between quantity and quality water issues when considering discounting formulations.

4.1 Problem Description

The objective of this problem is to maximize utility of groundwater pumping for irrigation for a system where irrigation itself leads to salinization. Salinization occurs because of concentration of salts due to evaporation when the pumped water is applied to a crop. In this formulation we assume that natural recharge is a fixed quantity; both recharge rate and recharge salt concentration. The primary decision variable is pumping rate.

The fluid flux balance for the system portrayed in Figure 4-1 is;

$$R = L + qE \tag{4.1}$$

where E is a non-dimensional evaporation factor. Note that this equation is steady state. We assume that the aquifer volume responds immediately to pumping. This way we may focus on the changes in salt concentrations rather than water flux; as was the case with the groundwater

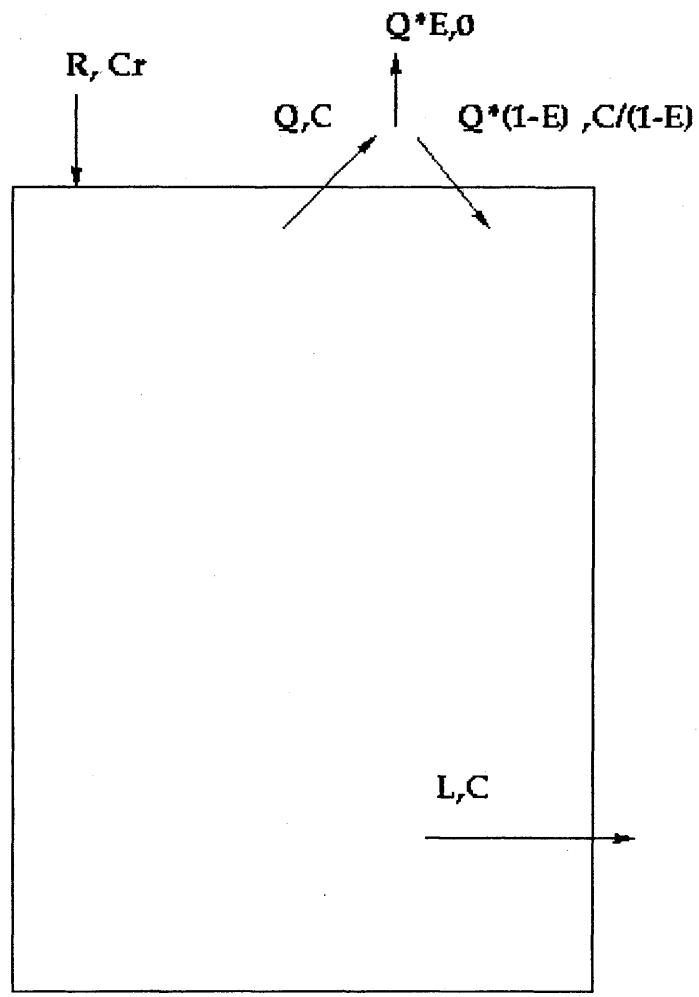

Figure 4-1: Schematic for dryland salinization problem. The term before the comma is flux, and the term after the comma is concentration.

mining problem. The variables q and c are related to each other by a salt mass balance equation for the aquifer system.

$$h\frac{dc}{dt} = Rc_r - Lc \tag{4.2}$$

where c_r is the recharge solute concentration [–], h is the aquifer depth [m], R is recharge into the system [m/t], L is leakage out of the system [$\frac{m}{t}$], and c is the aquifer solute concentration [–]. Initial condition for aquifer concentration is $c = 0.05$.

We may now solve for L in the fluid flux equation (4.1)and substitute into the salt balance equation yielding,

$$q = \frac{1}{cE}[hc' + R(c - c_r)] \tag{4.3}$$

The maximization problem takes the form,

$$V = max \int_0^{\infty} \mathcal{D}(t) f(q, c, t) dt \tag{4.4}$$

where the benefit function is

$$f(q, c, t) = \alpha Y(c) q \tag{4.5}$$

V has units of [\$], f is the net benefit function [\$/t], q is the pumping rate [$\frac{m}{t}$], α is a benefit factor [\$/kg], and Y is the yield function [kg/m]. The yield function includes a penalty for salty water; which has the effect of decreasing the water's utility.

$$Y = Y_m(1 - \frac{c}{c_m}) \tag{4.6}$$

Y_m is the maximum yield [kg/m], and c_m represents a maximum water salt concentration, which for this study is basically seawater, $c_m = 0.3$. As $c \rightarrow c_m$ yield, and hence benefit, goes to zero.

4.2 Non-dimensional Formulation

It is useful to non-dimensionalize the objective and state equations. They may be non-dimensionalized using h as a characteristic length scale, R as a scaling factor for time, α as a scaling factor for dollars, and Y_m as the scaling factor for yield. The non-dimensional groups are $\rho = \frac{rh}{R}$, $\tau = \frac{Rt}{h}$,

$q^* = \frac{q}{R}$, $V^* = \frac{V}{\alpha h Y_m}$, $\rho_h = \frac{rh}{R}$, and $L^* = \frac{L}{R}$. Concentrations are already assumed to be expressed in a dimensionless mass fraction form. The group $\rho = \frac{rh}{R}$ is the *time-scale factor* for the salinization problem. It is the ratio of the rate of discounting to the rate of recharge into the system.

The salt balance equation becomes,

$$\frac{dc}{d\tau} = c_r - L^* c \tag{4.7}$$

and the fluid flux equation reduces to,

$$1 = L^* + q^* E \tag{4.8}$$

Combining these two equation through the leakage term,

$$q^* = \frac{1}{cE}(c' - c_r + c) \tag{4.9}$$

The non-dimensional form of the objective function, after inserting the yield function, is

$$V^* = max \int_0^\infty \mathcal{D}(\tau) q^* (1 - \frac{c}{c_m}) d\tau \tag{4.10}$$

Substituting in for q^* the final, non-dimensional maximization problem is

$$V^*(c', c, \tau) = max \int_0^\infty \mathcal{D}(\tau) P(c', c, \tau) d\tau \tag{4.11}$$

where $P(c', c, \tau)$ is,

$$P = \frac{1}{cE}(1 - \frac{c}{c_m})(c' - c_r + c) \tag{4.12}$$

The corresponding terms needed to satisfy the Euler-Lagrange equation are:

$$\frac{\partial P}{\partial c} = \frac{1}{E}(-\frac{c'}{c^2} + \frac{c_r}{c^2} - \frac{1}{c_m}) \tag{4.13}$$

$$\frac{\partial P}{\partial c'} = \frac{1}{E}(\frac{1}{c} - \frac{1}{c_m}) \tag{4.14}$$

$$\frac{d}{d\tau}(\frac{\partial P}{\partial c'}) = -\frac{c'}{Ec^2} \tag{4.15}$$

Solving the optimization problem by substituting into Equation 3.12:

$$c = \frac{-\frac{\mathcal{D}'}{\mathcal{D}}c_m \pm \sqrt{(\frac{\mathcal{D}'}{\mathcal{D}}c_m)^2 + 4(1-\frac{\mathcal{D}'}{\mathcal{D}})(c_m c_r)}}{2(1-\frac{\mathcal{D}'}{\mathcal{D}})} \tag{4.16}$$

This solution applies no matter the discounting function used. As with the groundwater mining problem, we see that if the discount rate $(\frac{\mathcal{D}'}{\mathcal{D}})$ is constant then the concentration optimal trajectory is also constant in time.

4.3 Exponential Discounting

We first consider the case when $\mathcal{D}(t) = e^{-rt}$, or $\mathcal{D}(\tau) = e^{-\rho\tau}$ in non-dimensional form. Utilizing Equation 4.16 from above:

$$c = \frac{\rho c_m \pm \sqrt{\rho^2 {c_m}^2 + 4(1+\rho)(c_m c_r)}}{2(1+\rho)} \tag{4.17}$$

The corresponding optimal pumping rate is found by substituting the solution for c into 4.9:

$$q^* = \frac{1}{E}[1 - \frac{2c_r(1+\rho)}{\rho c_m \pm \sqrt{\rho^2 {c_m}^2 + 4(1+\rho)(c_m c_r)}}] \tag{4.18}$$

Note that the $\pm$ in the quadratic equation solution forces us to select the correct solution based on physical plausibility. Since concentrations must be greater than or equal to zero, the correct sign is positive for all cases except when $c_r = 0$ or $c_m = 0$. We assume c_m always greater than zero.

However, when $c_r = 0$ it is found that we must in fact choose the negative sign for the solution to make physical sense. When $c_r = 0$ the system must eventually reach a state of $c = 0$, since all incoming water is fresh and *we assume leakage can only be out of the system.* Allowing leakage into the system would allow for $c \neq 0$ when $c_r = 0$ due to initially saline conditions in the aquifer.

Therefore, for all cases except when $c_r = 0$:

$$c = \frac{\rho c_m + \sqrt{\rho^2 {c_m}^2 + 4(1+\rho)(c_m c_r)}}{2(1+\rho)} \tag{4.19}$$

$$q^* = \frac{1}{E}[1 - \frac{2c_r(1+\rho)}{\rho c_m + \sqrt{\rho^2 {c_m}^2 + 4(1+\rho)(c_m c_r)}}] \tag{4.20}$$

A further physical constraint imposed here is that pumping must be positive. Therefore, the previous equation for pumping implies:

$$0 \leq \frac{2c_r(1+\rho)}{\rho c_m + \sqrt{\rho^2 {c_m}^2 + 4(1+\rho)(c_m c_r)}} \leq 1 \tag{4.21}$$

This condition may be neglected if one allows the possibility of injecting water.

Substituting our optimal solutions for c and q^* into the objective function (4.10),

$$V^* = \int_0^\infty e^{-\rho\tau} \frac{1}{E}[1 - \frac{2c_r(1+\rho)}{\rho c_m + \sqrt{\rho^2 {c_m}^2 + 4(1+\rho)(c_m c_r)}}][1 - \frac{\rho c_m + \sqrt{\rho^2 {c_m}^2 + 4(1+\rho)(c_m c_r)}}{2c_m(1+\rho)}]d\tau \tag{4.22}$$

Integrating over the limits,

$$V^* = \frac{1}{\rho E}[1 - \frac{2c_r(1+\rho)}{\rho c_m + \sqrt{\rho^2 {c_m}^2 + 4(1+\rho)(c_m c_r)}}][1 - \frac{\rho c_m + \sqrt{\rho^2 {c_m}^2 + 4(1+\rho)(c_m c_r)}}{2c_m(1+\rho)}]. \tag{4.23}$$

4.4 Hyperbolic Discounting

The hyperbolic function, as in the groundwater mining example, is $\mathcal{D}(t) = (\frac{1}{1+bt})^2$, where b has units of $[\frac{1}{t}]$ like r in exponential discounting. Non-dimensionalizing and substituting into Equation 4.16, the optimal concentration trajectory is:

$$c(\tau) = \frac{\frac{c_m \rho_h}{1+\rho_h \tau} + \sqrt{(\frac{c_m \rho_h}{1+\rho_h \tau})^2 + c_m c_r (1 + \frac{2\rho_h}{1+\rho_h \tau})}}{1 + \frac{2\rho_h}{1+\rho_h \tau}} \tag{4.24}$$

Since $\frac{\mathcal{D}'}{\mathcal{D}}$ is not constant, this solution is a function of time. As a check on correctness, we may examine the solution's behavior as $\tau \to \infty$ to insure it asymptotically approaches the

no-discounting solution as is necessary.

$$\lim_{\tau \to \infty} c = \sqrt{c_m c_r} \tag{4.25}$$

Note that if the incoming recharge concentration (c_r) is totally fresh the whole system will be freshened over time.

To solve for the optimal pumping trajectory it is necessary to to compute c', and then substitute into the state equation (4.9). Though straightforward, the resultant equations for c' and q^* are very tedious and not shown here. As with the exponential solutions, a non-negativity constraint on pumping may also be imposed for the hyperbolic case; but the actual constraint formula is equally cumbersome and also omitted here. However, parameters in our test cases were found to insure a positive pumping rate at all times.

Substituting back into the objective function (4.10) and solving for the optimal net discounted benefit is straightforward. Just insert for q^* in,

$$V^* = \int_0^\infty (\frac{1}{1+\rho_h \tau})^2 q^* [1 - \frac{\frac{\rho_h}{1+\rho_h \tau} c_m + \sqrt{\frac{\rho_h}{1+\rho_h \tau}^2 c_m{}^2 + c_m c_r (1 + \frac{2\rho_h}{1+\rho_h \tau})}}{c_m (1 + \frac{2\rho_h}{1+\rho_h \tau})}] d\tau \tag{4.26}$$

As was the case for the groundwater mining problem with $a = 2$, this integral is convergent.

4.5 Results

4.5.1 Parameters for the Control Model

The following table gives the parameter values used in the control model or base case. Both dimensional and dimensionless values are shown.

Parameter	Dimensional	Dimensionless
Aquifer Depth (h)	50 m	1
Profit Factor (α)	5 \$/kg	1
Recharge Rate (R)	0.5 m/y	1
Max. Yield (Y_m)	10 kg/m	1
Discount Rate ($\rho = \frac{rh}{R}$)	0.04 /y	8
Max. Concentration (c_m)	–	0.3
Recharge Conc. (c_r)	–	0.05
Evaporation (E)	–	0.1

4.5.2 Summary of Results

The exponential pumping solution is constant at a non-dimensional pumping rate of 8; after the initial Dirac delta of pumping. The hyperbolic solution starts at 4.71, rises slowly, passes the GGR value of 6 at 115 years, and continues to rise with time. This hyperbolic trajectory will begin to decline in the very far future and asymptotically approaches the GGR solution.

The exponential concentration solution is constant at a non-dimensional concentration of 0.25. The hyperbolic solution starts at 0.27 then asymptotically approaches the no-discounting solution of c = 0.12; bottom of Figure 4-2. The hyperbolic solution salinizes the aquifer more than the exponential solution for about 25 years, before reductions in pumping allow the aquifer to slowly reduce salt concentrations to a better overall condition than the exponential solution in the long run.

4.5.3 Sensitivity Analyses

Sensitivity to time-scale factor, $\rho = \frac{rh}{R}$: For the exponential model, pumping increases with ρ since the future is discounted more. The exponential solutions are insensitive to changes in ρ for high values, $\rho > 20$, and moderately sensitive for the lower range of values. How much the hyperbolic trajectory changes with ρ depends on what point in time is being considered, but the solution is also more sensitive for $\rho > 20$.

It is useful to compare the range of pumping trajectories obtained using the extreme values for the non-dimensional discount rate. For the exponential discounting case:

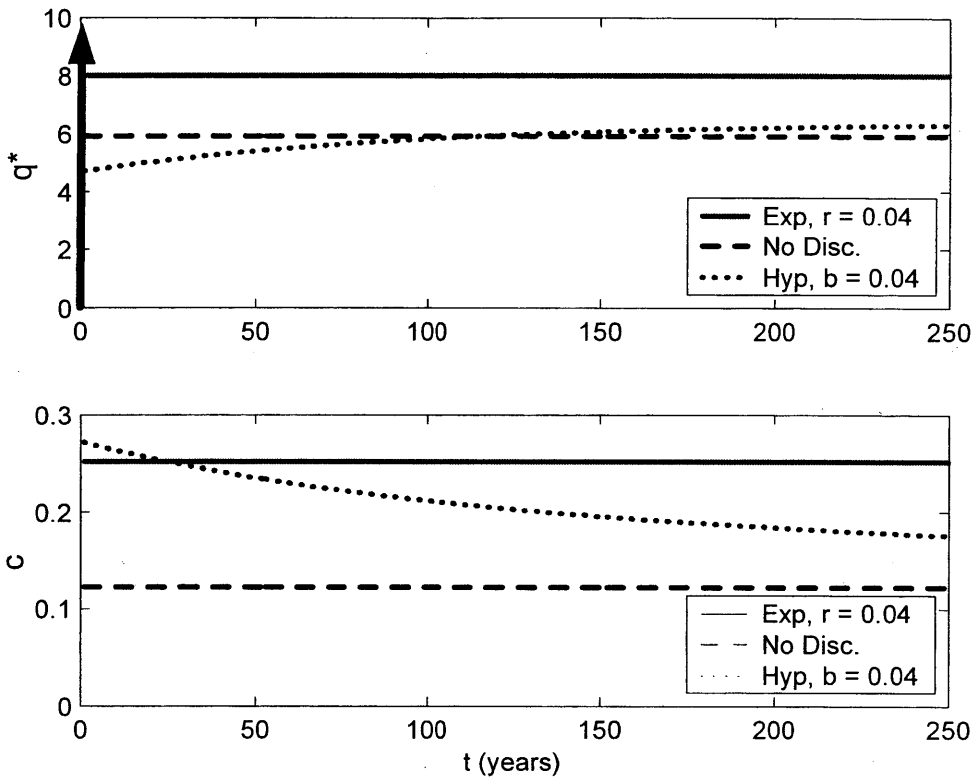

Figure 4-2: Salinization results for optimal pumping trajectory and corresponding salinity. The bold arrow at t = 0 represents the initial burst of pumping from initial conditions.

For r $<< \gamma$:

$$\lim_{\rho \to 0} q^* = \frac{1}{E}[1 - \frac{\sqrt{c_r}}{\sqrt{c_m}}] \tag{4.27}$$

For r $>> \gamma$:

$$\lim_{\rho \to \infty} q^* = \frac{1}{E}[1 - \frac{c_r}{c_m}] \tag{4.28}$$

Therefore, your choice of discount rate may at most affect your pumping management trajectory by the factor:

$$\frac{c_m - c_r}{c_m - \sqrt{c_m c_r}}.$$

It is interesting that this factor, given that c_r and c_m vary between 0 and 1, may only vary between 0 and 2. Therefore, as in the groundwater pumping example, the exponential optimal solution may only change by at most a factor of 2. The maximum factor of change is 1.4 given the parameters for this base case..

The hyperbolic case is more complicated. The optimal hyperbolic pumping trajectory for the two extreme ρ_h values are, with $a = 2$:

For b $<< \gamma$:

$$\lim_{\rho_h \to 0} q^* = \frac{1}{E}[1 - \frac{\sqrt{c_r}}{\sqrt{c_m}}] \tag{4.29}$$

For b $>> \gamma$:

$$\lim_{\rho_h \to \infty} q^* = \frac{c_m c_r(\tau^3 + 4\tau^2 + 5\tau + 2) + (1+\tau)({c_m}^2 - 4c_r A\tau + c_m A\tau) - c_r A\tau^3}{AE\tau(c_m + A\tau)(\tau + 2)} \tag{4.30}$$

$$A = \frac{\sqrt{c_m(c_m + 2c_r\tau + c_r\tau^2)}}{\tau} \tag{4.31}$$

At the lower bound the hyperbolic solution is the same as the lower bound for the exponential formulation; this is just no discounting. At the upperbound for we have a complicated equation (4.30) that is a function of time as well as the other parameters. However, as $t \to \infty$ this upper limit does go to the necessary no-discounting asymptote as is necessary. For the hyperbolic case, over the whole range of non-dimensional discount rates, the solution may only change at most by a factor of 1.08 at $\tau = 4.7$ (470 years); Figure 4-3.

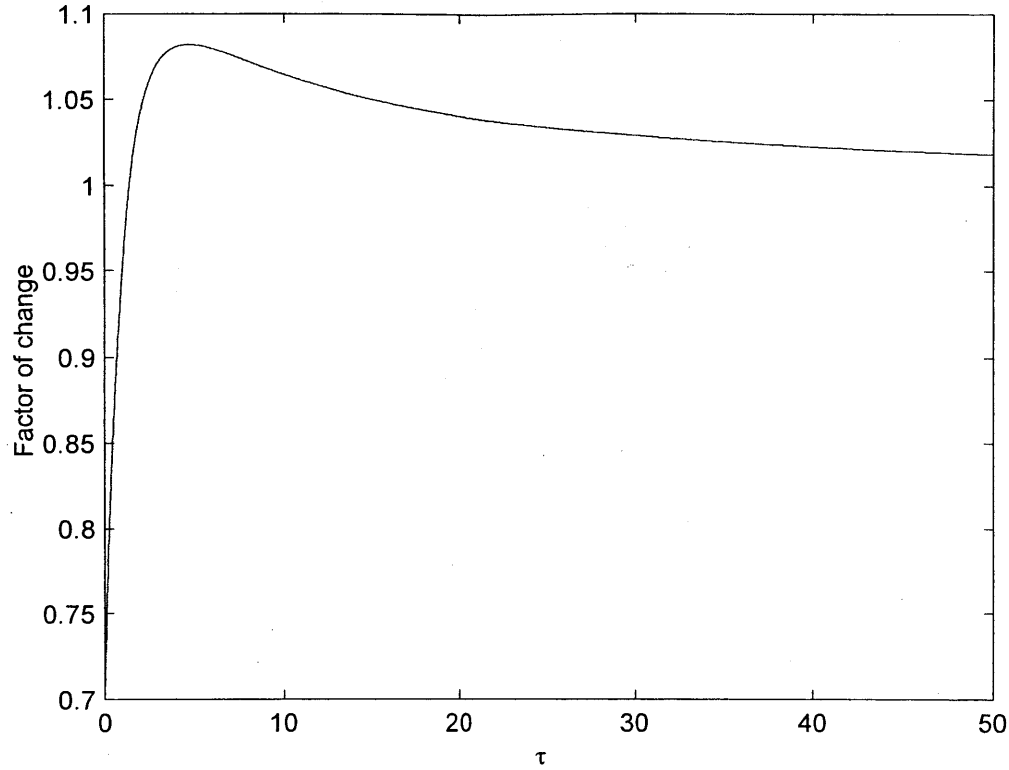

Figure 4-3: Factor of change over time for the hyperbolic salinization problem as $t \to \infty$.

As was the case for the groundwater mining problem, the exponential solution is more sensitive to the discount rate. However, it should be noted that unlike for the groundwater mining problem, the sensitivity to discount rate is a function of water quality parameters, c_m and c_r. In effect, the user defined contamination threshold, c_m, and the source of contamination, c_r, have direct bearing on not only the optimal solution, but on the optimal solution's *sensitivity* to the chosen discount rate.

Sensitivity to recharge concentration, c_r: A higher recharge concentration leads to less pumping and a higher optimal aquifer concentration if everything else is held constant. The exponential model decreases linearly with c_r. The sensitivity of the hyperbolic solutions depends on time. At early times, after the initial spike of pumping, the hyperbolic solution is less sensitive to c_r, while at late times the sensitivity to recharge concentration increases. In other words, a change in recharge concentration may significantly affect your long-term

hyperbolic optimal trajectory.

4.5.4 Objective Function Results

As with the groundwater mining problem, there is a benefit gained from the initial pumping that occus at time $t = \epsilon$. The Euler-Lagrange Equation must satisfy the system's initial conditions. It does this via a Dirac delta of pumping (or possibly injecting) at time $t = \epsilon$, that immediately takes the system to the optimal trajectory. There is a profit gained from this initial pumping that has to be counted for the analysis to be consistent.

The instantaneous profit is found by first assuming that $q^* = \frac{c'}{cE}$ since the rate of change of concentration dominates under such strongly transient conditions. Substituting into the objective function and integrating from 0 to ϵ, time when the optimal trajectory takes over, we may solve for the initial profit $V_i{}^*$:

$$V_i{}^* = \int_0^{\epsilon} \frac{c'}{cE}(1 - \frac{c}{c_m})d\tau \tag{4.32}$$

$$V_i{}^* = \frac{1}{E}\int_0^{\epsilon} \frac{dc}{d\tau}(\frac{1}{c} - \frac{1}{c_m})d\tau \tag{4.33}$$

$$V_i{}^* = \frac{1}{E}\int_{c_i}^{c_{opt}} (\frac{1}{c} - \frac{1}{c_m})dc \tag{4.34}$$

$$V_i{}^* = \frac{1}{E}[ln(\frac{c_{opt}}{c_i}) + \frac{(c_i - c_{opt})}{c_m}] \tag{4.35}$$

Note that c_i is the aquifer's initial salt concentration at t = 0. Now we just substitute for c_{opt} and c_i to get the initial profit. For the base case we assume $c_i = 0.05$; which is the steady-state aquifer concentration. Note that for $c_i = 0$ we yield $V_i{}^* = \infty$, since with no maximum pumping constraint the system pumps furiously if all the water is fresh. The exponential solution yields an initial profit of 9.44, and hyperbolic solution yields an initial profit of 9.53.

Plotted in Figure 4-4 is the non-discounted function P^*, which is the non-dimensional rate of profit from the objective function (4.10):

$$P^* = q^*(1 - \frac{c}{c_m}) \tag{4.36}$$

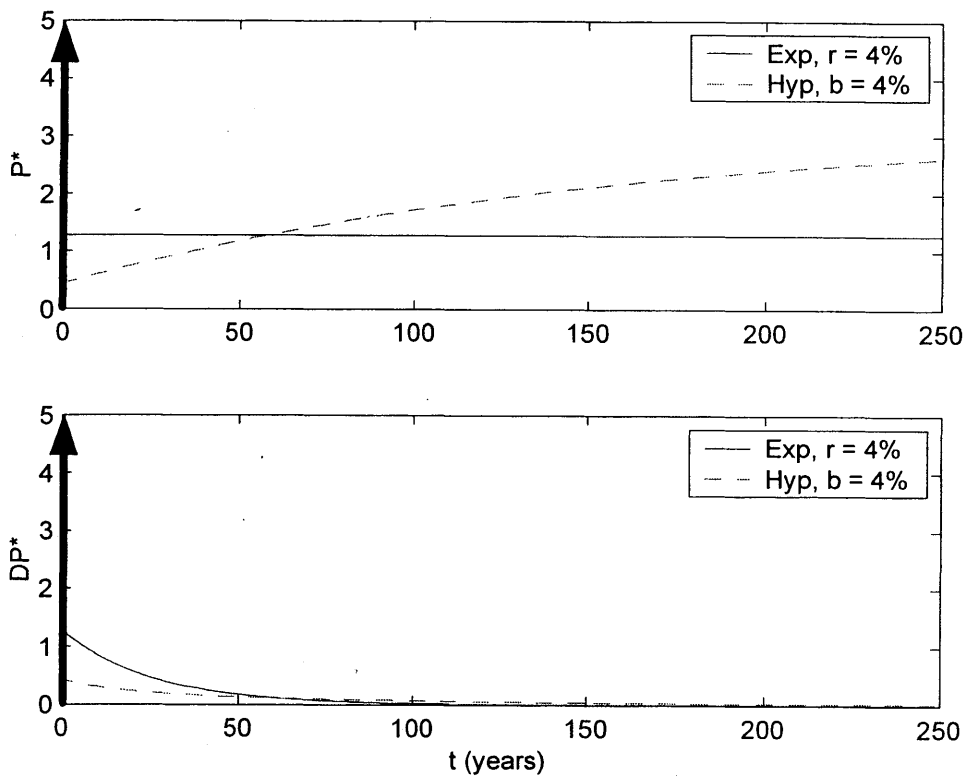

Figure 4-4: Non-discounted and discounted salinization objective function results.

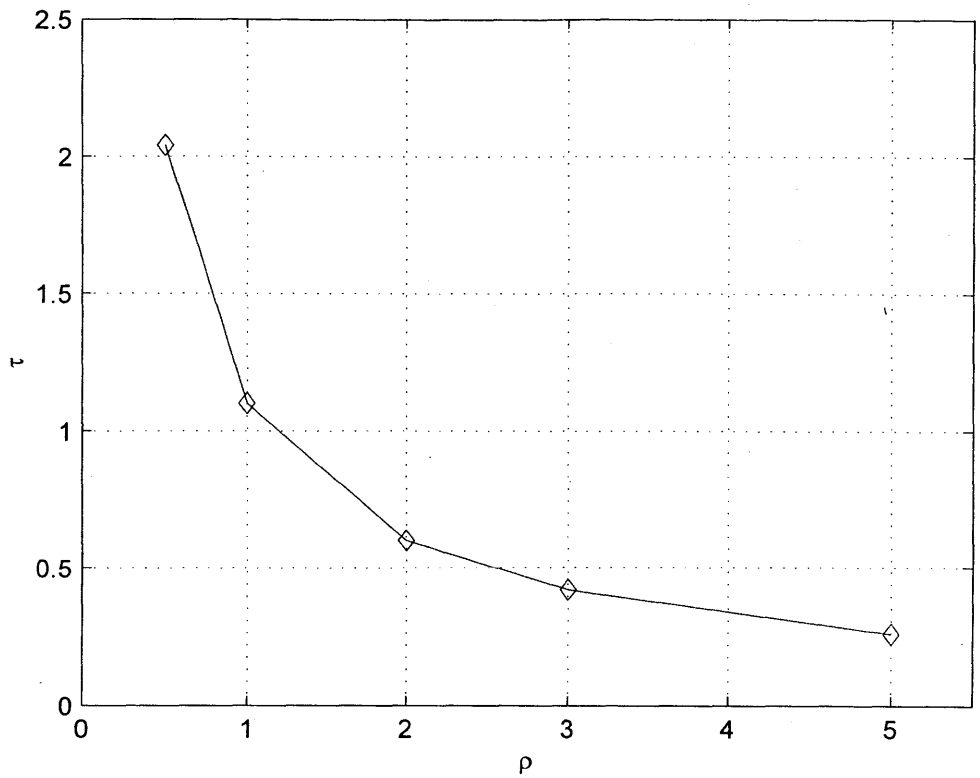

Figure 4-5: Plot of hyperbolic takeover time, HTT, for various time-scale factors for the salinization example.

As with the groundwater mining problem, a plot of Hyperbolic Takeover Time (HTT) may be constructed to give the decision maker a better idea of how the economic and physical time scales compare, and how this may affect long-term management decisions; Figure 4-5. Discount rates between 0.01 and 0.05 ($1 < \rho < 5$) yield HTT between 25 and 100 years ($0.25 < \tau < 1$).

Chapter 5

Stochastic Discount Rate

In this section a numerical model is developed for the groundwater mining problem in order to look at the effects of non-linearity in the benefit function and of a stochastic discount rate. Analytical results by Weitzman, Sozou and Azfar [55][1][56][50] are explained and compared to the numerical results.

5.1 Set-up of the Numerical Model

To facilitate the stochastic analyses, the deterministic model is transcribed using GAMS [5] and then solved using the MINOS optimization code. The analytical results of the deterministic problem are used to test and verify the numerical model. There is good agreement between the GAMS solutions and the analytical solutions for both the exponential and hyperbolic test cases[1]. The only discrepancy is at early times when the numerical model has difficulty resolving the initial spike of pumping found in the analytical solution. Decreasing the time step (Δt) in the numerical model will sharpen the peak, but at the expense of computational time and

[1] All models were run over 500 years in order to safely remove any numerical excursions that occur towards the end of the time horizon being optimized over. These numerical "blips" are to be expected and reflect the fact that the model does not recognize a future after 500 years and therefore uses up the resource during the final time steps.

In addition, for some GAMS simulations there are excursions at times before the 500 years. These are due to accuracy limits in GAMS and the fact that quantities are discounted to very low values at large times. When the discount factor gets so small that the numerical model can't distinquish it from zero the solution after that point is meaningless. Tested vigorously, this effect is proportional to the magnitude of the discount rate. It goes away for very small r.

effort. After experimenting with different time steps we found that a time step of 0.2 years is a good compromise of speed and accuracy for the purposes of this study. This time step leads to a Dirac delta that is spread out over about 10 years before the numerical and analytical solutions match exactly.

5.2 Non-Linear Benefit Function

Recall that in the formulation of the groundwater mining problem the objective function is given as,

$$V = max \int_0^\infty \mathcal{D}(t)[\alpha q - \beta sq]dt \tag{5.1}$$

where the first term in the brackets is benefit of using the water per unit time and is simply a coefficient of utility multiplied by the pumping rate. This formulation is convenient for analytical solution but not realistic. In reality there is a point after which the marginal value of more water approaches zero and may even decrease.

To include this information in the analyses the benefit function was modified to increase linearly at small pumping values, but taper off at some given level. The non-linear function

$$B(q,t) = \alpha \left(\frac{\eta q}{1 + \eta q} \right) \tag{5.2}$$

is used to simulate this effect. The constant η $[\frac{t}{m}]$ determines how quickly the benefit levels off with Q, and α $[\frac{\$}{t}]$ is the same benefit coefficient as for the analytical analyses. In this analysis η is set to 2 as a reasonable test case based on max pumping magnitudes in the linear benefit deterministic results. The function B(q,t) is plotted in Figure 5-1.

The objective function is now of the form:

$$V = max \int_0^\infty e^{-rt}[\alpha \left(\frac{\eta q}{1 + \eta q} \right) - \beta sq]dt \tag{5.3}$$

5.2.1 Results for Non-linear Benefit Function

As shown in Figure 5-2, the non-linear benefit function has a definite effect on the resulting optimal pumping trajectory and resulting water table depth. Pumping increases rapidly to

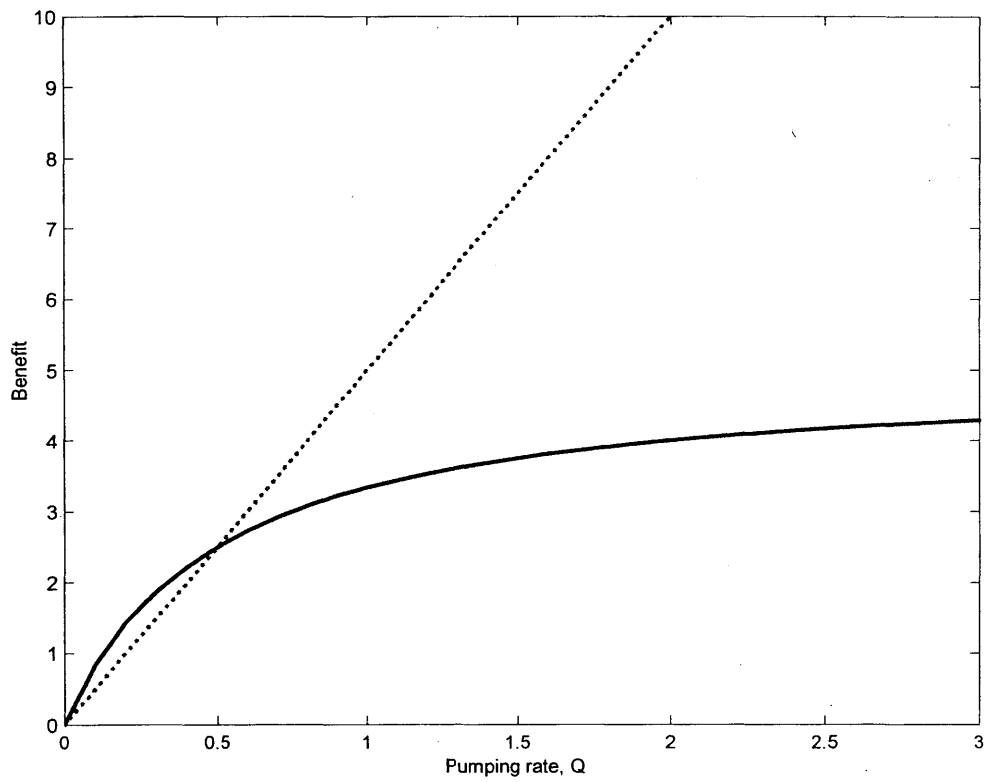

Figure 5-1: Linear benefit function and non-linear benefit function.

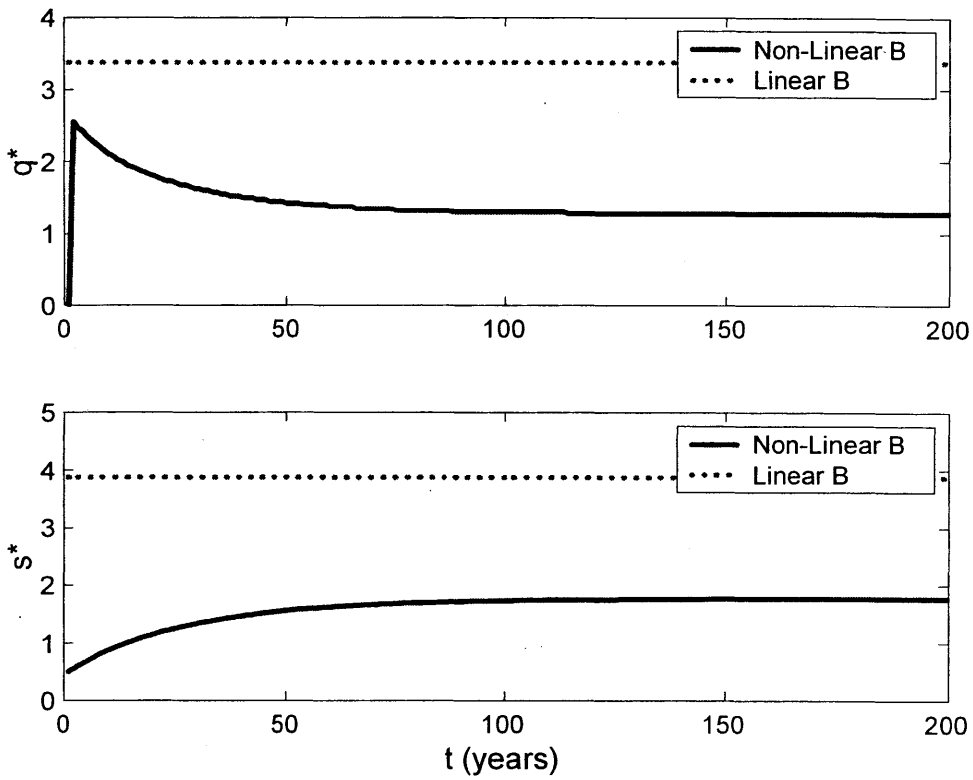

Figure 5-2: Optimal solution for non-linear benefit function.

about 2.25, then declines and asymptotically approaches 1.3. This produces a water table that increases smoothly from the steady-state depth to about $s^* = 2$ (40 m). Pumping is reduced from the linear benefit case since the value of increasing volumes of water decreases while the cost of supplying those additional volumes continues to increase.

5.3 Stochastic Discount Rate

In this section the analysis is extended to consider uncertainty in the exponential discount rate; both analytical and numerical solutions are developed.

5.3.1 Problem Description

This analysis is motivated by recent papers by Sozou [50], Weitzman [55, 56] and Azfar [1] indicating that uncertainty in the discount rate when using exponential discounting will naturally yield a discounting trajectory which declines slower in time than with a constant discount rate. The implication of this result is that if one is uncertain about future discount rates, then one should naturally use a non-constant discount rate that declines over time from the prevailing average discount rate. Equivalently, one could implement a hyperbolic discounting framework with a constant discount rate parameter.

5.3.2 Weitzman's Analytical Analysis

A summary of Weitzman's work [56] is given to clarify the problem and to facilitate comparison with the numerical results. To obtain his result, Weitzman surveyed over 2,000 economists and found a histogram of discount rates that is well fit by a gamma distribution; Figure 5-3. The gamma probability density function is given by,

$$f(x) = \frac{\beta^\alpha}{\Gamma(\alpha)} x^{\alpha-1} e^{-\beta x} \tag{5.4}$$

where α and β are estimated from the data using the following relations; Figure 5-3.

$$\alpha = \frac{\mu^2}{\sigma^2} \tag{5.5}$$

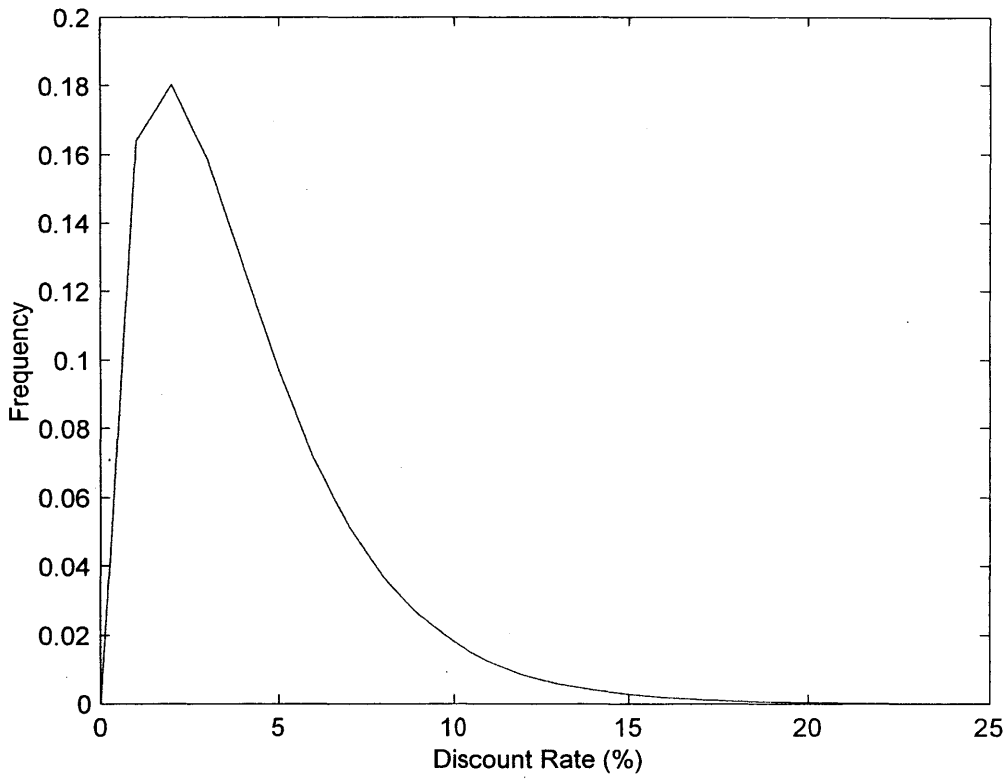

Figure 5-3: Gamma distribution of discount rates; $\mu = 0.04, \sigma = 0.03$.

$$\beta = \frac{\mu}{\sigma^2} \tag{5.6}$$

Following Weitzman's notation, μ is the mean discount rate and σ is the standard deviation. Define an *effective discount function*, $A(t)$, that is the exponential discount factor weighted by the probability of the discount rate:

$$A(t) = \int_0^\infty e^{-xt} f(x) dx \tag{5.7}$$

Given f(x) is gamma distributed, then A(t) reduces to,

$$A(t) = (\frac{\beta}{\beta + t})^\alpha \tag{5.8}$$

or, equivalently,

$$A(t) = \frac{1}{(1 + t\sigma^2/\mu)^{\mu^2/\sigma^2}} \tag{5.9}$$

The corresponding *effective discount rate* at any time t is

$$R(t) = \frac{\mu}{1 + t\sigma^2/\mu} \tag{5.10}$$

The bottom line is that uncertainty in your rate of discounting, assuming an exponential discounting scheme, will naturally give rise to an effective discount function which is hyperbolic in nature. Azfar and Sozou proceed along similar lines, using a hazard function to define an effective discount function, and go on to show that this naturally leads to a discount rate which declines with futurity.

5.3.3 Numerical Analysis of Stochastic Discount Rate

In the numerical model we use the same probability distribution of discount rate used by Weitzman, Figure 5-3. The numerical model generates N realizations, each with a different random discount rate chosen from the gamma distribution, and optimizes the expected benefit of **all** the realizations taken together. Each scenario is weighted equally in the objective function. All results presented are for exponential discounting with a stochastic discount rate. The goal is to compare the stochastic exponential solution to the deterministic hyperbolic solutions.

The optimal trajectories generated by different runs of the *same* model are similar but do differ slightly. This merely reflects the randomness in choosing r for each realization, and this difference between simulations becomes smaller the more realizations are included *in each* simulation. The more scenarios done, the more fully is the true gamma distribution being represented. Conversely, if one only tries to optimize a few realizations, then the result is highly affected by low probability discount rates that may be chosen. One hundred realizations seems to yield sufficiently stable solutions between simulations and is the number of realizations used in all results discussed below.

5.3.4 Results

Sensitivity to σ

Adding a stochastic discount rate does indeed produce an optimal solution which is hyperbolic in nature. As the uncertainty in the discount rate decreases, smaller σ, the optimal decision trajectory approaches that of deterministic exponential discounting using the expected value ($\mu = 0.04$); Figure 5-4. This merely verifies Weitzman's results.

Comparison with Hyperbolic Models

The stochastic exponential solutions are now compared to both the one and two parameter hyperbolic discounting weights.

$$\mathcal{D}(t) = \frac{1}{(1+bt)^2} \tag{5.11}$$

$$\mathcal{D}(t) = (\frac{1}{1+bt})^a \tag{5.12}$$

The second formulation corresponds to Weitzman's solution with $a = \frac{\mu^2}{\sigma^2}$ and $b = \frac{\sigma^2}{\mu}$. Obviously, if μ is equal to $\sqrt{2}\sigma$ then this formulation reduces to the one parameter formulation model with $b = \sigma/\sqrt{2}$. Figure 5-5 plots the optimal trajectories for the stochastic exponential model with $\mu = 0.04$ and $\sigma = 0.03$; plotted for comparison is the deterministic exponential model, the two parameter hyperbolic model, and the one parameter hyperbolic model. As expected, the stochastic exponential solution is equal to using the two parameter model with the corresponding mean and standard deviation. They are not the same at early times due to the

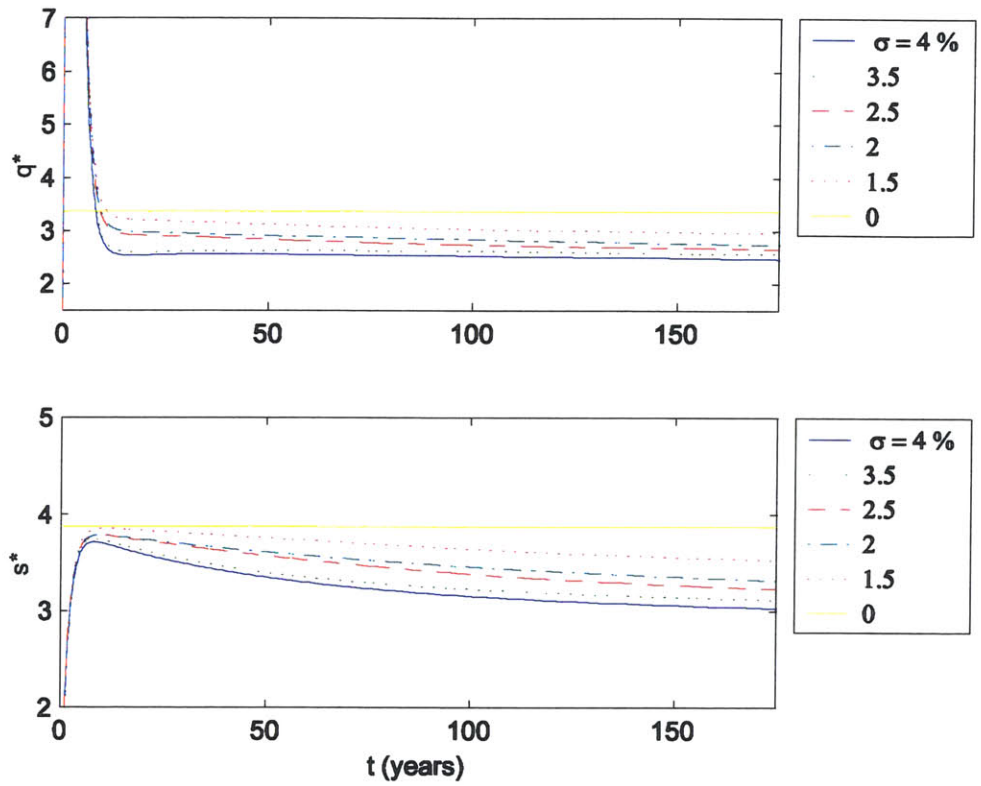

Figure 5-4: Stochastic results for various standard deviations (σ) of the discount rate distribution. Note that the numerical model exhibits a spike of pumping over about 10 years rather than the Dirac delta at t = ϵ for the analytical solution.

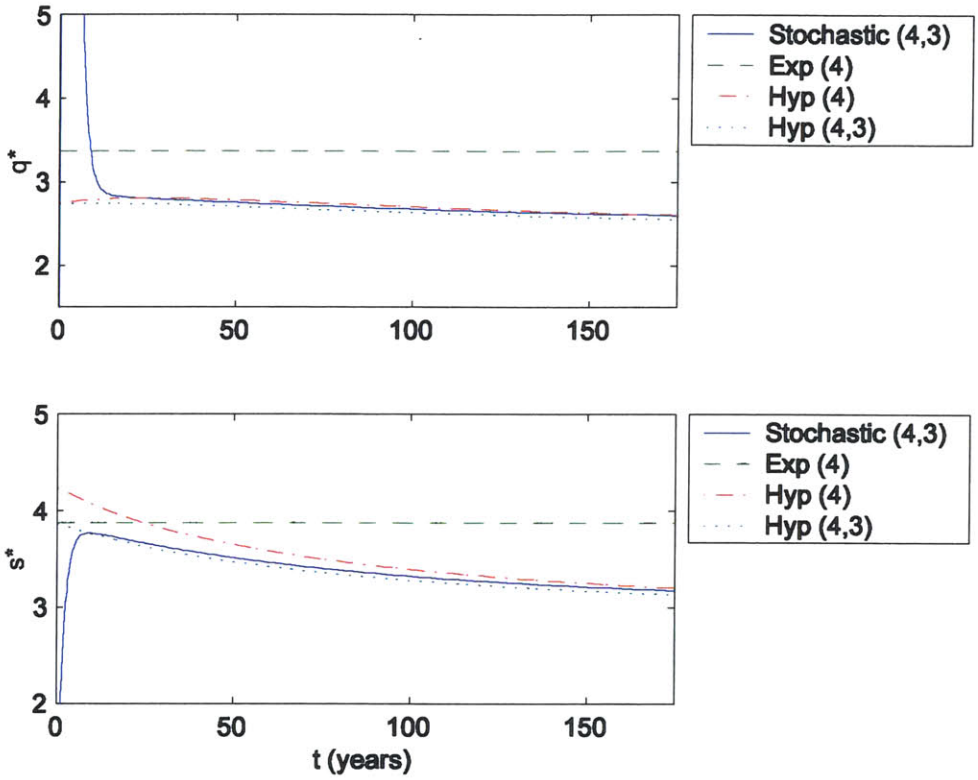

Figure 5-5: Comparison of the stochastic exponential solution, deterministic exponential solution, one parameter hyperbolic solution, and the two parameter hyperbolic solution. The μ and σ values (%) are shown in parentheses.

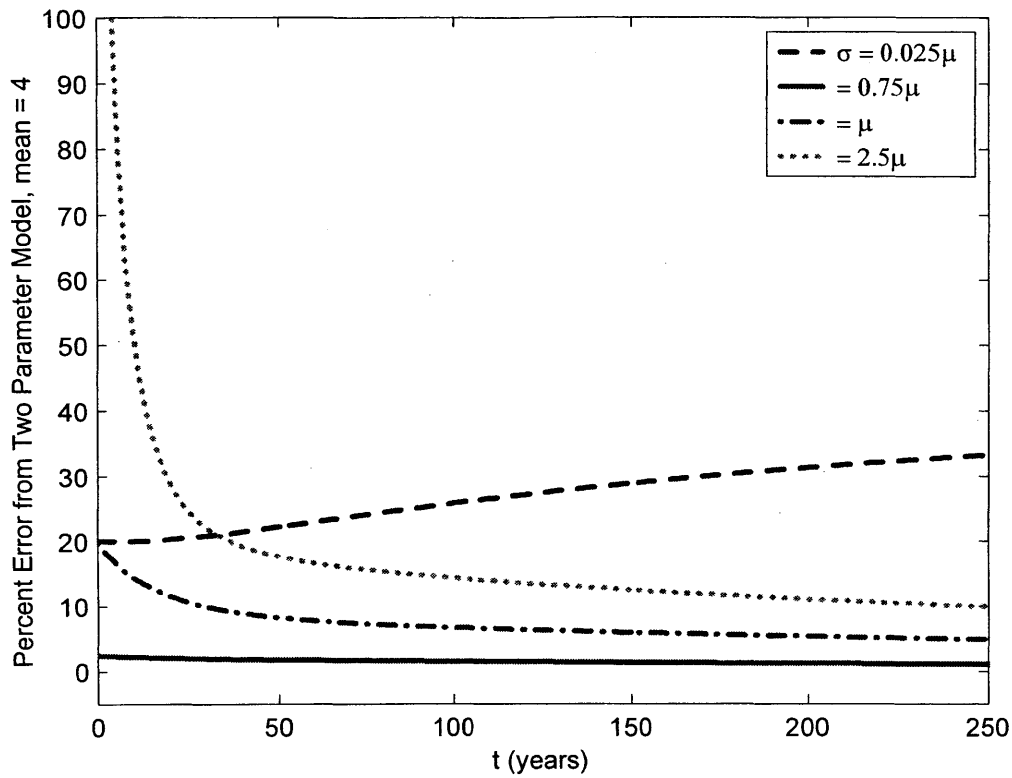

Figure 5-6: Percent difference/error of the one parameter hyperbolic model compared to the two parameter model for a given mean and various standard deviation values (shown as percent deviation from the mean).

inability of the numerical model to capture the Dirac delta.[2]

The one parameter hyperbolic model using the mean discount matches the two-parameter model fairly well, especially at later times. Plotted in Figure 5-6 is how badly the one parameter model does in fitting the two parameter model with various σ values. The one parameter model is taken to have the parameter b equal to the average discount rate. Interestingly, the one parameter model performs poorly if the discount rate is known with great certainty or if it's known with little certainty. However, it does very well if your uncertainty, σ, is approximately equal to the expected value, μ.

[2]The fact that they do not lie exactly on each other after the Dirac delta is due to (1) the finite number of realizations run and (2) numerical error.

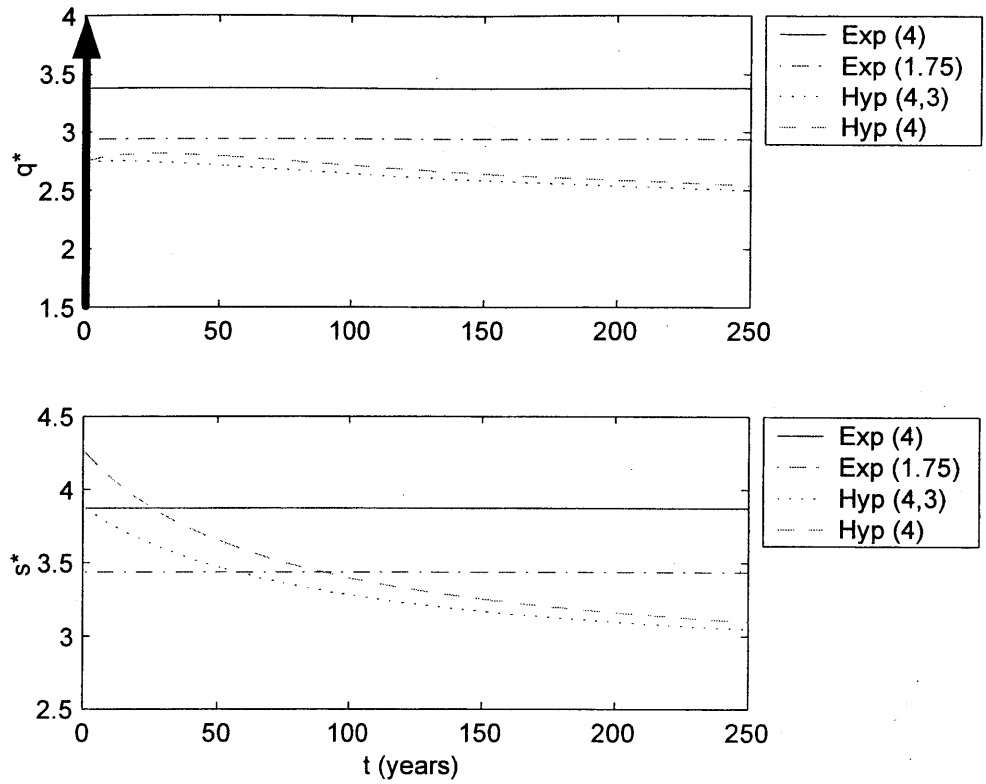

Figure 5-7: Optimal decision trajectory for constant equivalent solution; plotted against the other formulations.

Comparison to a Constant-Equivalent Discount Rate

Weitzman states that "if one were forced here to choose a single constant-equivalent discount rate $\bar{r}$ " [56], *assuming an exponential formulation*, then it would be given by:

$$\bar{r} = \frac{1}{\int_0^\infty A(t)dt} \tag{5.13}$$

$$\bar{r} = \frac{(\mu - \sigma)(\mu + \sigma)}{\mu} \tag{5.14}$$

Using this constant-equivalent discount rate, in this case $r = 0.0175$, simply yields an exponential decision trajectory which is more conservative; Figure 5-7. However, if one is unsure of future discount rates this constant-equivalent rate may not be the best alternative.

First of all, it will yield less profit in the short term than using hyperbolic discounting.

Using the constant equivalent discount rate of 0.0175 would mean about a 15% loss in initial benefit over the other three formulations.

Secondly, it is just as easy to implement the hyperbolic discounting function. If one is forced to pick one number, using the mean discount rate in the one parameter hyperbolic model, especially if one suspects $\sigma \approx \mu$, may be a better alternative than the potentially detrimental short-term changes Weitzman's constant-equivalent discount rate would entail[3].

[3]The only time the constant-equivalent model could be useful is if for some reason the optimization problem could not be solved with the hyperbolic discounting function. However, if not possible analytically, it should almost always be possible using a numerical model.

Chapter 6

Conclusions for Part I

6.1 Deterministic model conclusions

It was found that the optimal pumping trajectory and depth to the water table is dependent on time for any solutions with a hyperbolic discounting function. Depending on the leakage rate, this may lead to unusual periods of peak pumping in the near to mid-future. The solutions asymptotically approach the no-discounting or Green Golden Rule solution in the very far future. If the discount rate is constant, which can only be the case for an exponential discounting formulation, the optimal decision trajectory will also be constant in time. No other discounting formulation can have a solution independent of time.

There is a period of groundwater mining or reduction in resource stock which occurs initially. This is true for both discounting formulations tested. For the analytical solutions this manifests itself as a Dirac delta of instantaneous pumping at time $t = \epsilon$, which brings the system from its initial condition to the optimal trajectory. In reality however, this period of stock reduction would occur over a period of time dependent on the system physics and economics.

Interestingly, the optimal decision trajectories are not that sensitive to the non-dimensional discount rate, ρ. For the groundwater mining problem the degree of pumping varies at most by a factor of 2 for the exponential discounting case, and by most a factor of 1.25 for the hyperbolic case. However, it should be noted that a factor of 2 could be a significant difference for some water resource systems. The salinization problem solutions vary at most by a factor of 1.4

for the exponential formulation and by most 1.08 for the hyperbolic formulation. Both the groundwater mining problem and the salinization problem are more sensitive in the discount rate to the exponential formulation than to the hyperbolic formulation. The salinization problem's sensitivity to discount rate is dependent on the quality of the incoming water and the maximum allowable contaminant concentration.

As a management decison tool, a plot of Hyperbolic Takeover Time (HTT) may be constructed to determine how long it will take for the hyperbolic solution to yield a rate of non-discounted benefit equal to or larger than the exponential discounting solution. This plot is based on a non-dimensional ratio of economic to physical times scales, and as such gives an idea of the time frame until hyperbolic discounting will yield significantly different solutions from the exponential discounting formulation.

6.2 Stochastic discount rate conclusions

Weitzman's analytical results were verified numerically with a real physical model. Uncertainty in the discount rate does lead to optimal trajectories which are hyperbolic in nature. The one parameter hyperbolic model with $\mathcal{D}(t) = \frac{1}{(1+bt)^2}$ produces optimal trajectories which are very close to those generated by the two parameter model, $\mathcal{D}(t) = (\frac{1}{1+bt})^a$, with a and b as defined by Weitzman's analysis. Therefore, just using a one-parameter hyperbolic model with the mean discount rate would yield optimal decision trajectories near trajectories generated with a full stochastic analysis.

If one is forced to choose one discounting parameter, using hyperbolic discounting may be a better alternative than Weitzman's constant-equivalent discount rate. The constant-equivalent discount rate could severely affect short-term benefits.

6.3 General Conclusions

This study does not, nor did it expect to, prove that one method of discounting the future is "better" than another. The decision to use exponential or hyperbolic discounting depends on how the decision maker values the future. However, as outlined in Chapter 2, there are reasons to use one or the other. For instance, a descriptive arguement is that empirical studies indicate

humans act hyperbolically. Normatively, which discounting function one chooses is dependent on the temporal preferences and accompaning axioms one accepts. Neither is right or wrong, they are just different.

What this study does present is how one's decision strategy may change depending on which method of discounting one chooses. The discount rate itself doesn't appear to affect optimal strategies dramatically, but the discount factor may. It ultimately becomes the choice of the decision maker(s) to determine which type of long-term management strategy, and accompanying future valuation, meets the project's goals. This will often manifest itself as a socio-political decision.

6.4 Summary of original contributions

1. A general framework was developed in which to optimize simple water resource systems under various forms of discounting.

2. Analytical solutions were generated and used to critically examine the effects of discounting on a groundwater mining problem and a dryland salinization problem.

3. A numerical model was developed to further test the effects of discounting on water resource management problems that aren't amenable to analytical solution. The numerical model is used to test for sensitivity to uncertainty in the discount rate.

6.5 Recommendations for future research

- Application of these methods to more complex water resource systems with varying time-scales of system response and various economic constraints.

- Statistical work on the range of time-scales of response for typical water systems we find in nature.

- More investigation into how the time-scale of the movement of fluid in a system compares to the time-scales of contaminant movement (i.e. dispersion/diffusion), and how that affects optimizaton under alternative discounting formulations.

- Take a serious look at how alternative discounting formulations such as hyperbolic discounting could be used to meet sustainability goals. What are the mathematical, philosophical, and socio-political implications? Do they have a place in modern management studies and strategies?

Part II

Long-term management of water resources at Kuki'o, Hawai'i

Chapter 7

Introduction

Due to population growth in the islands, Hawai'i has been faced with rapidly increasing water demand on relatively small islands with finite resources. Water issues are constantly in the news, and developers are faced with the need not only to better manage resources in-house, but also to start cooperating with neighbors to insure water resource availability in their respective regions. As such, private and public agencies alike are beginning to take a fresh look at how to more sustainably manage the islands' very unique water systems. The physical and economic parameters defining these systems make for very good case studies of long-term water resource management.

In this study a hydrologic-economic model is formulated to investigate sustainable management strategies for dual coastal and high-level aquifer island systems. The optimization framework developed for the physical system is flexible enough to be applied to any aquifer system with a basal lens and inland high-level water body connected through a leaky barrier. The economic framework is also fairly flexible with general equations and constraints dealing with energy costs, desalinization costs, capital costs, and consumer demand curves. The hydrologic-economic model developed is applied to the Kuki'o region on the island of Hawai'i as a case study and test of the methods.

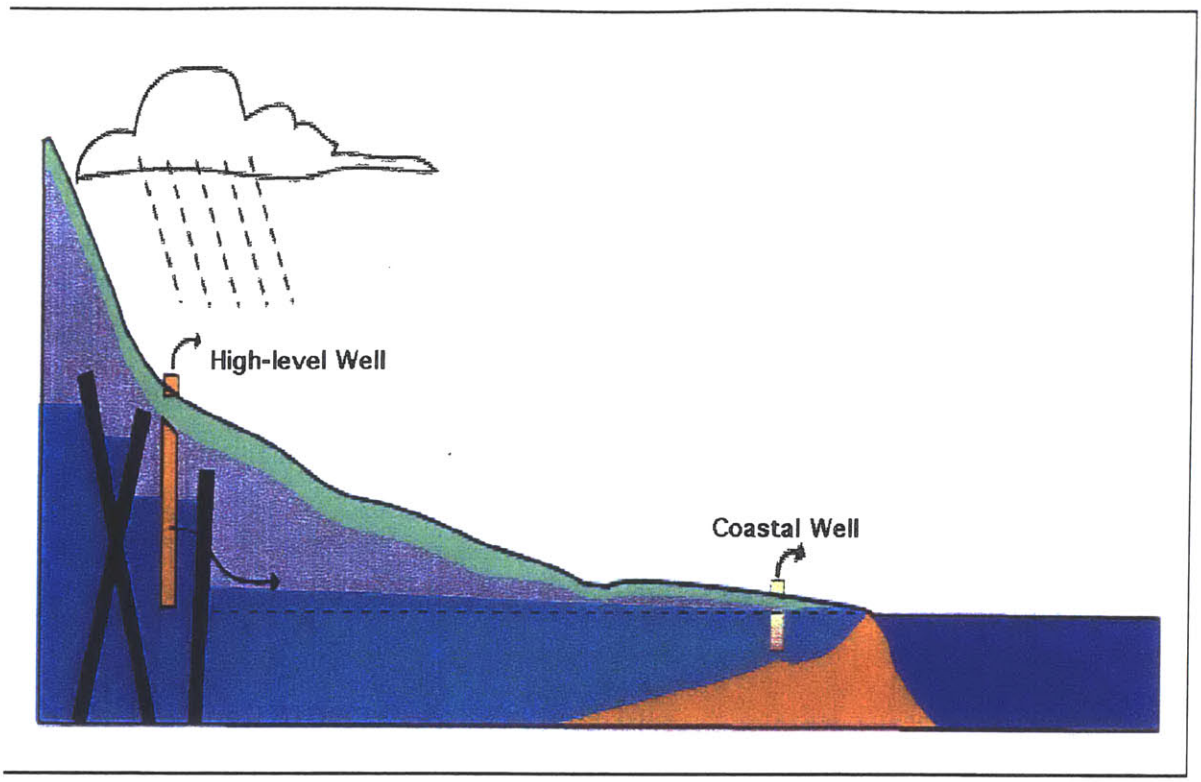

Figure 7-1: Cartoon of typical high-level and coastal aquifer in Hawai'i (not to scale). Note upconing/intrusion at coastal well.

7.1 Coastal Basal Lens

Almost every coastline in Hawai'i exhibits some form of a basal or Ghyben-Herzberg lens. This is simply the result of less-dense freshwater floating on the denser seawater as it makes it's way from inland to the sea and discharges into the ocean. The lens is recharged primarily in the wetter uplands on most islands, and may have a fairly sharp or broad transition zone depending on the region's geology and resultant hydraulics. Water resource managers in Hawai'i have typically tapped this resource with skimming wells that extend to about sea-level and capture the freshwater on its way to the sea. However, overpumping of this resource can lead to the related phenomena of saltwater upconing and saltwater instrusion.

7.1.1 Saltwater Upconing

Saltwater upconing occurs due to pumping of the less-dense freshwater. This pumping will begin to draw the transition zone and underlying saltwater towards the low-potential pump intake, hence reducing the water's quality. The resultant flow system resembles a cone rising. The extent and characteristics of this cone depends on pumping rate and the area geology. In the very hydraulically conductive aquifers of Hawai'i, especially in areas such as our field site, the cone is thought to be very broad and thin.

Saltwater upconing has been a common problem in Hawai'i and in coastal regions worldwide, and striking a balance between quantity and quality in such regions has always been a challenge. In some geologic environs where there are fairly impermeable clayey layers, inducing critical upconing conditions could adversely affect an area's water quality for a significant amount of time [3]. In highly permeable regions such as most of Hawai'i it is thought that the aquifer can recover in a much shorter period of time.

7.1.2 Saltwater Intrusion

Closely related is the concept of saltwater intrusion. Whatever freshwater a well takes from the freshwater lens takes away from the ambient flow to the sea. This decrease in flow results in a decrease in inland hydraulic head. Therefore, seawater may intrude further inland. An area's geology, hence hydraulic conductivity (K) values, strongly influences the degree of saltwater intrusion.

In many cases it may be hard to distinguish whether saltwater intrusion or saltwater upconing is contaminating a well, and indeed the two often go hand-in-hand. However, near the coast it's likely that pumping will quickly pull in seawater hence causing saltwater intrusion, while inland well contamination is likely due to upconing from the underlying lens. At medium distances, which tend to be brackish water, the dominance of one or the other is debatable and depends on variables such as geology, tides, and pumping characteristics.

7.1.3 Engineering Solutions to Coastal Salinization Phenomena

Though a definite problem in the islands, there are a number of alternatives to limit the effects of upconing and saltwater intrusion.

1. Spread the demand over more wells that pump at lower rates and that are separated from each other hydraulically.

2. Desalinization water treatment plants.

3. Supply most demand with inland high-level wells.

4. Limit saltwater intrusion with coastal injection wells.

5. Devise optimal control schedules for coastal wells such that upconing in minimized.

All of these options, except number 4, will be discussed in this study. Limiting intrusion with injection wells is an infeasible solution in Hawai'i due to the prohibitive costs of drilling in volcanic rock, the lack of excess water to inject, and the possible effects on sensitive reef species.

7.2 High-level Aquifers in Hawai'i

The other primary groundwater source in Hawai'i is so-called high-level aquifers. These aquifers are termed high-level because the geology of inland volcanoes often traps upland recharge so that the water table is significantly higher than it is in the coastal basal lens. The dike complexes in many volcanoes will often impound water in compartments that may resemble leaky buckets. Faults are also known to impede flow and cause a build-up of hydraulic head.

Though a potentially huge source of very good water, high-level aquifers are not without their drawbacks. The primary problem is getting to the water. Though the water is "high-level", the mountains in Hawai'i are often steep enough that wells would have to be drilled thousands of feet to reach these aquifers. Therefore, potential sources that are far inland or far upslope are either in inaccessible areas, too expensive to drill and transport, or taxing the limits of drilling rigs and/or pumping equipment as they exist in Hawai'i now.

7.3 Need for an Integrated Framework

The two aquifer systems are connected hydraulically, and hence economically, by leakage from the high-level aquifer to the coastal aquifer. This occurs through the leaky hydraulic barrier

that separates the two. As mentioned earlier, exactly what type of geologic structure this would be is debatable. However, it is mostly likely either a fault or dike structure.

Though long-term projected demand numbers for the islands could not be found, it is well known in the development community that water is a primary limiting factor for development on the leeward side of the islands (various personal communication). So as Hawai'i moves into the 21st century, and as development projects are becoming increasingly large-scale and long-term, there is a need to look at managing these two sources of water jointly, and the economics of tapping these resources needs to be considered along with the physics. The study described herein attempts to combine the relavent physics of coastal and high-level aquifers with the crucial economic and environmental constraints. Following in the spirit of Part 1, emphasis will be on long-term management strategies.

7.4 Research Issues

1. How to optimally manage a dual-aquifer coastal and high-level system. Do we use one or the other, or a combination of both? If both, how so?

2. Assess the importance of the leaky barrier separating the two aquifer systems.

3. Analyze the economics of desalinization plants in coastal regions.

4. Look at the effects of alternative discounting schemes on long-term optimal pumping strategies.

5. Critically examine the effects of user demand economics on the solution. Specifically, how does the demand curve and associated water elasticities reflect on optimal decision trajectories.

Chapter 8

Kuki'o Study Area

8.1 General Description

The Kuki'o study area is located on lands being developed by WB Kuki'o Resorts, LLC. Kuki'o is situated along the North Kona coast of the island of Hawai'i, Figure 8-1. This soon-to-be luxury community sits on 650 acres and will support an 18-hole golf course, a 10-hole golf course, custom home lots, and pre-designed home complexes. The lands of Kuki'o extend from the seashore inland about 2 miles to the 600 foot topographic contour and are part of the larger Ka'upulehu district. The properties immediately north of Kuki'o are also under construction for luxury communities. The State of Hawai'i owns the lands to the south, while Kuki'o's mauka[1] neighbor is the Kamehameha Schools private land trust. In an attempt to develop the district water resources sustainably, Kuki'o and Kamehameha Schools have been working with Waimea Water Services, Inc. to study the available groundwater resources. As part of this effort, they have graciously allowed the use of their wells and all pertinent data for this case study.

[1] *Mauka* is a Hawaiian word meaning "upland direction; towards the mountain; inland side". It's opposite is *makai*, meaning "seaward direction; towards the seashore; by the beach/ocean". These are convenient directionals for an island locale and are sometimes used in this manuscript.

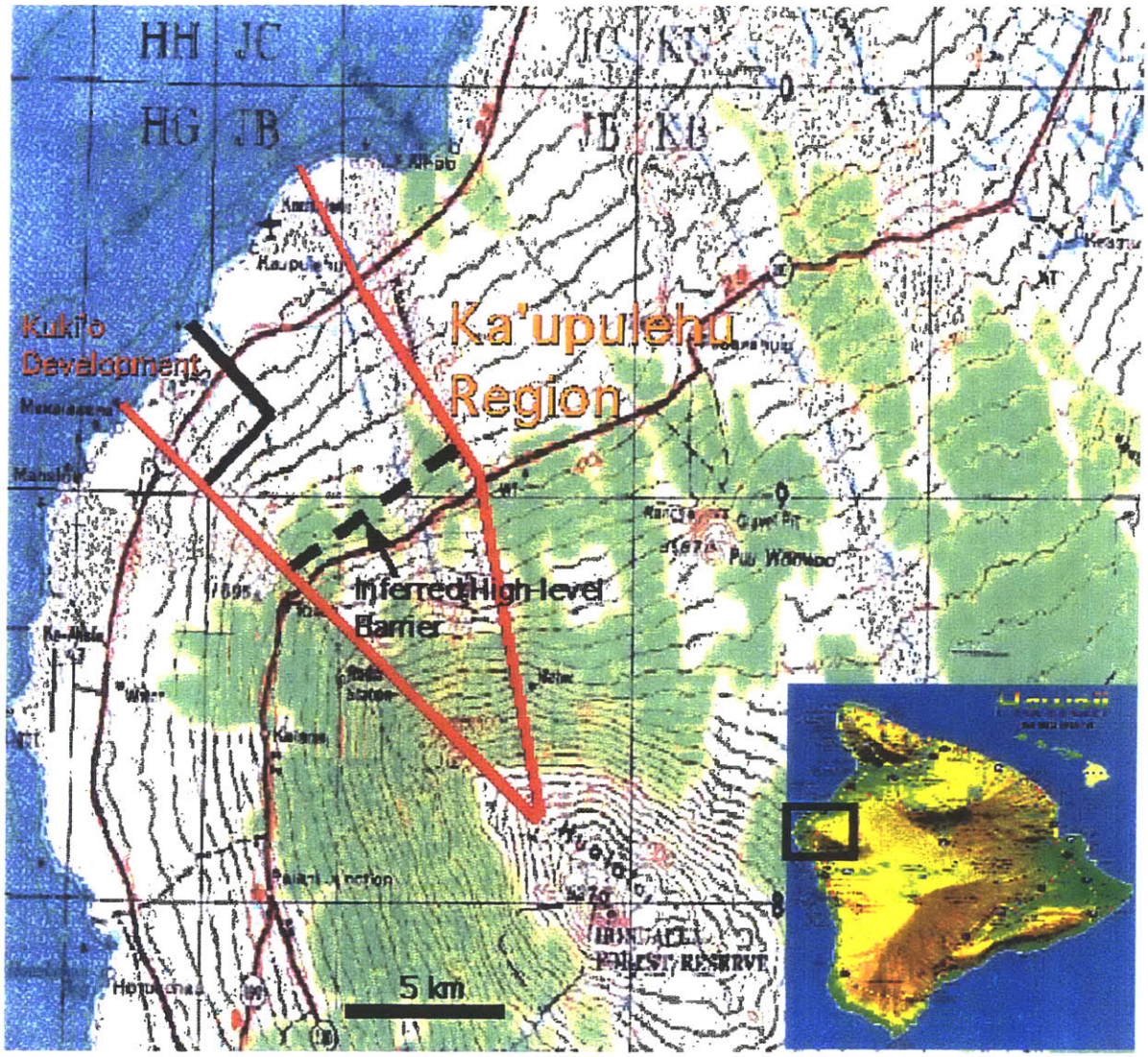

Figure 8-1: Map of the study area.

8.2 History

Native Hawaiians lived in the makai part of Kuki'o until the early part of this century. Descendents of Kuki'o's original inhabitants still visit the area for cultural reasons and were involved in some of the development planning near the ocean. The makai portion is dotted with numerous brackish water ponds that were once used by Hawaiians to raise fish and 'opae[2] for sustenance. The middle elevations were likely uninhabited, being mostly barren lava, but were probably traveled upon by Hawaiians to visit others living in the lush uplands or to collect birds, pigs, and upland trees for canoes. Kuki'o would have also been a ideal resting place for Hawaiians traveling up and down the coast from larger settlements to the north and south.

8.3 Geology and Soils

Kuki'o consists primarily of fairly young basaltic lavas from Hualalai volcano, and the site is actually located on or very near the northwest rift zone of Hualalai. There is very little to no soil cover over most of the lands, with most of the area being barren 'a'a and pahoehoe lava rock. There is a large volcanic cinder cone located on Kuki'o lands, with about 2 acres covered with mostly cinder.

At depth one encounters a typical Hawaiian volcanic sequence of alternating pahoehoe and 'a'a layers, which consists of highly permeable clinker layers and somewhat less permeable cracked 'a'a cores. Clinker is the chaotic, brittle, very permeable lava rock that forms on top of lava as it is flowing; the hard cores form beneath the flow surface where slower, less chaotic cooling can occur. These layers can range from a few centimeters to tens of meters thick, but road cuts at the site indicate an average thickness near 1 meter. As is also common in young volcanic terrain, and as exhibited by road cuts and drilling, there are lava tubes throughout the subsurface; Figure 8-2. Some of these lava tubes are large enough for a man to stand upright in. Given all these geologic conditions, the aquifer underlying Kuki'o is extremely permeable and heterogeneous.

Within the rift zone and in mauka areas there may be subsurface barriers to groundwater flow caused by volcanic intrusions such as dikes or by faults. Due to a lack of observation wells

[2] Brackish water shrimp.

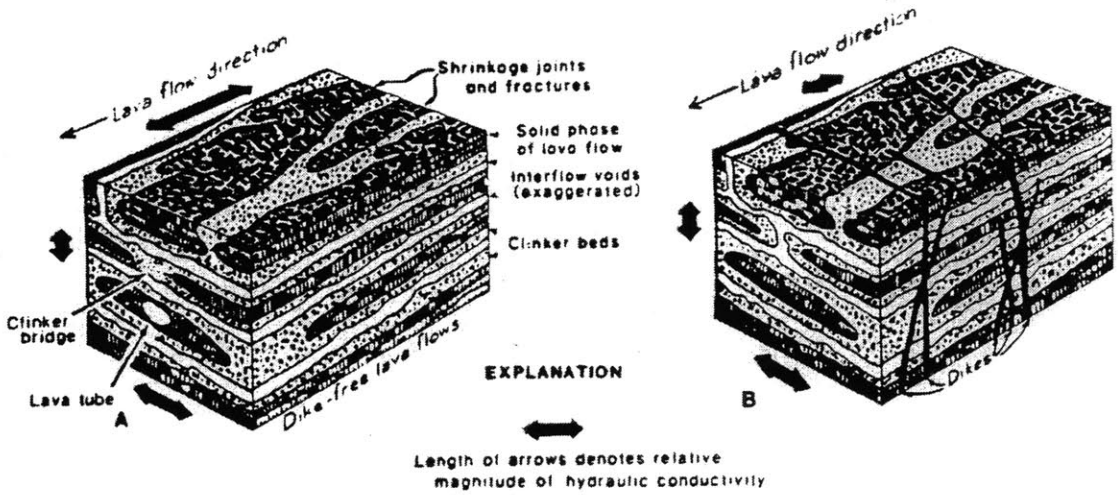

Figure 8-2: Cross section of a typical young Hawaiian volcano showing lava tubes, clinker layers, dense cores, and dikes [24].

the existence of these features in the area is not well documented, but are known to exist on the south, southwest flank of Hualalai. These barriers to flow can significantly alter a regions groundwater hydrology and resultant water management decisions.

8.4 Water Resources

8.4.1 Surface Water

Surface water sources are non-existent in the area. The only water bodies are the brackish water ponds near the ocean, which are really exposed pieces of the coastal basal lens.

8.4.2 Precipitation, Evapotranspiration, and Net Recharge

Kuki'o is located on the leeward side of the island and receives very little rainfall from the moist tradewinds that hit the very wet windward coast of Hawai'i. The predominant wind pattern and most precipitation on the leeward side is from convective processes due to daily heating and cooling of a land surface near the relatively thermally stable ocean. Most precipitation occurs in the late afternoons and evenings, and primarily falls at higher elevations (305-1525 meters);

Figure 8-3. As a result Kuki'o and most of the northwest corner of Hawai'i are relatively dry compared to the rest of the island. Kuki'o makai averages less than 10 inches per year [36]. However, the presence or lack of winter storms can greatly affect the yearly rainfall total.

Due to windy conditions and the region's high temperatures (70 - 85 degrees), evaporation is very high. Except during winter storm showers, most of the area's very light rains are immediately consumed by existing vegetation or evaporated immediately. Water budget tests conducted on golf course irrigation systems at Kuki'o indicate an evapotranspiration rate of about 0.66 cm per day (0.26" per day); which is obviously more than the average daily rainfall (Steve Bowles, WWS Inc., oral communication).

Recharge to the coastal basal lens is therefore primarily due to rainfall and fog drip in the middle and upper elevations that infiltrates the subsurface and flows towards the coast. Maps of average net recharge with and without fog drip are shown in Figure 8-3.

8.4.3 Groundwater

Groundwater is basically the only source of brackish and freshwater in the area. The sources of groundwater may be conveniently divided into two types: high-level groundwater in the uplands and coastal basal lens water. Though high-level groundwater is almost always fresh, coastal basal lens water may be brackish or fresh depending on conditions.

In the Kuki'o area, only one well (HR-5) is known to be in high-level conditions. HR-5 is located within the rift zone of Hualalai and exhibits water levels of 7 m (23 feet), which is about 3 times higher than nearby wells which are at the same elevation. All of Kuki'o's other wells are considered to be part of the coastal basal lens. The existence of high-level water at higher elevations is likely but has not yet been explored due to prohibitive costs. However, the populous Kona district immediately south of Kuki'o gets almost all of its freshwater from a number of very successful high-level wells.

The coastal lens displays a very thick transition zone with brackish water extending at least to the 183 m (600') contour which is about 3 km inland. The KI wells analyzed in this study are at the 183 m contour and exhibit heads of only about 0.3 m relative to mean sea level (MSL). Wells at the 457 m (1500') contour are fairly fresh and exhibit heads in the 2 m range. The direction of groundwater flow in the area has not been extensively studied, but based on head

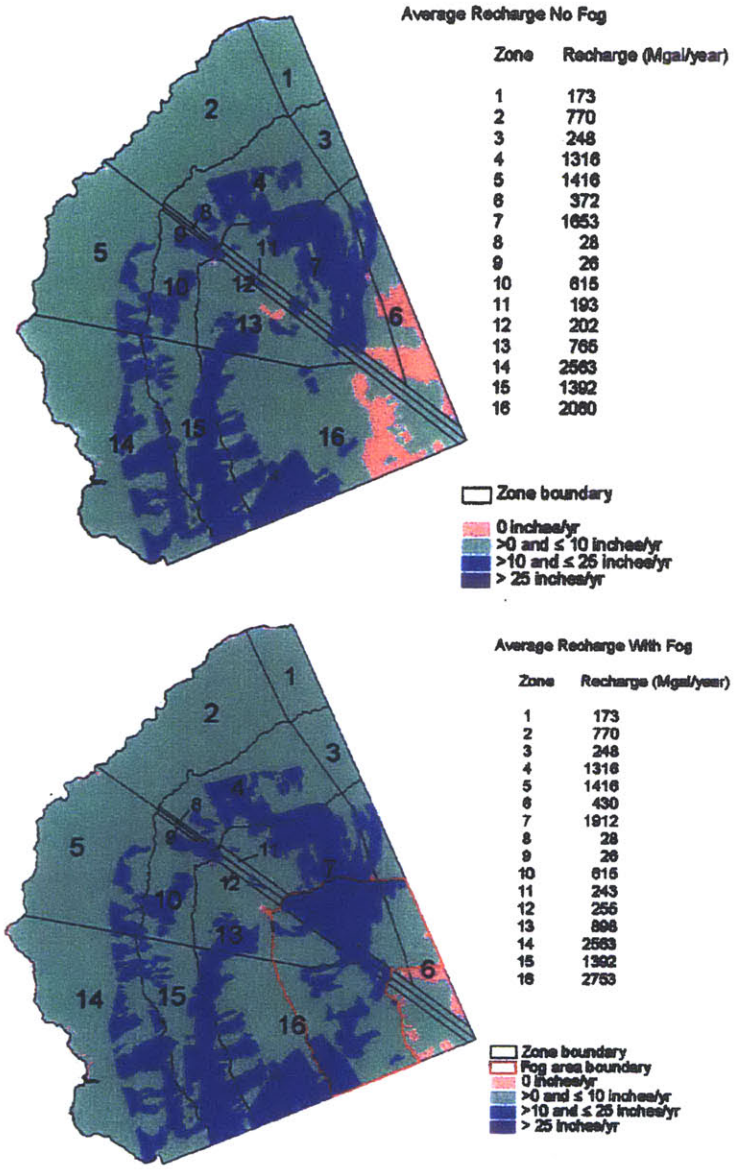

Figure 8-3: **Recharge with and without fog drip for the northwest riftzone of Hualalai (prepared by WWS, Inc.).**

	Projected Water Use (GPD)	Projected Water Use (m^3/day)
Potable Water	992,550	3757
Non-Potable Water	1,764,260	6678

Table 8.1: Summary of water demand for Kuki'o Project; estimated post-construction

gradients between wells appears to flow in the south-west direction. This is slightly southward from a straight line drawn from the mountain top to the ocean for the Ka'upulehu area.

8.5 Water Demands

There are two types of water demand for Kuki'o: non-potable irrigation water and potable water. The non-potable (brackish) water will be used primarily for golf course grasses and landscaping with salt-tolerant species. Potable water is for the residential uses and salt-sensitive landscaping uses. Table 8.1 summarizes expected demand (Memorandum, PBR Hawaii). This amounts to a total projected demand of over $1x10^4$ m^3/d ($3.8x10^6$ m^3/yr) of mixed potable and non-potable water for the Kuki'o project. This demand is projected to become a reality as soon as construction is finished is the next few years. [See A-2 and A-3 for a more detailed list of water demand]

Though Kuki'o's immediate water demands are important, the regional management model considered in this study is also concerned with determining sustainable supply for the Ka'upulehu region in general. In other words, "Just how much demand can the aquifers of Kuki'o/Ka'upulehu support in the long-term?". When I refer to the Ka'upulehu region for this study I am referring to recharge Areas 2, 4, and 7 as shown in Figure 8-3; or see Figure 8-1. The Kuki'o development project primarily occupies the southern half of Area 2. It should be noted that parts of Areas 2 and 4 are occupied by other developments. The final results will concern long-term management strategies for all of the Ka'upulehu region, and Kuki'o is used as a representative 2-D slice to test the model and to investigate the resultant water management implications.

8.6 Available Supply

8.6.1 Freshwater

There are three potential sources of freshwater for Kuki'o. The first is the fresh inland coastal wells. The second is desalting brackish water from the KI wells with the RO (reverse osmosis) water treatment plant currently under construction. The third is a possible high-level well.

It should be noted that pumping from fresher inland coastal wells would draw water from any lower elevation brackish wells that are down-gradient. In effect, it is advisable to determine the optimal location to develop a coastal well field and optimize water management for that well field alone. In this study we assume that the brackish water KI wells are the well field to be optimized since there is data available, and because these types of brackish water well fields are an increasing reality for coastal water managers and beg more study.

How much supply there is to sustainably meet demand will be deduced later with the model, but it is reasonable to present the total recharge in the demand area as an upper-bound/maximum **long-term** pumping rate. From Area's 2 and 4 (coastal) and Area 7 (high-level) in Figure 8-3 we determine this to be about 1.5×10^7 m^3/yr. This is about 4 times the projected demand of 3.8×10^4 m^3/yr (1×10^4 m^3/d).

8.6.2 Brackish water

Brackish water is to be supplied from the KI wells analyzed in this study and from the Maniniowali well currently under construction. It is thought that the KI wells will be able to sustainably supply 4921 m^3/d (1.3 MGD) and Maniniowali 2839 m^3/d (750,000 GPD), (Waimea Water Services, Inc., personnal communication). This prediction will be assessed in the next chapter.

8.6.3 Supply Issues and Tradeoffs

There are numerous supply issues to be considered in the management decision and optimization model. There are physical and economic factors which will affect any long-term management decisions. The primary decision will be between developing only coastal wells, only high-level wells, or a mixture of the two. The pros and cons of each source are summarized in the Table 8.2, and will be explored at length with the dual-aquifer model developed for the study.

	Coastal Well	**High-level Well**
Lift Costs	Moderate	High
Transmission Cost	Low	High
Treatment Costs	High	Low

Table 8.2: Pros and Cons of coastal versus high-level wells

Chapter 9

Coastal Well Experiments and Results

9.1 Introduction

This chapter focuses on the coastal basal lens portion of the study area. Due to a lack of data on the area's basal lens, we undertook a series of pumping experiments at Kuki'o. It was first thought to use existing analytical solutions for basal lens upconing and saltwater intrusion, but what little data exists seems to indicate that Hawaii's unique hydrogeological environment is not very amenable to these relatively simple solutions. It would be too unrealistic to use such equations in the hydrologic-economic optimization model. On the other hand, attempting to develop a good numerical model of the system would be an enormous task in and of itself, and depart from the primary focus of this dissertation.

As a result, we attempted to use direct field data to derive empirical equations of aquifer response. These empirical state equations may be used with more confidence in the optimization model, and are also much easier to implement in an optimization model than a coupled dual-density, numerical model. The empirical state equations generated are specific to Kuki'o, but it is thought that the general management guidelines produced will be broadly applicable; especially in the Hawaiian islands or geologically similar locations.

However, it was found that even pumping at the maximum rate did not induce critical

upconing conditions. It appears that a new sustainable equilibrium is reached. There may be a long-term trend to critical conditions if the wells are not managed correctly, but the experiments conducted did not capture such long-term effects. In addition, the effect of pumping the high-level aquifer on the coastal well could not be determined with these experiments. Even though the results are valuable for numerical model calibration and for optimal management of the KI wells on short time-scales, these results could not be incorporated into the regional, long-term model. Nonetheless, the on-site knowledge gained from the experiments do serve to guide the model formulation.

9.2 Research Questions

The primary goal of the pumping tests was to assess the response of the basal lens salinity to pumping. Both the rise and fall in salinity with time are observed. The interdependence of nearby wells and the head responses are also monitored. The key research topics are listed below:

1. Salinity rise with pumping
2. Rebound in freshness when a pump is turned off
3. Head response to pumping
4. Effect of pumping on salinity and head at nearby wells
5. Time scale of aquifer response to perturbations

9.3 Experimental Set-up

9.3.1 Site specifics

The three irrigation wells tested are on the mauka boundary of Kuki'o's property; see Figure ?? for exact locations. The wells are spaced at about 457 m (1500 ft) from each other. KI-1 was built first and is the southernmost well. This well is the focus of our study. KI-2 is the northernmost, and KI-3 is in the middle of the other two. The well field is located on the flanks

Figure 9-1: KI3 well site showing pipelines and pump.

of the large cinder cone located on Kuki'o property. The surface geology is of very permeable cinder and/or 'a'a. There is also a large storage reservoir located between KI-1 and KI-3 which is used to store water from the KI wells. Water is transported to the reservoir via 20.32 cm (8") pipes and then tranported to standpipes or landscaping systems from the reservoir also using 8 inch pipe.

9.3.2 Wells and Pumps

The KI wells are all brackish water wells, Figure 9-1. Their primary role is to provide brackish water for use on the salt tolerant grasses being used for much of Kuki'o's golf course. Some water will also be desalinized or mixed with fresher water to produce a water of sufficient quality to be used for non-salt tolerant plant species. All three KI wells are located at around the 183 m (600 foot) elevation contour and are drilled to about 6.1 m (20 ft) below sea level. The

125 HP U.S. Motors' Pumps are set at sea-level. As-built well pump sections are located in A-1. These pump motors are of fixed running capacity, and any decrease or increase in pumping rate is done through opening or closing the outlet valve. In normal operating mode, fully open, these pumps generate about 2.02 m^3/min (540 GPM) depending on elevation and pipeline pressures.

9.3.3 Measuring hydraulic head

Hydraulic head measurements were made via a bubbler level monitor system supplied by Digital Control Corporation [1], Figure 9-2. The bubbler system works by pumping air into a tube which extends from the surface to below the water table. The pressure required to force air through the tube is proportional to depth of water. Luckily, airlines were already installed on all three KI wells. KI-1 also had a 3.81 cm (1.5") tube running down 183 m in which a sounder could be lowered to double-check water levels.

9.3.4 Measuring salinity

Salinity was measured with a Corning conductivity meter. Samples were taken from the outlet pipe and stored in plastic tubes. Samples were taken every 10 minutes at the start of the experiment, but at an increasingly slower sample rate as the conductivity values leveled off. This is true for both the pumping and rebound experiments. The probe was calibrated in air and with 12.88 mS solution. Conversion from conductivity to salinity is calculated using 1 mS/cm = 0.6 ppt (psu) = 640 ppm = 0.06% mass fraction (temperature variations were negligible in the samples tested).

9.4 Experimental Results

9.4.1 Salinity results

As shown in Figure 9-3, the salinity rises fairly quickly during the first 24 hours, and then continues to rise at a much smaller rate. In fact, 75% of the salinity rise over a one week period occurs during the first 24 hours.

[1] Largo, Florida. www.digitalcc.com

Figure 9-2: DCC bubbler setup with solar panel and Madgetch datalogger. Snow-capped Mauna Kea in the background.

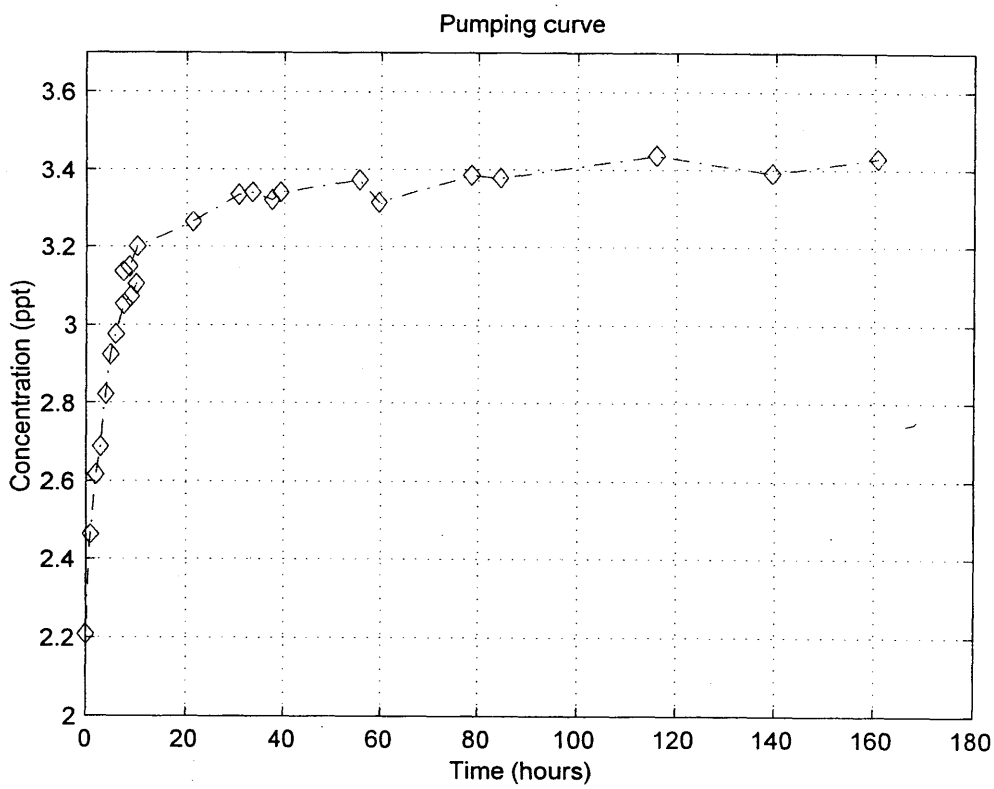

Figure 9-3: Pumping test for KI1.

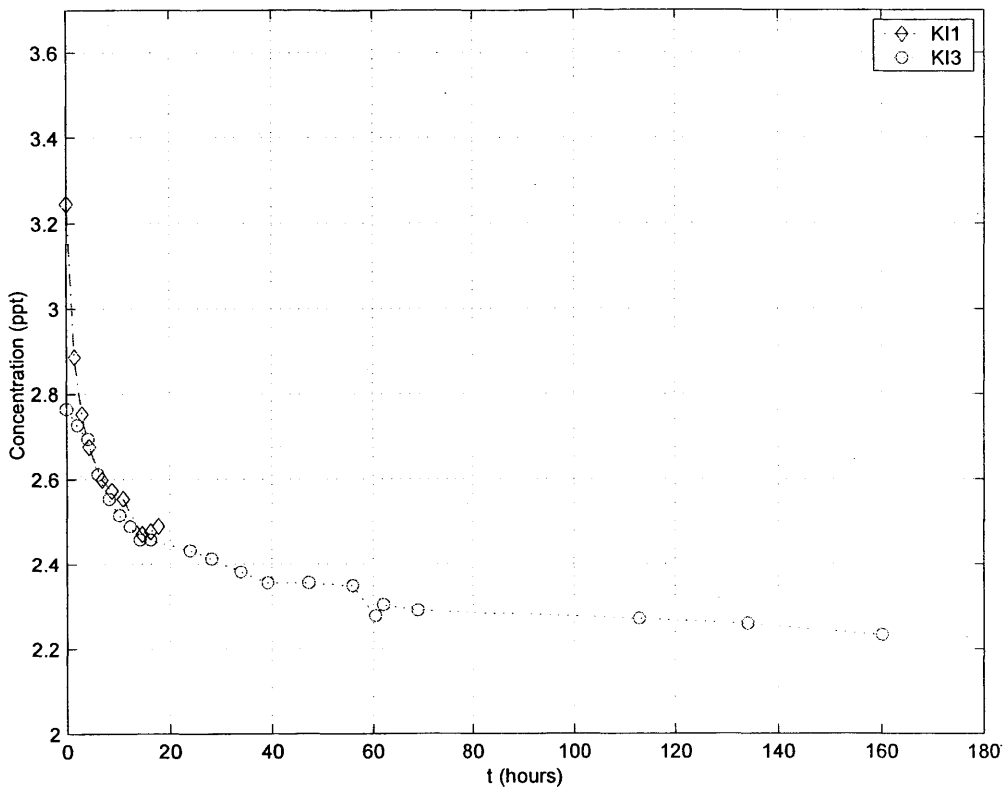

Figure 9-4: Rebound in salinity for KI1 and KI3.

The rebound data displayed in Figure 9-4 is a compilation of data from rebound tests conducted on wells KI1 and KI3. It was impossible to conduct a week long rebound test on KI1 due to the demand for water for construction. KI1 is the primary supply well at this time. However, we were able to conduct a rebound test on KI3 for nearly one week. Though the initial points of the rebound curves do not correspond exactly, after only a few hours they overlap amazingly well. Therefore, given the additional fact that these wells are only 457 m apart, I assume my rebound curve to be a smooth curve starting with the KI1 initial concentration and smoothly merging with the KI3 rebound curve. For the purposes of the study this is a reasonable assumption.

Short-term pumping and rebound tests were also conducted on KI1 and KI2 and KI3. These results are plotted in Figure 9-5. Interestingly, in all cases it takes longer to recover than it takes to get salty. Even the short 8 hour pump test on KI2 does not recover quickly (it took

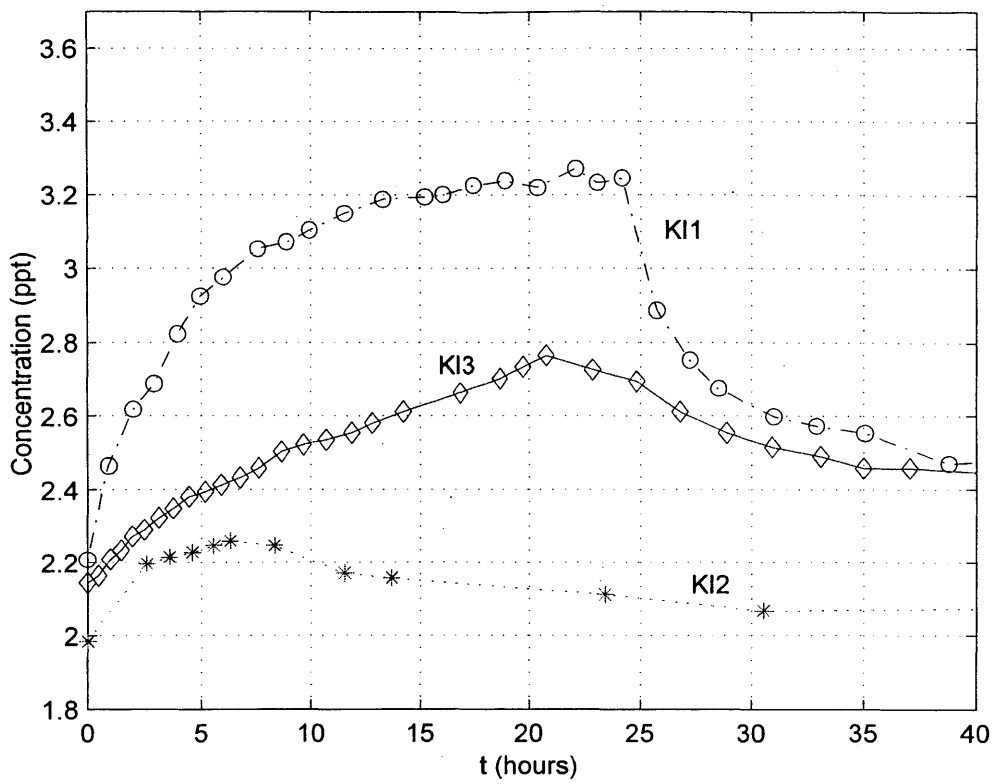

Figure 9-5:

6 days to get back to initial conditions). This indicates that the current pumping schedule of Kuki'o management, of 12 hrs on and 12 hours off, would lead to a ratcheting effect that would drive the salinity very high. However, this has not happened. The salinity seems to max out at less than 3.52 ppt (5.5 mS) as shown in Figure 9-3. This indicates that given the pump capacity and current hydrologic conditions, the system reaches a new equilibrium that does not lead to a critical upconing situation; even at steady pumping. It may ratchet up to this new position from a lower salinity situation, but it does not pass this ceiling.

9.4.2 Head results

Bubbler data for wells KI1 and KI2 were taken successfully. The bubbler at KI3 generated very erratic data and was impossible to calibrate well. It is thought that the bubble line is clogged or ruptured somewhere along its length. Figure 9-6 shows the head data from the week

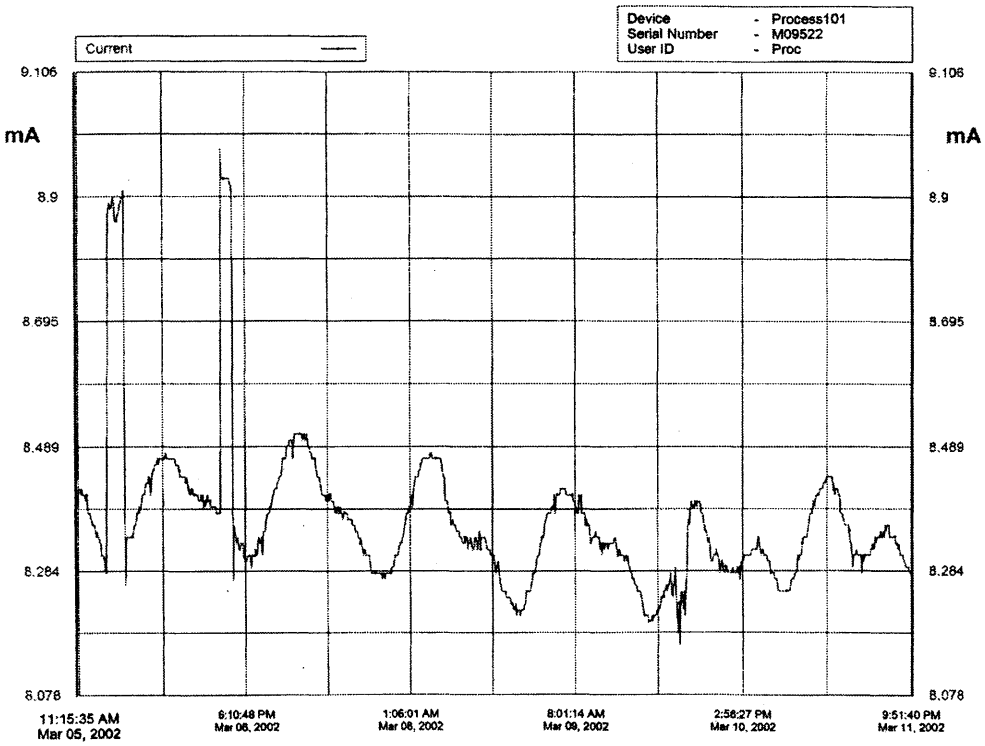

Figure 9-6: 1 mA is equal to one foot of head change.

long pump test at KI1. The sinusoidal curve is the tides, while the two spikes on March 5 and 6th are when the pump shut off due to electrical surges. Note the lack of a typical drawdown curve. There is likely a drawdown curve, but it has very steep sides and develops very quickly.

Shown in Figure 9-7 is the head data taken at KI2 while the KI1 test was going on.

9.4.3 Comparison to analytical saltwater upconing solutions

It is useful to briefly compare the experimental results at Kuki'o with some existing analytical saltwater upconing results. Schmorak and Mercado [47] give a much used and simple approximate analytical solution based on the sharp interface assumption. The new equilibrium elevation to the sharp interface due to pumping is given by

$$z = \frac{Q\rho_f}{2\pi z_b K(\rho_s - \rho_f)}$$

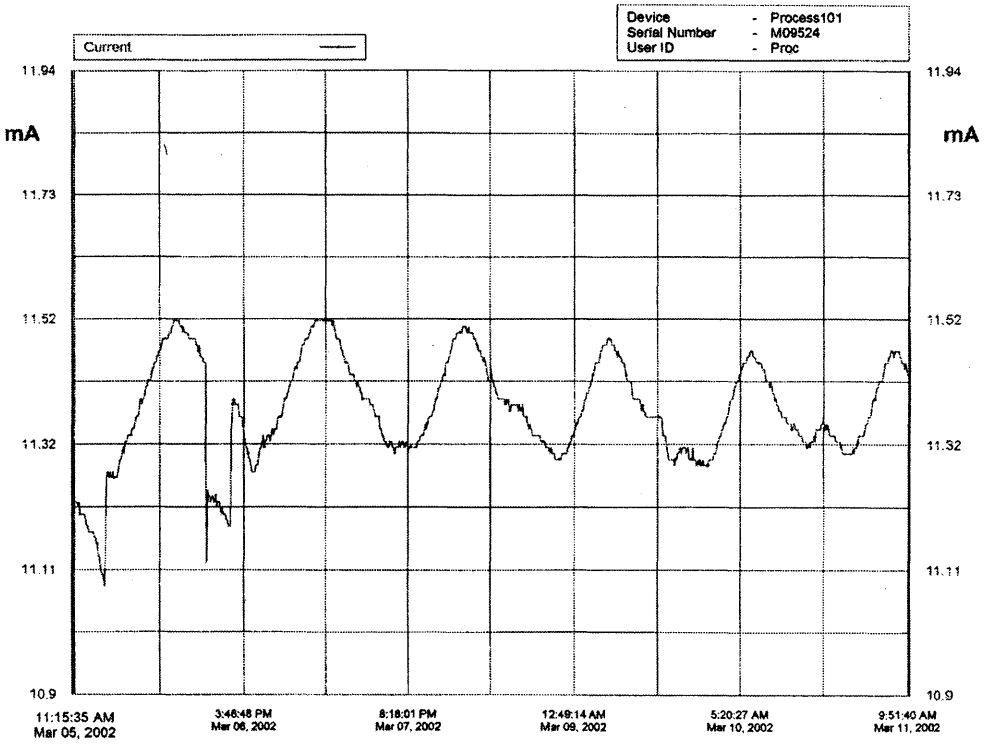

Figure 9-7: 1 mA is equal to one foot of head change.

where z is the new equilibrium elevation, Q is the pumping rate, z_b is the original depth to the interface from the bottom of the well screen, K is hydraulic conductivity, and ρ_f and ρ_s are the densities of fresh and saltwater respectively; Figure 9-8. The results for z plotted versus various K values are shown in Figure 9-9. Q = 2955 m^3/day (540 GPM), z_b = 18.29 m, and K = 30.48 – 3048 m/day (100 – 10,000 ft/day). Though we have no way of knowing what the actual cone rise due to pumping is at the Kuki'o site, this simple approximation indicates that the aquifer must have very high conductivities. Work by Dagan and Bear [11] suggest that the upconed height should not exceed $0.3z_b$ since there is a very non-linear jump from the smooth rise in cone height to the critical situation leading to cone capture by the well. In this case $0.3z_b \approx$ 5.5 m, which corresponds to K = 190 m/day (623 ft/day). Since no cone capture occurred at Kuki'o, we can safely assume, based on this simple method, that K values are in excess of 200 m/day.

One more layer of complexity may be added to these analytical solutions without too much effort. As described by Wirojanagud and Charbeneau [59], the effects of hydrodynamic dispersion may be superimposed upon the sharp interface upconing solution with a simple error function solution which is based on a one-dimensional upward, solute transport model.

$$c = \frac{1}{2} \operatorname{erf} c \left(\frac{z - z_{rise}}{2\sqrt{\alpha z_{rise}}} \right)$$

c(z) = dimensionless concentration

z = vertical distance from the initial interface (m)

z_{rise} = how far the interface center traveled (m)

α = dispersivity (m)

It is reasonable to use the conservative value z_{rise} = 5.5 m as described above, and a distance to the well screen of 18.29 m based on Ghyben-Herzberg. A value for the dispersivity, α, is not documented for Kuki'o so I have plotted concentration with depth for various dispersivity values; Figure 9-10. This dispersivity is longitudinal dispersivity to the vertical transport model, but would correspond to vertical dispersivity in reality (in relation to the geologic strata).

The mass fraction of sea-water is 3.5%, which is approximately 35 ppt. The concentration at KI1 after a week of pumping only rose to about 5.4 mS/cm = 3.5 ppt, which is 10% of seawater. According to Figure 9-10 this would require longitudinal dispersivity values of

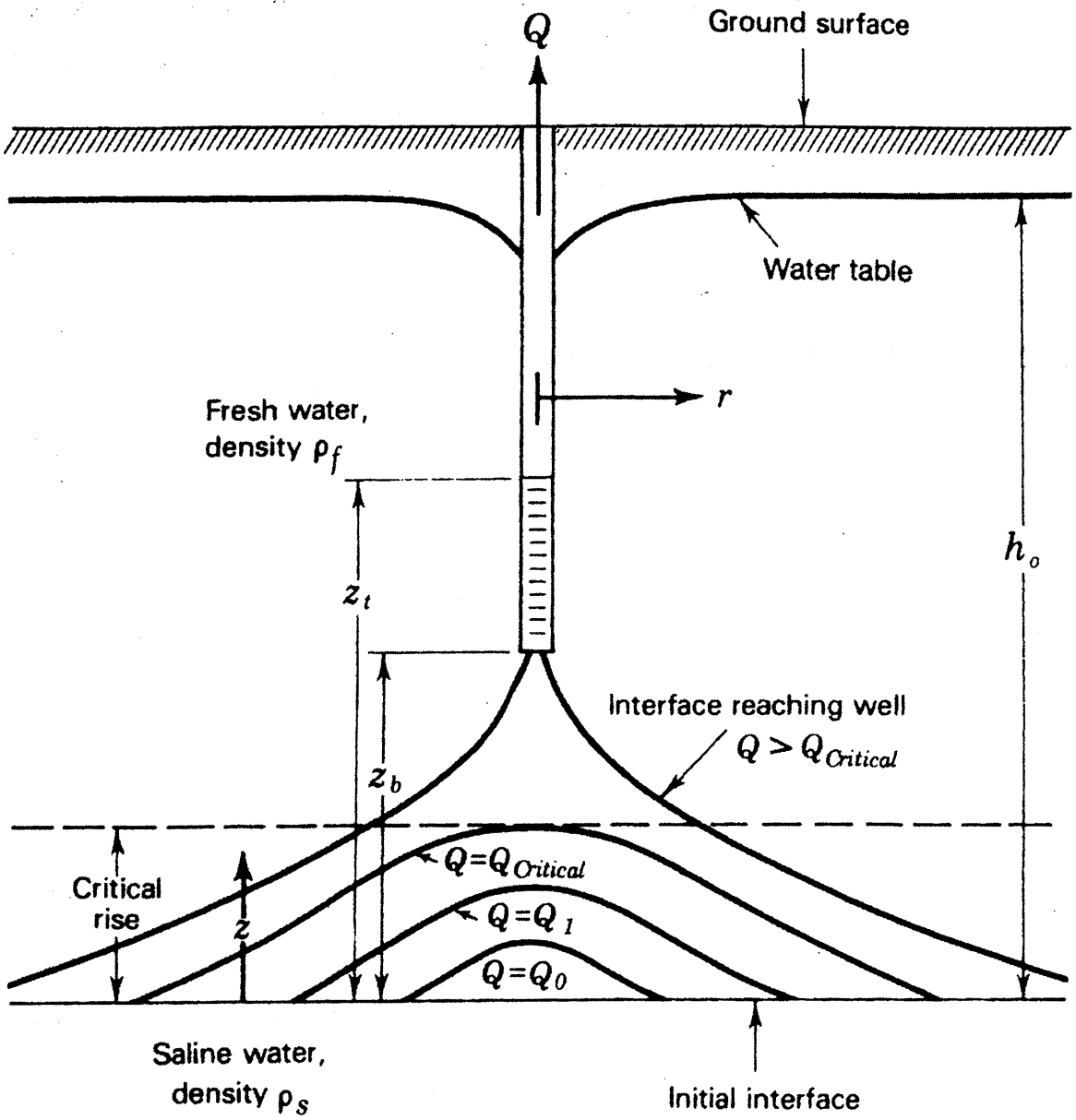

Figure 9-8: Schematic for analytical solution for upconing conditions (Reilly and Goodman, [45]).

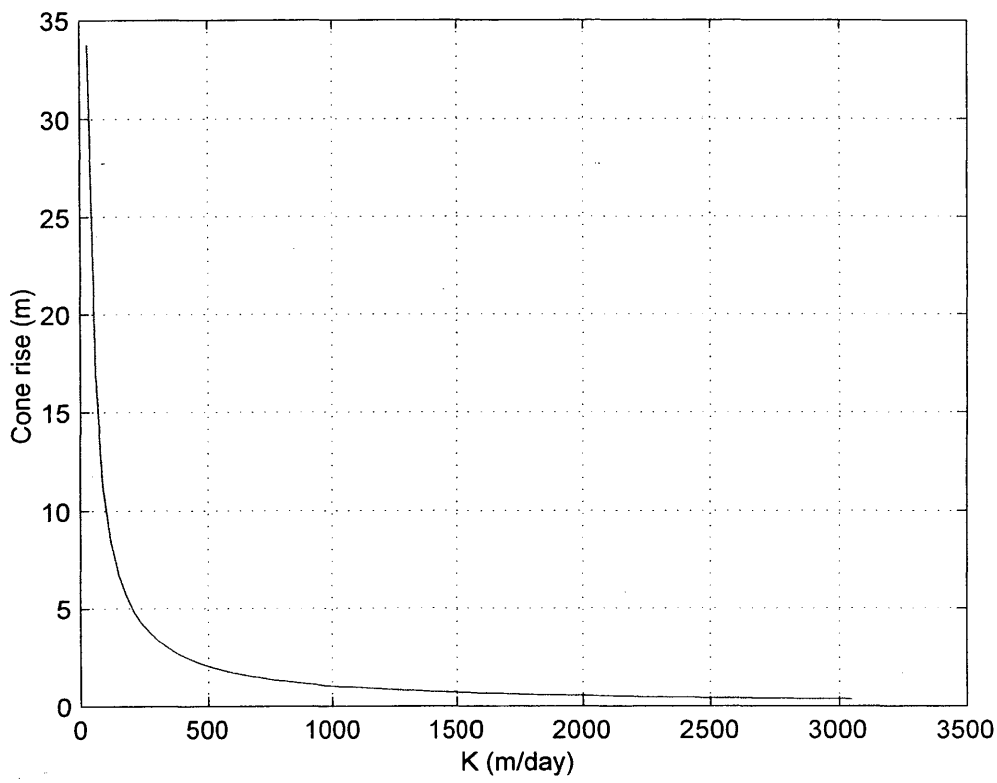

Figure 9-9: Saltwater cone rise using Schmorak and Mercado approximate solution.

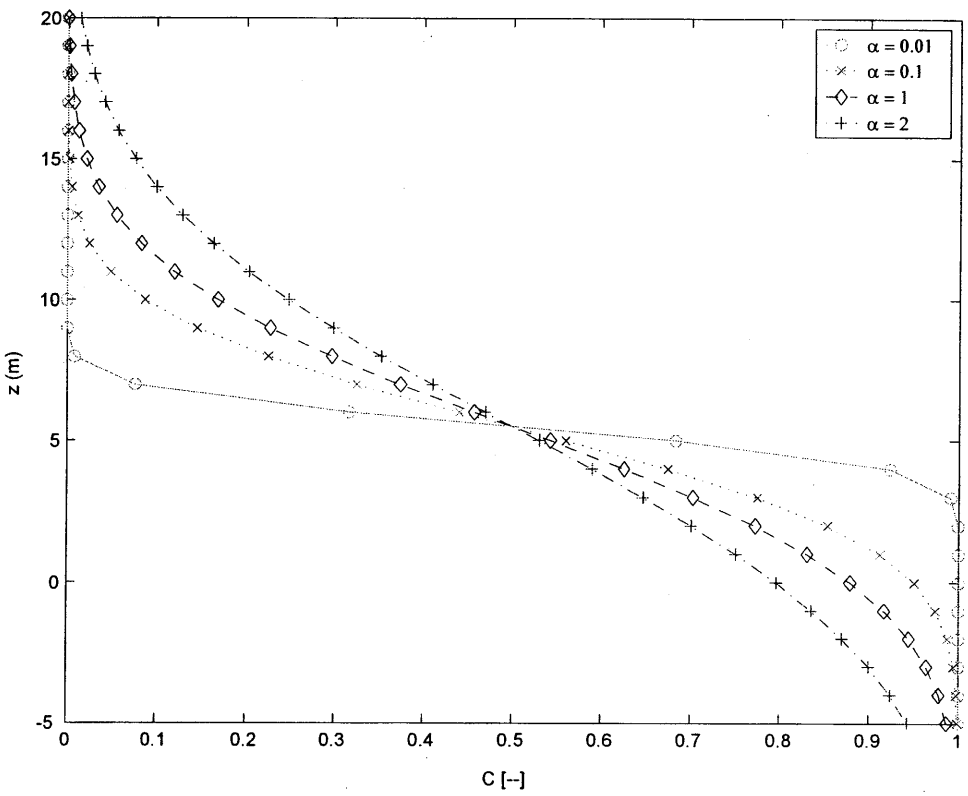

Figure 9-10: Dispersion of a transition zone a saltwater cone that has risen 5.5 m.

about 2 m to have that much salt reach the pump bottom by dispersive processes. Such high vertical dispersivities are possible in volcanic terrain, but it is likely that tidal effects are also contributing to such a thick transition zone. This simple 1-D model neglects these dynamic effects.

Though these approximate solutions could account for the test results at Kuki'o, the nature of these analytical methods highlight the need for direct field measurements or numerical modeling when studying complex aquifers such as at Kuki'o. The heterogeneity and anisotropy of the volcanic pile makes it very difficult to chose a correct K value in the highly sensitive equation for upconing under sharp interface conditions. Complex boundary conditions such as tides and the lack of any good dispersion parameters renders analytical solutions for the transition zone equally unreliable. Comparison of the field data to more complex numerical models of upconing are warranted, but left for another time.

9.4.4 Interdependence of the KI wells

The bubbler data from KI2 and KI3 was checked for any response to pumping and pump shutdown at KI1. In addition, water samples were taken to test for salinity changes during the KI1 tests. None of the head or salinity data indicate any interaction between the wells. However, there may be some long-term interactions that this relatively short-term study cannot detect. It is useful to do a rough calculation of the capture zone width for these wells in order to asses the validity of this apparent lack of inter-well interaction. The simplest approximation is for a pumping well in uniform flow. The following solution is for a homogeneous, isotropic confined aquifer, but is a reasonable first-cut approximation. This solution may be found in most groundwater textbooks; see, for example, Bear, 1979 [2].

The groundwater divide bounding the area of aquifer suppling the pumping well, i.e. capture zone, is a streamline defined by;

$$y/x = \pm \tan(2\pi q_o B y/Q_w) \ [+y \text{ for} > 0 \text{ and } -y \text{ for} < 0]$$

Q_w is the pumping rate of the well [m^3/day], B is the thickness of the aquifer [m], and q_o is the regional uniform flow rate [m/day]. This streamline asymptotes to the lines, $y = \pm Q_w/2q_oB$, which, taken from the centerline, is the width of the widest part of the zone of influence for the

well. The primary unknown in this equation for the KI wells is the value for the uniform flow, q_o. However, we can substitute in Darcy's law using head values between two of the KI wells. The primary unknown becomes hydraulic conductivity, K.

$$y = \pm \frac{Q_w}{2BK\nabla h}$$

where ∇h is the gradient between two of the wells. Using pre-pumping head data for KI1 and KI3, the value for ∇h is found to be 0.00048. The aquifer thickness beneath KI1, assuming Ghyben-Herzberg, is $B = 18.3$ m (60 ft). Q_w is 2943 m^3/day. Substituting in all known values, one may now plot the maximum width of the capture zone versus various K values; Figure 9-11. The plot indicates that K values in excess of 460 m/day (1500 ft/day) are necessary to have a zone of influence which is less than 457 m wide (the approximate distance between the KI wells). The lack of data indicating well interaction, together with this back-of-the-envelope estimation, is an indicator that horizontal K values in the Kuki'o region are around 500 m/day or larger.

9.5 Coastal wells conclusions

Even though more research needs to be done, a number of the key research questions were successfully answered by the KI well experiments:

Salinity rise with pumping

It was determined that for Kuki'o, given the current pump configuration, no critical upconing situation seems likely. This assumes that salinity values of around 3 - 3.6 ppt (5-6 mS) are acceptable for supply. Apparently the system reaches a new equilibrium that appears sustainable at least on the time scales investigated. It may be that there is a slow increase in salinity that is impossible to detect given the tides and the time frame of the completed experiment, but that will only be made known with continuous monitoring in the years to come.

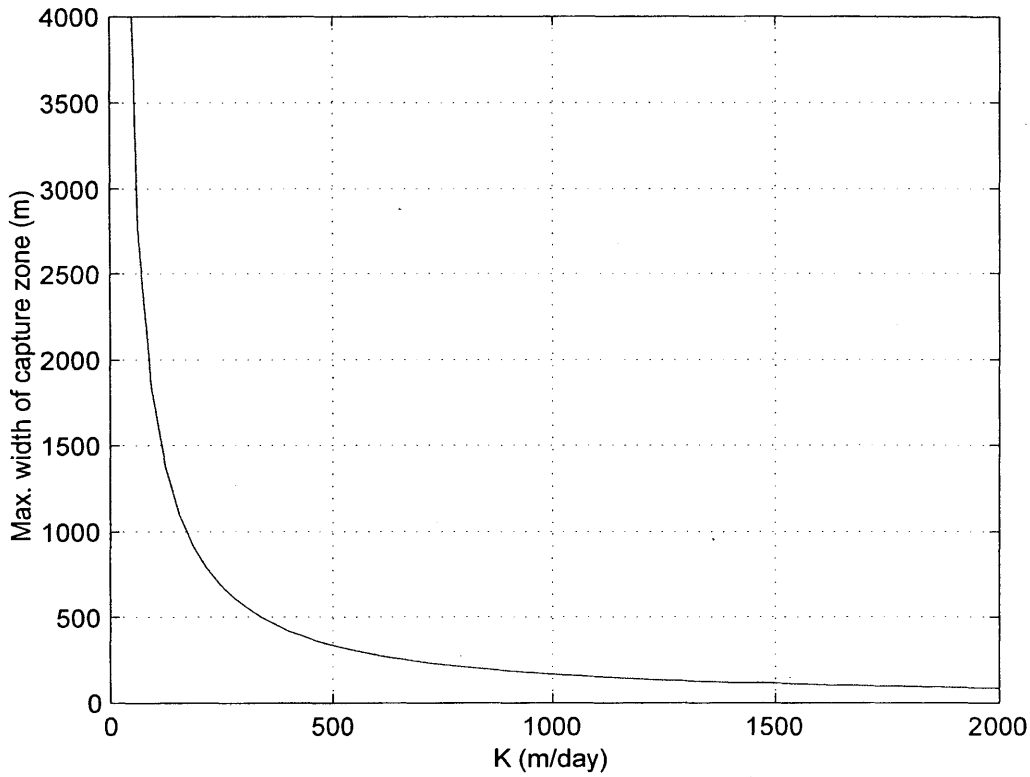

Figure 9-11: Approximate width of zone of influence for KI1, $\frac{Q_w}{2q_oB}$.

Rebound in freshness when pump is turned off

The system takes longer to rebound back to original conditions than it takes to salinize. This is most likely due to dispersion effects, as a sharp interface would theoretically recover at least as fast as it upconed (possibly faster due to the density effects). However, the time to recovery at Kuki'o is not excessive. In some numerical studies it takes on the order of years to decades for recovery [3][32], but at Kuki'o full recovery to initial conditions is on the order of weeks. This is a significant difference to be noted.

Head response to pumping

The head in the wells responds almost instantaneously to pumping. The 4 minute sampling interval of the bubbler apparatus can't detect a drawdown cone. The decrease in head is about 17.78 cm (7 in.) for KI1 and 7.62 cm (3 in.) for KI2. This signal shows up as a jump on the continuous and remarkably smooth tidal signal detected by the bubbler. This verifies the intuition that the highly permeable basalt yields water readily to the pumping well.

Effect of pumping on nearby wells

Head and salinity data don't indicate any influence of one well on any of the others. It seems that the very high K values of the geologic pile facilitate high flow rates to the well without the need to draw from great distances. Therefore, the capture zone for the wells is fairly narrow.

Implications for Kuki'o

In summary, it appears that Kuki'o's stated brackish demand for the KI wells of 4921 m^3/d (1.3 MGD) could be sustainably met by the wells assuming brackish water levels near 3.5 ppt are acceptable. A pumping schedule which allows the wells to freshen after periods of pumping may better insure that excessive salinity values are never encountered, but that is not verifiable at this time. An optimization model (optimal control model) using the pumping and rebound curves derived here would be useful for determining an optimal pumping schedule for a daily or weekly management schedule.

However instructive in understanding the dynamics of pumping in this region, the coastal experiment results are not valid for constructing an effective model of the long-term effects of

pumping from this coastal aquifer. The primary reasons include:

1. The lack of experiment sensitivity to up-gradient pumping wells.
2. No data on how sensitive the system is to recharge. The coastal experiments were conducted during two of the wettest months in the Kuki'o area in decades.
3. The time scale of the experiments were too short. Monitoring of the wells needs to be an on-going process that may take years to complete.

Therefore, as discussed in the following sections, an alternative method for determining salinity with pumping from the coastal aquifer is developed and implemented in the long-term regional model.

Chapter 10

Regional Hydrologic-Economic Model

10.1 Introduction

The regional hydrologic-economic model for Kuki'o jointly optimizes groundwater use for the two important aquifer systems in the Ka'upulehu region; the high-level and coastal aquifers. The two are linked through a semi-permeable geologic formation. It should be noted that the existence of a high-level aquifer for Ka'upulehu has not been verified. We formulate the model assuming its existence, and it is almost certainly true that as one drills further and further into Hualalai mountain high-level water will be discovered at some point.

Though we are using data and parameters from Kuki'o, the methodology employed here is general enough to be used in any joint aquifer system. As far as I know, this is the first dual-aquifer, regional scale, long-term hydrologic-economic model attempted in Hawai'i. It is hoped that the framework developed is a positive first step to sustainably managing Hawai'i's precious water resources.

It should be stressed that the model developed here is only useful as a "management tool" to aid in determining water policies. Successful use of the methods are contigent upon input from hydrologists, economists, social planners, and local community members. This tool is only as good as its inputs and assumptions; which should always be stated clearly. If done so,

we feel this can be a useful tool for strategizing water management in coastal areas. Sensitivity to key parameters and constraints, whether physical, economic or social, can easily be tested once the basic model is set-up.

The model will **not** pop-out the "correct answer". Rather, it allows the user to see how the system generally responds to different inputs and strategies. A range of possible solutions is the most useful output. It is still up to socio-political forces to make the final decision.

10.2 Hydrologic-Economic Model Formulation

10.2.1 Major Assumptions

We assume that the dual-aquifer system modeled is an independent, closed system. This means that water only enters the system through recharge on-site, and exits through wells or to the ocean. No leakage into or out the sides of the aquifers (besides the ocean boundary) is permitted; the no-flow boundaries follow streamlines to the sea. In reality these streamlines may not follow the model boundaries perfectly and some water exits (or enters) since the groundwater system is not 2D, but how so and how much is unknown. However, since we are only using a simple box model to conserve mass the no-flow boundary conditions are assumed to be adequate for the general purposes of this study. Given that the island geometry is more cylindrical than cartesian, it is as if we are taking a representative wedge out of the mountain and assuming that wedges taken to either side would look similar and behave in the same way.

The model is also independent in the sense that the potential contribution of water from other districts and aquifers is not considered. As mentioned earlier, our goal is to sustainably manage the area's existing water resources.

Only one well in the high-level aquifer and one well in the coastal aquifer are considered. The primary decision variable for each aquifer is *total pumping*. In reality a number of wells would likely be necessary to support total pumping, but, again, our goal is to develop general guidelines for developing these resources. The added complexity of added wells is unnecessary to this end.

The positions of the two wells are fixed in space; they are not decision variables. Even though the decision variable is total pumping, the well position does matter since we use data

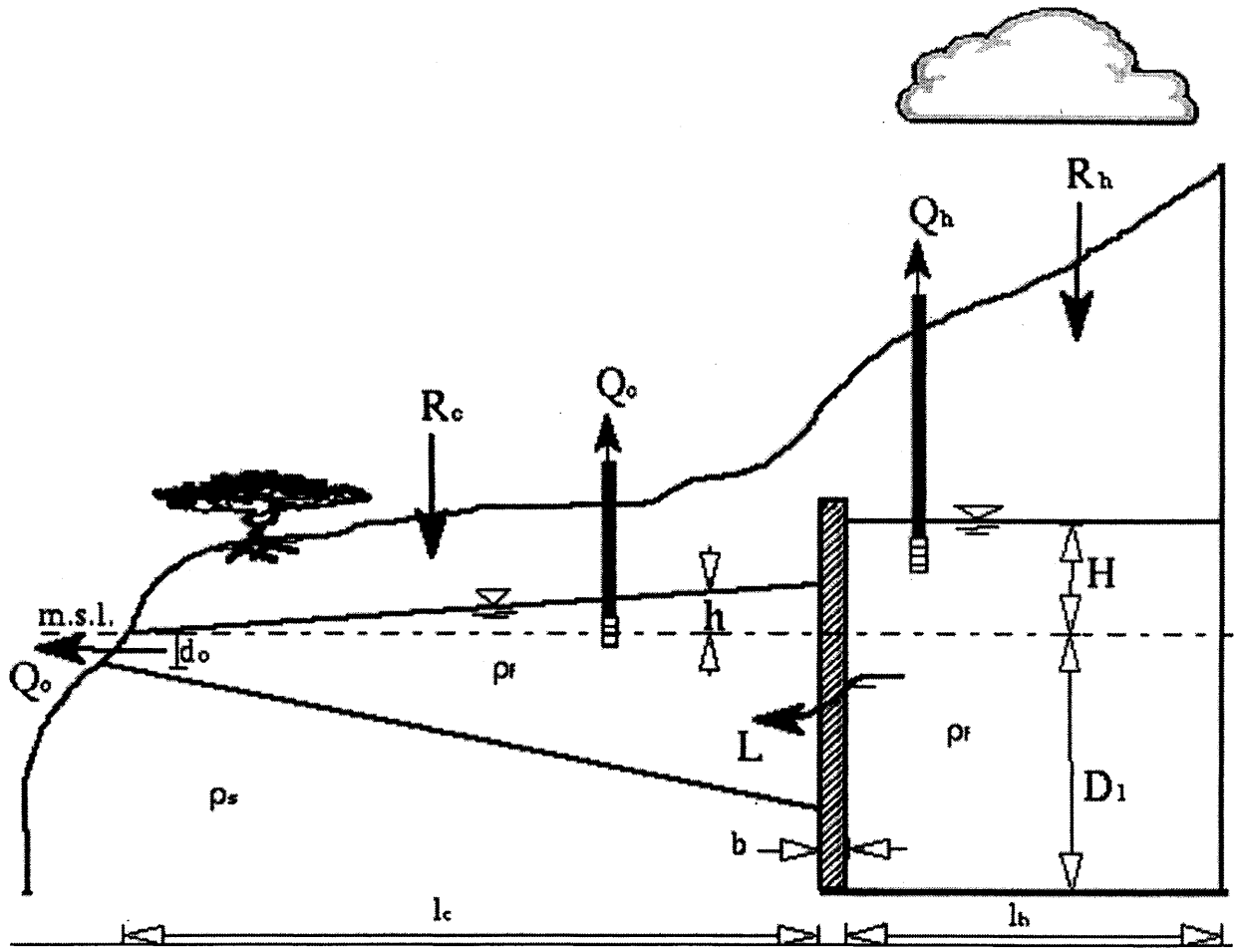

Figure 10-1: Schematic for dual-aquifer model.

from the KI wells for the coastal well. The high-level well position must also be set since capital costs and lift costs are dependent on its elevation and distance from the coastline.

Finally, it is important to mention that the spatial gradients in groundwater head are *not* modeled here. This is a box model approach which conserves mass through conservation of aquifer pore water volume. This means a sharp interface approximation is used. The effects of salinization and salt dispersion are superimposed upon the water balance solutions with independent, empirical equations. This is explained in more detail in the following sections.

10.2.2 High-level Aquifer State Equation

The high-level aquifer is the simpler of the two-aquifers. It may be reasonably modeled as a typical "bucket-like" unconfined aquifer not too unlike the groundwater pumping problem described in Part1, Chapter 4. It is treated as a two-dimensional problem with a unit width, Figure 10-1. All parameters are normalized by the average system width of 6000m. The high-level aquifer extends from the semi-permeable barrier on its ocean (makai) end to an inferred groundwater divide upgradient (mauka end). The summit of Hualalai and its ridge-like rift zone may be reasonably considered groundwater divides. Aquifer recharge, R_h, is precipitation plus fog-drip minus evapotranspiration. Input values were taken from a recharge map developed for the Kuki'o area by Waimea Water Services (see Figure 8-3). Output from this aquifer is high-level well pumping, Q_h, and leakage into the coastal aquifer, L. The water is assumed fresh throughout, which is true for all high-level aquifers currently being tapped.

The governing fluid balance equation is given by,

$$\frac{dV_h}{dt} = R_h - Q_h(t) - L(t)$$

or, since the total volume of the high-level aquifer is given by $V_h(t) = \theta W l_h \left(D_l + H(t)\right)$,

$$\theta W l_h \frac{dH}{dt} = R_h - Q_h(t) - L(t)$$

$H(t)$ = high-level aquifer hydraulic head [m]

D_l = depth of high-level water below mean sea-level (assumed constant) [m]

W = width of aquifer (set to a unit width) [m]

V_h = total volume of water in the high-level aquifer for a unit width [m^3]

l_h = lateral extent of high-level aquifer [m]

R_h = net recharge to high-level aquifer [m^3/yr]

$Q_h(t)$ = pumping rate from high–level well [m^3/yr]

$L(t)$ = leakage from high-level aquifer to the coastal aquifer [m^3/yr]

θ = porosity [-]

In GAMS the state equation is discretized using a simple finite difference numerical approximation for the derivative with time. The resultant discretized state equation is:

$$H^t = H^{t-1} + \left(\frac{\Delta t}{\theta W l_h}\right)\left(R_h - Q_h^t - L^t\right)$$

For the long time scales considered here Δt is set at 1 year in the numerical model.

10.2.3 Leakage Equation

The flow equation needed to link the two aquifers is leakage from the high-level aquifer to the coastal aquifer. Leakage is determined with Darcy's Law through a semi-permeable barrier of thickness b. I assume that the leakage face is W wide and D_l deep.

$$L(t) = \frac{KWD_l}{b}[H(t) - h(t)]$$

D_l, K, and b are all relatively unknown quantities and may be incorporated into one **leakage factor** termed $K' = \frac{KD_l}{b}$ [m/yr]. W is taken as a unit width in the model. Therefore, leakage is written simply as

$$L(t) = K'W[H(t) - h(t)].$$

Note that the leakage face depth is assumed constant. Exactly how deep a high-level aquifer goes is unknown. However, it is unlikely its depth below mean sea-level obeys Ghyben-Herzberg for the highest high-level heads. This would lead to depths in excess of 4,267 m (14,000 ft) for high-level heads of 107 m (350 ft) observed in the Kona district. It is more likely that an effectively impermeable boundary is reached with depth due to compaction of the volcanic pile with depth. Here we assume that the depth to this impermeable boundary is the depth of the leakage face. Uncertainty in D_l is subsumed into K'. The leakage factor is tested over 3 orders of magnitudes to thoroughly test the model's sensitivity to this critical parameter.

The lengths of the arrows in Figure 10-2 are proportional to the degree of leakage from the high-level aquifer; assuming linear dependence on pressure variations. This leakage differs slightly from our assumptions in two ways. First, we are neglecting some leakage occuring over depth H in the section labeled 1. This is partially justified by the fact that D_l can be reasonably assumed to be much larger than H, $D_l >> H$. We also assume that leakage is constant and proportional to (H-h) over all of D_l. The bottom of Figure 10-2, labeled 3, shows

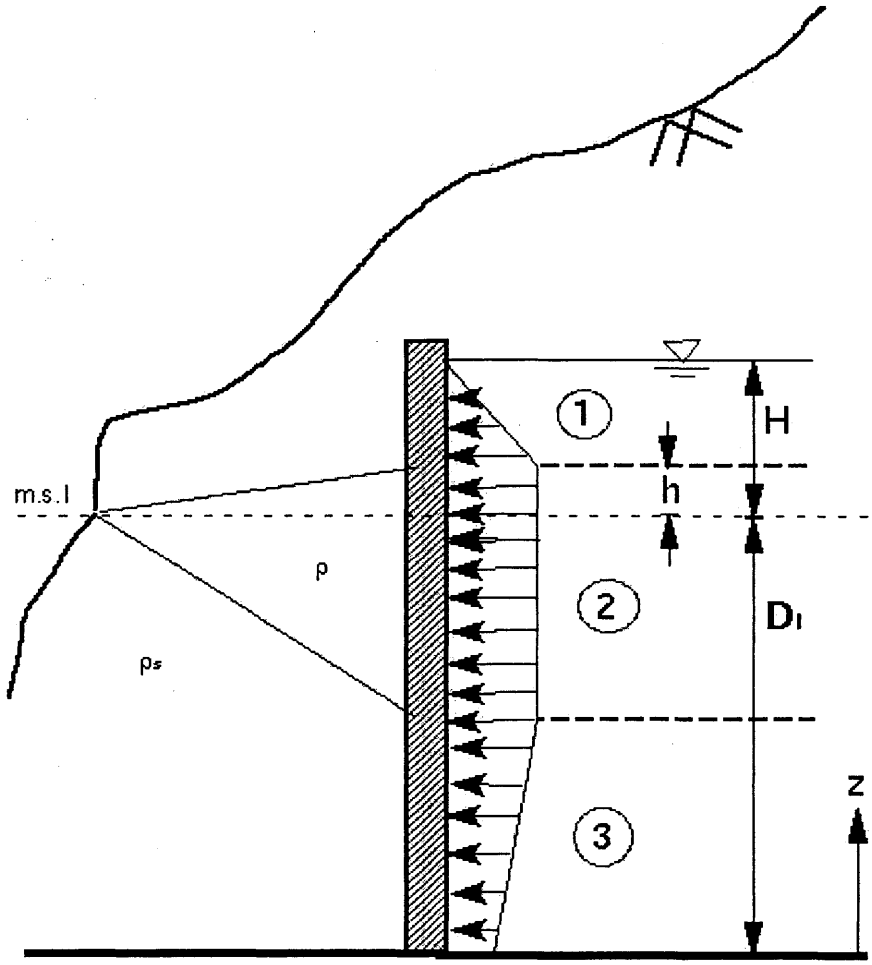

Figure 10-2: Diagram for leakage through the high-level barrier (not to scale).

that leakage will be somewhat less than that at depths greater than 40h. We are forced to neglect this since we simply don't know the true relation. However, gaining some leakage at depth and losing some at the very top may balance each other out.

10.2.4 Coastal Aquifer State Equation

The coastal aquifer is more difficult to model due to the presence of saltwater. This density difference leads to difficulty in computing the size of the freshwater basal lens with changing inputs; not to mention the presence of a thick transition zone and dispersion due to tides and pumping. As such, simplifications had to be made to make the optimization problem tractable.

The thickness and resultant volume of the basal lens are computed using the sharp-interface Ghyben-Herzberg relation. Transition zone and dispersion effects are superimposed through an empirical equation.

As with the high-level aquifer, we use a box model approach here. The governing fluid mass balance equation is straightforward.

$$\frac{dV_c}{dt} = L(t) + R_c - Q_c(t) - Q_o(t)$$

That is, the change in fluid volume for the coastal aquifer is equal to the input of water from high-level leakage (L) and coastal recharge (R_c), minus output due to coastal well pumping (Q_c) and discharge to the ocean (Q_o)[1]. The volume of water in the coastal aquifer, V_c, may be approximated as:

$$V_c = \theta W[\frac{1}{2}l_c h(t) + \frac{1}{2}(B(t) + d_o)l_c]$$

The first term is simply the area of water above sea-level approximated as a triangle, and the area below sea-level as a trapezoid; $h(t)$ is the coastal aquifer head and d_o is the depth of the discharge face at the coastline; see Figure 10-1. Simplifying and taking advantage of the Ghyben-Herzberg relation, assuming $\frac{\Delta\rho}{\rho} = 0.025$,

$$V_c = \frac{\theta W l_c}{2}[h(t) + B(t) + d_o]$$

$$V_c = \frac{\theta W l_c}{2}[41h(t) + d_o]$$

The derivative of V_c is similar to that of V_h, and I assume that the area of discharge at the ocean varies very little with time ($\frac{dd_o}{dt} \ll 0$).

$$\frac{dV_c}{dt} = \frac{41\theta W l_c}{2}\frac{dh}{dt}$$

[1] We assume that all water pumped is consumed. In reality there would be some wastewater that would re-infiltrate and discharge to the ocean or have to be disposed of elsewhere. This layer of complexity is not considered here.

The final fluid mass balance equation is therefore,

$$\frac{41\theta W l_c}{2}\frac{dh}{dt} = L(t) + R_c - Q_c(t) - Q_o(t)$$

Discretized for inclusion in GAMS:

$$h^t = h^{t-1} + \left(\frac{2\Delta t}{41\theta W l_c}\right)\left(L^t + R_c - Q_c^t - Q_o^t\right)$$

The final coastal equation needed is an equation constraining discharge to the ocean, $Q_o(t)$. If $Q_o(t)$ is left as purely a decision variable the maximization model would "turn off" discharge to the ocean in an effort to derive more water and hence benefit from the aquifer. We constrain $Q_o(t)$ by recognizing that the discharge to the ocean is proportional to the head in the basal lens. We may then define a linear relation between coastal head and ocean discharge:

$$Q_o(t) = ah(t) + b$$

However, we know two points on this line and can therefore determine a and b explicitly. First, $b = 0$ since when there is no head in the aquifer there is basically no freshwater discharge to the ocean[2]. Second, a is constrained by initial conditions in the aquifer.

$$Q_o(t) = \frac{Q_o^{initial}}{h^{initial}}h(t)$$

where $Q_o^{initial}$ is *not* an arbitrarily fixed number. It is automatically fixed once the known KI initial heads, pumping rates, and recharges are input into the model.

Initial conditions

Initial conditions were set with quantities taken from the KI well tests. Specifically, at t = 0 Q_c is set at the current pumping rate of 322 m^3/yr (this is normalized by the aquifer width of 6000 m), h is set at 0.3 m (KI1 current conditions), and Q_h is set at 0 m^3/yr. The last variable that needs to be set for the optimization to run feasibly is the initial high-level head.

[2]There is some ocean discharge even when h = 0 due to the tidal range. However, this discharge would be almost all saltwater.

Fortunately, this value is set automatically through the state equations given the other three initial conditions.

Note that this initial high-level head will depend on the leakage factor K'. Assuming the model is formulated correctly, varying K' is a reasonable way to back out an approximate high-level head value prior to exploratory drilling. As far as I know, there is currently no other model available to test possible high-level head values prior to drilling; aside from proximity to other successful wells of course. Conversely, drilling a high-level well would be useful to constrain K' values.

10.2.5 Coastal Aquifer Salinity State Equation

The effects of salinization of the coastal wells are incorporated via an empirical relation of salt concentrations to coastal head levels. This equation is based on well data from the northwest Hawai'i coastline. The chloride concentrations from 54 wells in the coastal plain from Kuki'o to Kawaihae were plotted versus well heads[3]. These chloride and head measurements are pre-development and represent roughly virgin aquifer conditions. The data was then fit with an exponential-type curve.

$$S(h) = 4922e^{-0.7377h} + 1.219x10^5e^{-10.91h}$$

As shown in Figure 10-3, there is some error near head levels between 0.15 m and about 1.5 m (0.5 to 5 ft) of head, but the curve captures the intuitive phenomenom of rising salinity with decreasing head levels. The coefficient of determination, r^2, for the regression is 0.91. This empirical equation is directly imbedded in the optimization model.

This is a fairly simplistic approach, but as exhibited in the previous chapter, the coastal well tests were unable to produce a more reliable salinity versus head relation. It would be useful to test this equation with a full numerical simulation of the coastal aquifer; which has not been done yet. It will be interesting to see how future models and data support or disprove this simple empirical approach.

[3] Conversion from chlorinity to psu (ppt) may be done using the relation: S = 0.03 + 1.805[Cl].

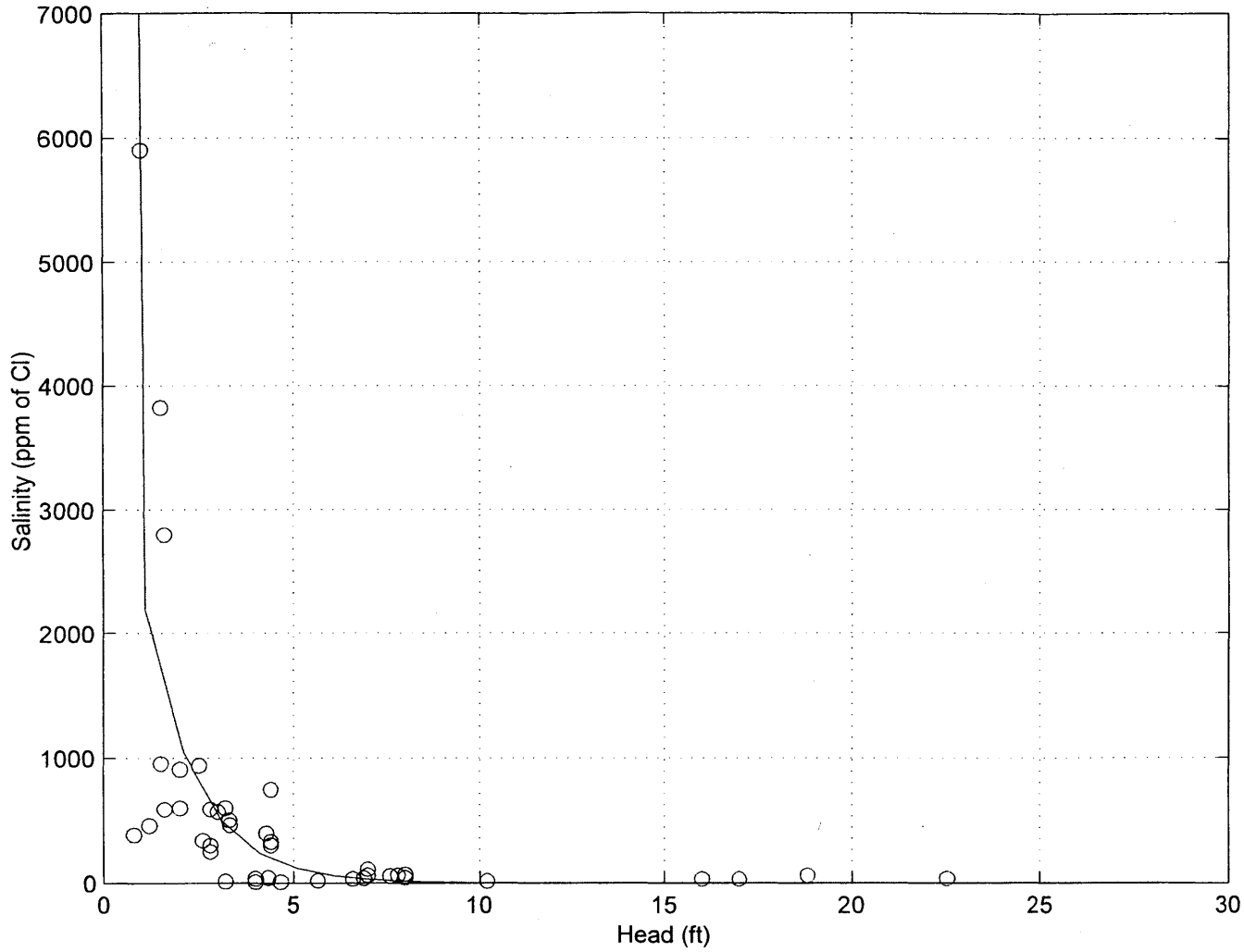

Figure 10-3: Coastal aquifer salinity versus coastal head levels. Data derived from 54 wells along the North Kona coastline.

10.2.6 Economic Constraints and Cost Equations

High-level Aquifer Energy Costs

Costs for the high-level aquifer are primarily due to energy needed to lift water to the ground surface. The energy equation used in the Kuki'o model assumes parameters common for in-well pumps currently in use in the area. The general equation is:

$$PE = Q \cdot (h_{grd} - h) \cdot ER \cdot K_e$$

PE is the resultant price of energy per day, Q is the pumping rate in GPM, h is the head in feet, h_{grd} is the ground elevation in feet, ER is the current energy rate in \$/KWH, and K_e is a constant that makes all the necessary conversions. It is important to note that this equation is only accurate for pumps that resemble the ones currently in use at Kuki'o. Though the dual-aquifer model only recognizes one pumping source in the high-level area and one in the coastal area, I assume that for large pumping rates the pumping stress is divided among N number of equally sized and rated pumps. In essence, I assume a well field instead of one huge, infeasible pump. This assumption is valid given the linearity of the energy equation with respect to Q (this ignores drawdown cones).

The base case cost of energy is based on a \$/KWH rate of \$0.21 for the North Kona area, assuming a 24 hour rate schedule (WWS. Inc.). K_e is 6.46x10^{-3} $\frac{KWH}{GPM \cdot ft \cdot day}$. The management model optimal trajectories will be tested for their sensitivity to energy rates.

Coastal Aquifer Energy Costs

Costs for the coastal aquifer are due to energy required to lift water to the ground surface and energy required for additional pressures needed to drive the Reverse Osmosis (RO) process. This additional desalinization pressure may be easily equated to a depth of water and directly added to the h term in the energy equation. All that is needed is an equation to calculate the additional pressure needed based on the salinity of the RO intake water. Such a relation is very difficult to determine exactly since the exact conditions of individual RO plants and configurations may vary significantly. However, an approximate relation based on data from the Hydranautics division of the Nitto Denko Corporation was used for our study [57]. Hy-

draunatics developed the RO membranes that will be in use at the Kuki'o RO treatment plant. The resultant approximate equation is:

$$ROP = 0.03164 \cdot S$$

where ROP is the additional pressure needed in feet and S is salinity in terms of ppm of chlorides.

Capital Costs

The primary capital cost for a high-level well is the pipeline to transmit water from the mountain to the user. For Kuki'o this is a distance of about 6 km. Based on a common "ready-to-go" price of $656 per meter ($200/ft) for a 0.3 m (12 inch) ductile main water line, a pipeline for Kuki'o would cost approximately $4,000,000 (ESH Engineers and Surveyors Hawai'i). The cost for a ready-to-go well at 457 m (1500') is $750,000, assuming a cost of $1,641 per meter ($500/ft) of depth. This is for a fully-cased 12-14" hole ready for a pump. The pump itself would run around $120,000, and additional controls and plumbing an additional $50,000 (WWS Inc., personal communication). The total high-level costs for a high-level well and pipeline are thus $4,920,000.

For the coastal system the RO treatment plant is the primary capital cost. The cost for an RO plant is approximately $1 per gallon of capacity. However, this cost will go up if the water being treated has a very high TDS concentration. This additional cost is usually about a 30% increase when moving from brackish water to very salty water (Pacific Keystone Inc., personal communication). I have treated this fact with a simple linear equation that has capital costs increasing with salinity up to a critical salinity level equal to seawater 35 ppt.

$$ROC = Q_{RO}\left(1 + 0.3\frac{S_{RO}}{S_c}\right)$$

ROC is RO capital cost, Q_{RO} is RO plant capacity [m^3/yr], S_{RO} is the salinity level [ppt]the RO plant is capable of treating, and S_c is the critical salinity level of 35 ppt. ROC is a decision variable in the hydrologic-economic model. This is a conservative formulation as we constrain Q_{RO} to be as large as the largest coastal pumping rate over the whole time horizon.

$$Q_c(t) \leq Q_{RO}$$

S_{RO} is taken to be the average coastal salinity over the whole time horizon (N is the number of time steps).

$$S_{RO} = \frac{1}{N} \sum S(t)$$

Drilling costs for a coastal well at 183 m would be \$300,000, the pump would cost around \$90,000, and additional plumbing and controls \$50,000. These costs are added to the RO capital cost which is not known *a priori.*

As is necessary, all capital costs are normalized to a unit width before inclusion in the model.

10.2.7 Benefit Function

The challenge in defining a reasonable benefit function is defining a reasonable demand curve for water. It is often difficult to accurately assess how people in a region value units of water. For the Kuki'o region the only "real" number we had to work with is a Public Utility Commission approved water price of \$1.27 per m^3 (\$4.80 for 1000 gallons at the current pumping rate). We determine how the solution depends on the demand curve by testing the model with a number of different curves. The demand curves are all either of a linear form or formulated as a power function with a constant elasticity of demand over time.

It should be noted that applying these various demand curves is an effort to investigate the full range of possible management strategies for a dual-aquifer system. Kuki'o itself is a unique case in which the developer really only wants the amount of water needed to satisfy the projected demands of the population at Kuki'o estates. More water does not really have more value to Kuki'o development unless they opt to buy more land in the Ka'upulehu region and start more development. Their interest in this project is to (1) get a general idea of how much groundwater is available in the area, (2) develop some general guidelines on how to use the two different aquifers, and (3) investigate any negative effects on the system.

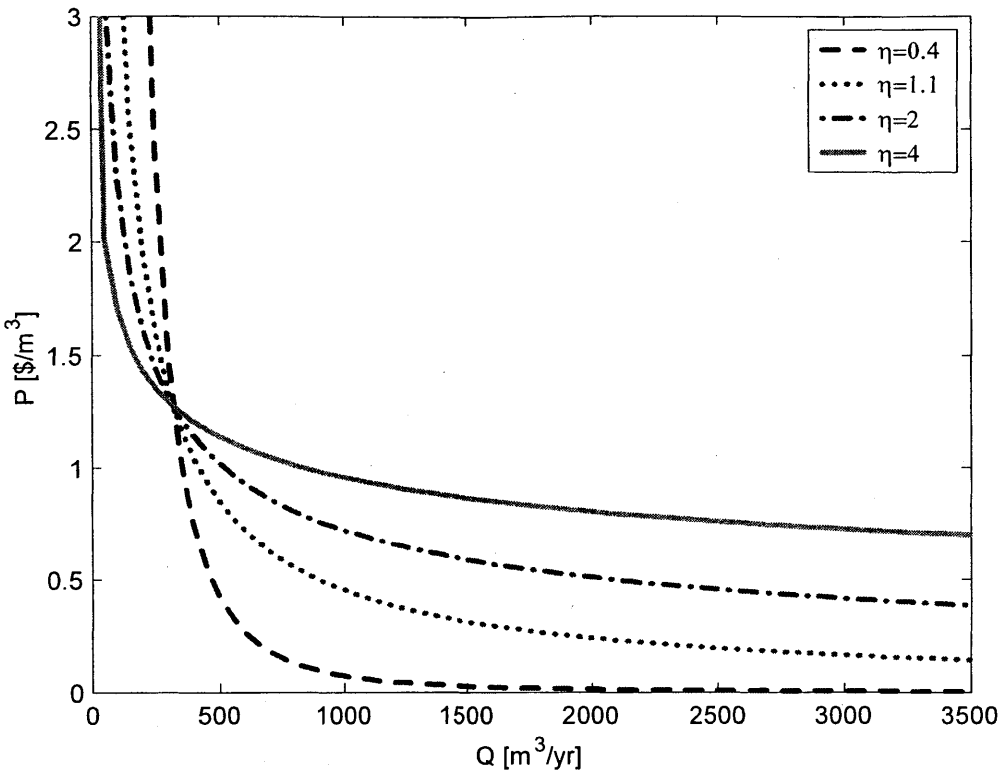

Figure 10-4: Demand curves with constant elasticities.

Constant elasticity demand curve

A constant elasticity demand curve is of the form:

$$P(t) = mQ(t)^{-\frac{1}{\eta}}$$

where m is a constant to be determined with the PUC price and η is the elasticity of demand. Various consumer elasticities may be easily tested with this model, Figure 10-4.

Total benefits (social benefits) at some time are found by integrating the demand curve from some minimum Q_m to the current pumping rate Q_t. Q_m is needed since the equation for P(t) is ill-defined at $Q = 0$, and at very low pumping rates (very high prices) constant elasticities with an absolute value less than unity are unrealistic [14]. The actual choice of Q_m will not affect the characteristics of the results of the optimization; only the absolute value of

the objective function. In our analyses Q_m is set to 10 m^3/yr.

$$Benefit = \int_{Q_m}^{Q_t} mQ^{\frac{1}{\eta}} dQ$$

$$B(t) = \frac{m}{\frac{1}{\eta}+1}\left[Q_t^{1+\frac{1}{\eta}} - Q_m^{1+\frac{1}{\eta}}\right]$$

This quantity B(t) will be positive as long as Q_m is small enough.

Linear demand curve

The linear demand curve is simply of the form:

$$P(t) = aQ(t) + b$$

where a is a slope which must be set by the user, and b is fixed by the PUC water price once a is chosen. The PUC price was applied with the quantity of water currently being extracted at Kuki'o, 1.38x10^6 m^3/yr. For instance, for a slope of $a = -0.0001$, $P(t) = -0.0001Q(t) + 1.316$. The dual-aquifer model was run with various slopes in order to see the affect on pumping strategies, Figure 10-5.

The choice of a is important because it figures into determining the elasticity of demand, η, for the water resource. Note that elasticity changes along the linear demand curve; it is a function of price and quantity at a given point as well as the slope.

$$\eta = \frac{P}{aQ}$$

Benefit is calculated as:

$$Benefit = \int_{Q_m}^{Q_t} (aQ + b)dQ$$

$$B(t) = \left[\frac{a}{2}Q_t^2 + bQ_t\right] - \left[\frac{a}{2}Q_m^2 + bQ_m\right]$$

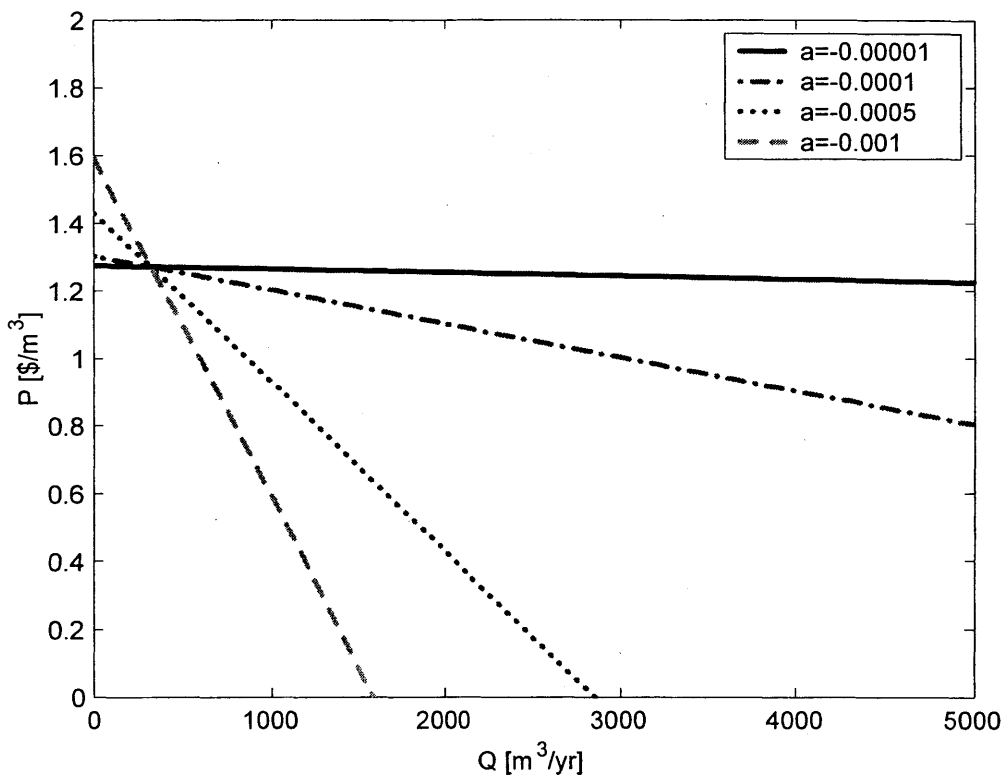

Figure 10-5: Linear demand curves with three different slopes.

10.2.8 Objective Function

The objective function is the discounted net benefits minus capital costs. Capital costs are not discounted since we assume they are incurred only at the beginning[4].

$$J_{opt} = \sum_t D^t(TB^t - TC^t) \text{ - Capital Costs}$$

where TC is the total energy costs and TB is the total benefits of water pumped. D^t is the discounting function. The discrete time version of the standard exponential discount factor is used in all scenarios; except when indicated for the hyperbolic test cases.

$$D^t = \frac{1}{(1+r)^t}$$

10.2.9 Comments on the Numerical Model and Optimization Solver

All scenarios tested were run with the GAMS/MINOS optimization interface/language and solver [5]. All scenarios were run for 150 years, but only 75 years will be shown in the plots. This is to both exclude erroneous output towards the end of the time horizon, and also to better visualize the important changes happening at early times. It was found that even at low discount rates the system usually reaches equilibrium conditions before 75 years.

[4] It is possible to modify the model so that it may decide **when** to implement the high-level well and associated pipeline. This may be particularly important if preliminary runs indicate that the high-level well is not needed for a number of years.

Chapter 11

Results

11.1 Introduction

This chapter presents the results of the dual-aquifer economic-hydrologic model. Following a description of the base case or Control, the model is tested for its sensitivity to physical, economic, and discounting parameters. The implications for pumping schedules, water levels, and the economics are explained for each scenario run.

11.2 Base Case

The Control was run with inputs that fit the Kuki'o region as much as possible. Recharge inputs, aquifer lengths, energy costs, transmission line costs, water pricing, and initial coastal aquifer heads and salinities were all taken from the Kuki'o coastal experiments and sources affiliated with Kuki'o. The porosity, thickness of the leaky barrier, and K value are approximations based on the KI experiments and prior research in the area or on volcanic terrain similar to that of Kuki'o [60][28]. Table 11.1 outlines key inputs into the Control model:

11.2.1 Pumping

The trajectory for *total pumping* in both aquifers is shown at the bottom of Figure 11-1. Total pumping is high initially since the aquifers' conditions are very favorable quantity and quality wise, and because the discount weight is near one. This is the groundwater mining portion of

Parameter	Explanation [units]	Value
θ	porosity [-]	0.3
K'	leakage factor [m/yr]	100
R_h	high-level net recharge [m^3/yr]	1366
Rc	coastal net recharge [m^3/yr]	1153
l_h	high-level aquifer length [m]	5300
l_c	coastal aquifer length [m]	6850
W	aquifer unit width [m]	1
EP	energy price [$/KWH]	0.21
TC	transmission costs [$/m]	656
r	discount rate [1/t]	0.03

Table 11.1: Control model key input parameters

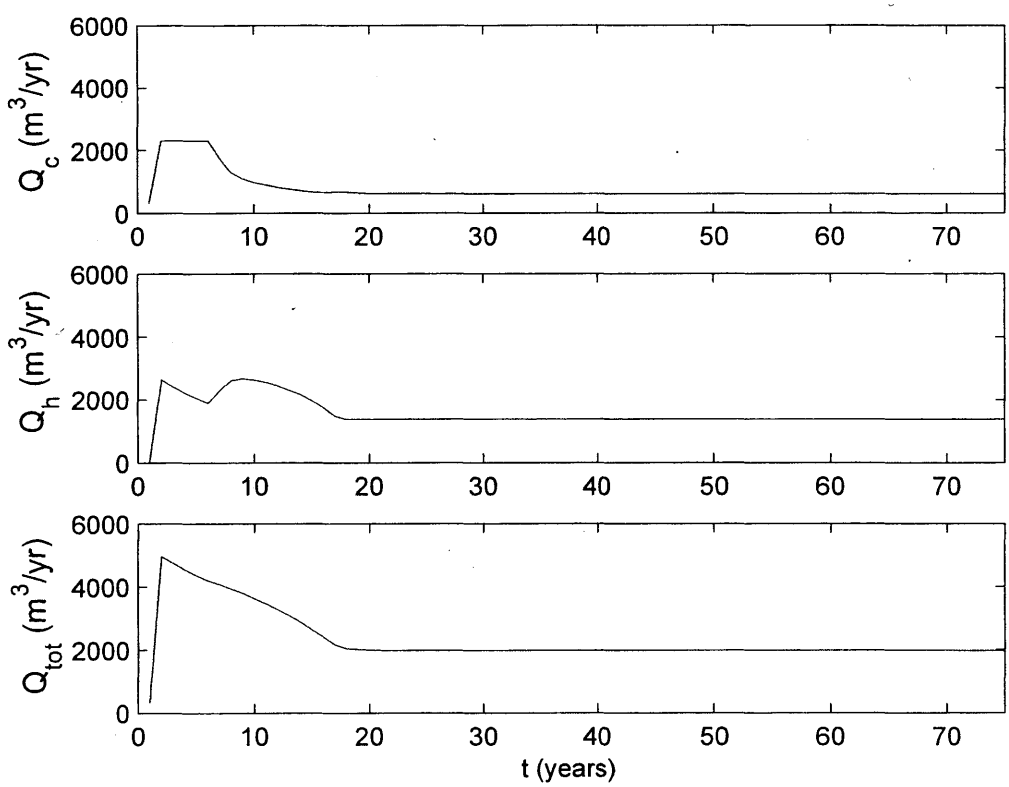

Figure 11-1: Optimal pumping trajectories for the base case.

the total pumping curve. Total pumping slowly declines as the aquifer conditions decline, and by year 18 a new equilibrium is reached which is economically optimal.

Both aquifers begin pumping at year 1 to satisfy the total pumping demand. Pumping in the coastal well quickly rises to 2304 m^3/yr and continues at this rate for about 5 years. It will not go above this level because pumping more water would drive RO capital costs too high. The high-level well also begins pumping immediately because the coastal well can't meet demand. However, after jumping to 2647 m^3/yr at year 1 the high-level well backs off slowly to 1889 m^3/yr by year 6. The increasing depth to the watertable leads to costs that are uneconomical given the demand curve and discount rate. However, after year 6 the coastal well is beginning to get so salty that it is uneconomical to continue pumping the coastal aquifer at such a high rate. Coastal pumping declines slowly while high-level pumping begins increasing to make up the difference in total demanded water. By year 10 the high-level well peaks a second time at 2682 m^3/yr, after which the depth to water becomes a limiting cost and high-level pumping also begins to decline with time.

By 18 - 20 years time the system has reached a new equilibrium where salinities, heads, leakage, and ocean discharge are stable at new levels. The degree of pumping fresh, deep high-level water is exactly that of yearly high-level recharge, 1366 m^3/yr. The degree of pumping salty, coastal water is only at about half of coastal recharge at 616 m^3/yr. It appears that the salty water becomes too expensive to treat if the coastal head is lowered anymore. Coastal pumping declines very slowly with time and is still only at 610 by year 75.

11.2.2 Heads and Leakage

Heads start at 0.3 m for the coastal aquifer and drop to about 0.1 m in the first 7 years; Figure 11-2. The new long-term equilibrium coastal level of 0.07 m is reached in about 18 years. The high level head starts at 14 m and declines fairly quickly with time, reaching the same long-term equilibrium of 0.07 m by year 18. These long-term equilibrium head levels of 0.07 m do *not* correspond to any lower-bound model constraints. The model is finding these heads to be optimal given the physical and economic constraints. Note that these heads are small compared to the depth to water; the ground surface is at 457 m.

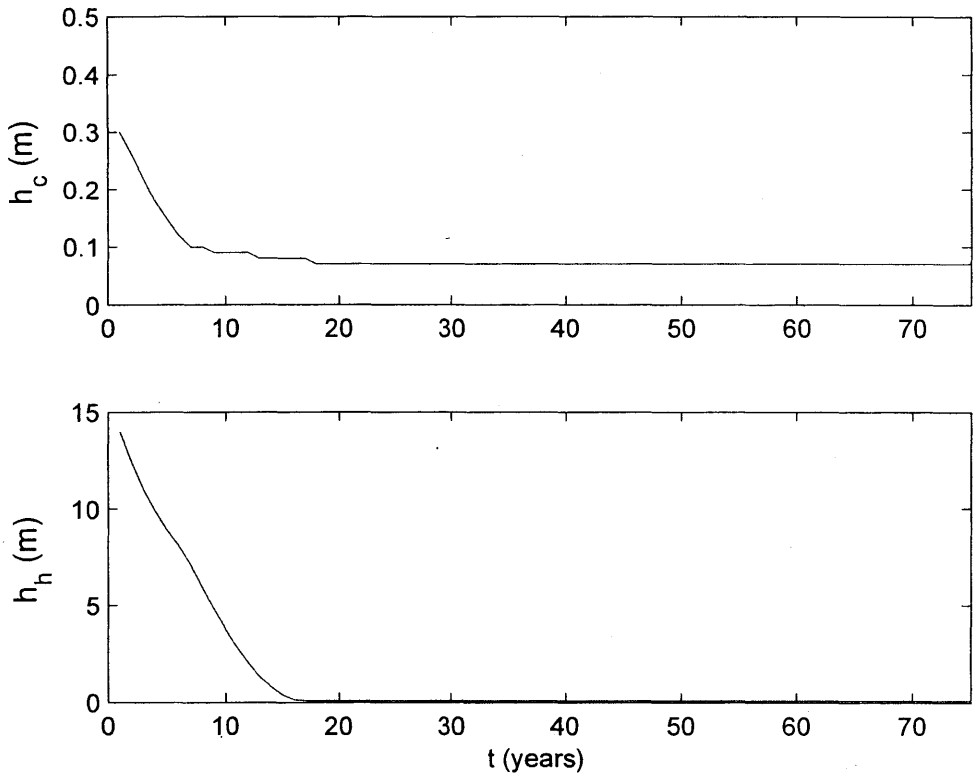

Figure 11-2: Head trajectories for base case.

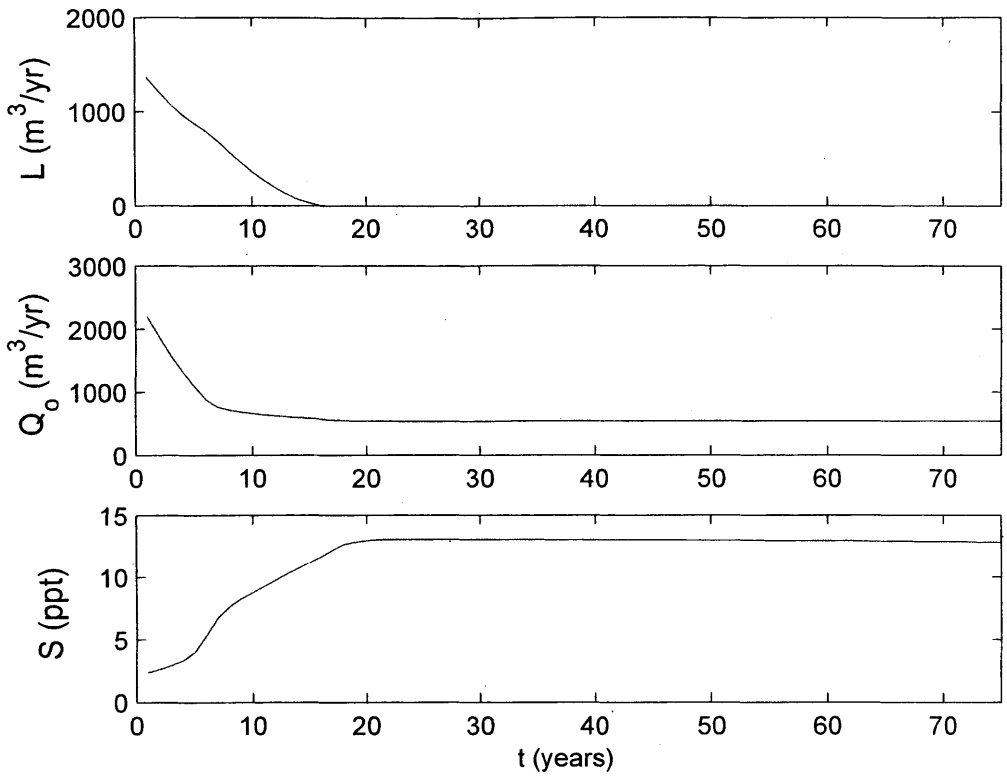

Figure 11-3: Leakage, ocean discharge, and salinity trajectories for the base case.

11.2.3 Leakage, Coastal Salinities and Ocean Discharge

Leakage starts high at 1366 m^3/yr, but goes to zero as the head gradient between the two aquifers goes to zero with time; Figure 11-3.

Initial salinities were at 2.4 ppt, and quickly rise during the heavy coastal pumping at early times. They continue to rise to 13 ppt at 20 years, after which they very slowly decline with time; in tandem with slowly declining coastal pumping rates.

Ocean discharge is initially at 2197 m^3/yr, but quickly declines to about a fourth of that. Q_o is 535 m^3/yr at 25 years and rises slowly as Q_c declines with time; it is still only at 539 m^3/yr by year 100.

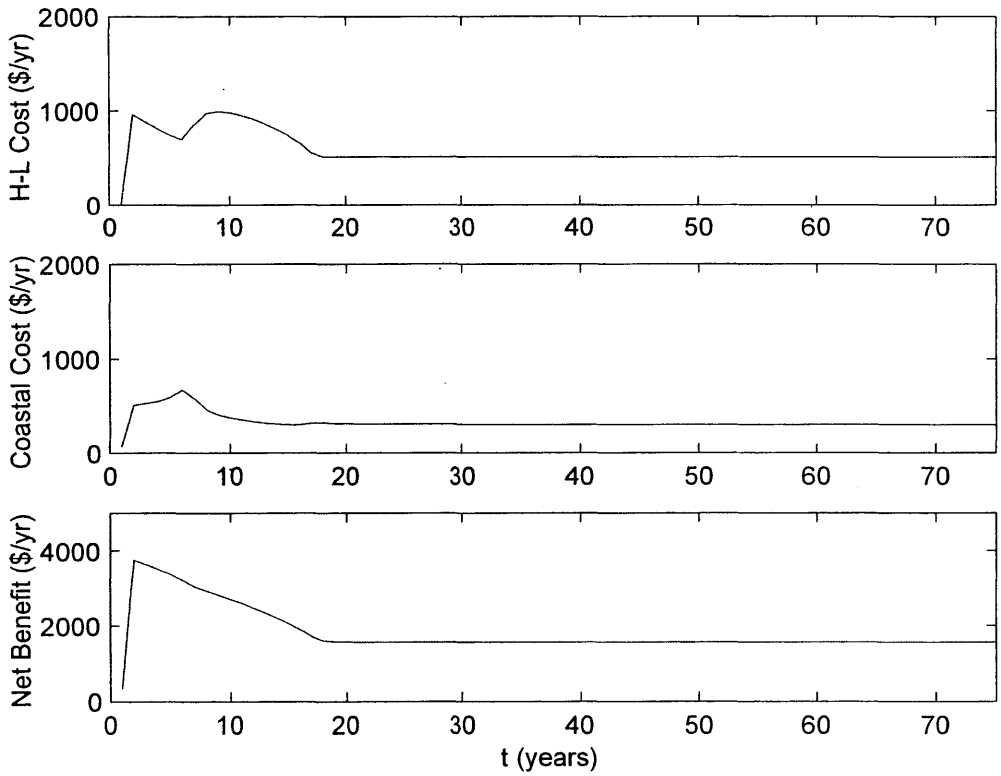

Figure 11-4: Cost and benefit trajectories for the base case.

11.2.4 Economics

Coastal costs rise quickly to 500 \$/yr and continue rising to a peak value of 663 \$/yr at 6 years. Coastal costs decline with coastal pumping after this and are at 300 \$/yr by year 15. They do decline very slowly with time, but for all intensive purposes are constant in time.

The high-level cost curve mimics its pumping curve and has two peaks before leveling off to an equilibrium value at 510 \$/yr by year 18.

Total capital costs equal \$2734 [1]. Of the total capital costs, \$1841 is for an RO treatment plant capable of treating about 6.3 m^3/day (1669 G/day). Keep in mind that this is all for a unit width. Total capital costs for the region amount to \$16.4 million dollars, and the RO plant will cost over \$11 million dollars and be able to treat 37,800 m^3/day (10 MGD).

As expected, the highest yearly benefits are at early years. Yearly benefit peaks at a little over 3745 \$/yr at year 2, but settles to 1563 \$/yr at later times. The objective value over 150 years is \$6.34x10^4 (per unit width). These numbers are not that important in and of themselves, but do serve as a guide for comparison to the various scenarios described below.

Note that the large amount of pumping at early times assumes that there will be a market for this "extra" water. For instance, the water may be sold to outside users or used for a short-term (< 18 years) project. If the water is used purely for residential development, it would be politically infeasible to curtail water use after 18 years. The model may be easily modified to account for the reality of a particular management/development project. For example, a constraint could be inserted that only allows for an increase in pumping with time. This would have the effect of getting rid of the early peak of pumping and allowing for a slightly higher long-term equilibrium pumping rate.

11.3 Summary of System Sensitivity to Input Parameters

Table 11.2 lists the important uncertain system inputs/parameters and how sensitive the optimal management solution is to the respective input. *Low* sensitivity means that the general

[1] This is not a mixed integer model, and therefore the decision to incur the capital cost of building the transmission line for the high-level aquifer was decided manually. The model was run with and without the high-level well to this end. In all cases it was found that the benefit of the additional high-level pumping outweighed the capital cost of the pipeline.

Parameter/Input	Sensitivity	Comments
Leakage Factor (K')	High	Especially important for the groundwater mining portion of the pumping curves. The high-level aquifer is most affected.
Energy Cost	Low	Does affect net benefits slightly, but the qualitative characteristics of the optimal trajectories remain relatively unchanged.
Discount Rate (r)	Moderate	The magnitude of high-level pumping is affected at early times, but the general shape of the curve remains unchanged.
Slope of Linear Demand Curve (**a**)	High	Affects both aquifers significantly. The high-level well never pumps for the steepest demand curve (a = -0.001).
η in Constant Elasticity Demand Curves	High	Affects both aquifers significantly. The high-level well never pumps for low elasticities ($\eta = 0.4, 1.1$).
Discounting Formulation	Moderate	High-level aquifer more sensitive when leakage factor is low, coastal more sensitive when leakage factor high.

Table 11.2: Relative sensitivity of the dual-aquifer model to the important uncertain system inputs

shape and magnitude of the optimal pumping strategies and resultant system conditions do not change significantly when the parameter is varied. *Moderate* sensitivity means that a particular parameter may have a significant effect depending on what other system parameters are and on the time horizon one is considering. *High* sensitivity means that the optimal trajectories may change in a significant fashion if the parameter is varied.

For brevity, only the high sensitivity cases are fully discussed in the following sections. The low and moderate sensitivity cases are summarized; the corresponding plots may be found in the Appendix.

11.4 Sensitivity to Conductivity of Leaky Barrier

In this section the model is tested for its sensitivity to leakage from the high-level aquifer to the coastal aquifer. The parameter varied is the leakage factor, K', which is the ratio of hydraulic conductivity, leakage face, and barrier thickness, $\frac{KD_l}{b}$ [m/yr]. The leakage factor is tested over four orders of magnitude.

11.4.1 Pumping

Changing the leakage factor does not significantly affect pumping from the coastal aquifer; Figure 11-5. Interestingly, the coastal trajectories do not change in a predictable, monotonic fashion with K'. The pumping plateau for K' = 10 is the lowest and the plateau for K' = 1000 lies right above it in magnitude. Then K' = 50, followed by K'= 100 with the highest plateau in pumping. This is an unexpected result that wouldn't have been predictable without the complete model. The solutions are most different between years 5 and 20, and change at most by a factor of 2 between scenarios.

The effect of low K' values on the high-level pumping trajectories are more dramatic. While the coastal well is already doing the best that it can, the high-level aquifer is seeing a larger store of water as the K' values decrease. This means that when the high-level pump starts up it has a much larger store of water to mine from. In addition, the high-level well will be mining water for a lot longer. High-level pumping is above the long-term equilibrium of 1366 m^3/yr for nearly 60 years when K' = 10 m/yr, as opposed to 10 years with K' = 1000 m/yr.

11.4.2 Heads

Following the logic in the pumping explanation, heads change most dramatically for the high-level case. Low K' values allow heads to rise to a maximum of 137 m for K' = 10, and 27.6 m for K' = 50. This is compared to a high-level max head of 14 m in the Control case. Heads will eventually all go to the long-term equilibrium value of 0.07 m, but with lower leakage factor values it takes longer for the system to reach that equilibrium.

Though not as dramatically, the coastal heads do exhibit changes with K'. Most noticeable is that the heads are above the long-term equilibrium of 0.07 m for a much longer period of time. For K' = 10 coastal heads are over 0.1 m until about 55 years time.

11.4.3 Leakage, Coastal Salinities, and Ocean Discharge

What is most interesting in the plot for leakage is not the differences in leakage magnitudes, but the shape and time frame of the leakage trajectories. For the highest leakage factor value, K' = 1000, the system time scale is very fast and the high-level aquifer leaks its store of water to the coastal aquifer at a high-rate and is "empty" in only about 4 years; except for a small

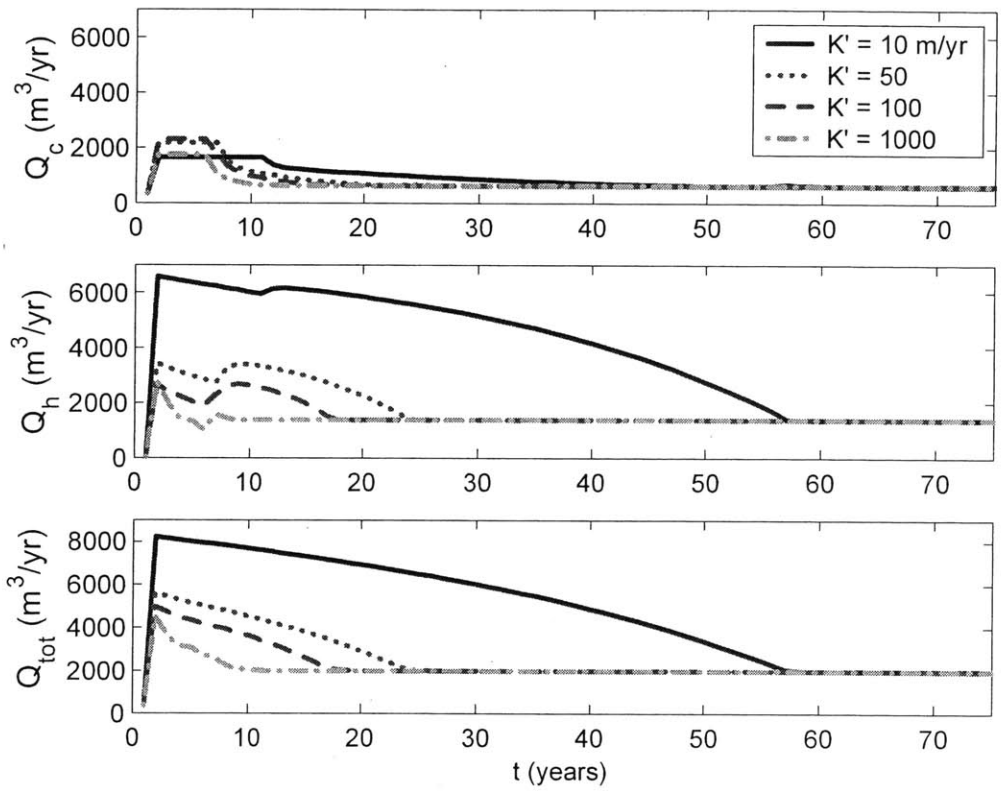

Figure 11-5: Optimal pumping trajectories for scenarios with K' varied.

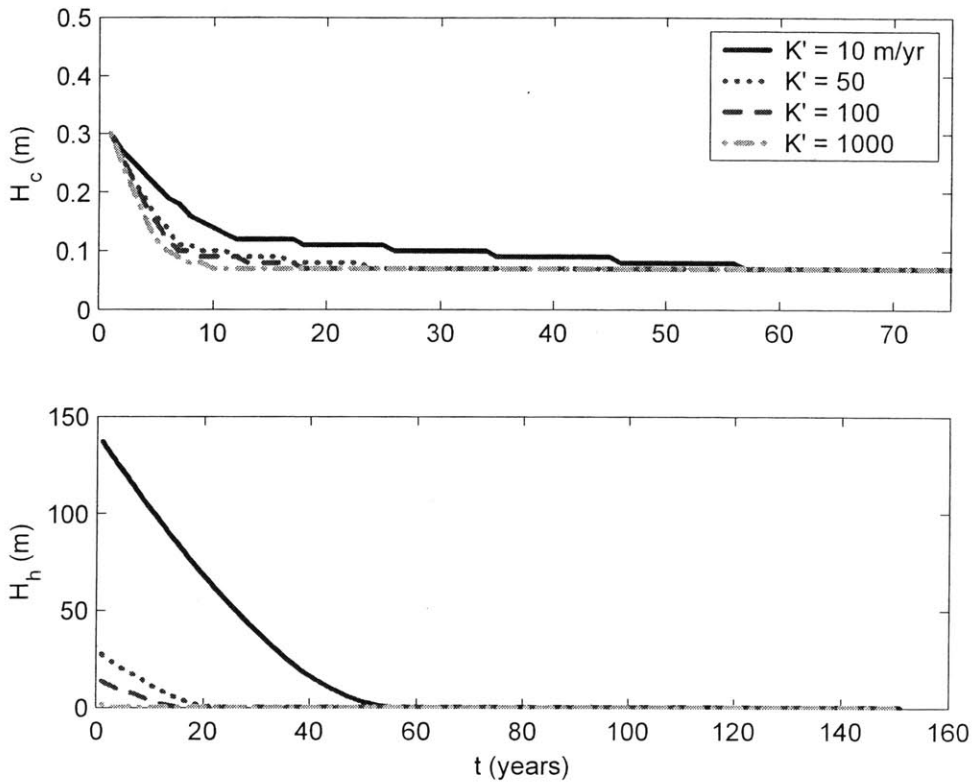

Figure 11-6: Optimal head trajectories for scenarios with K' varied.

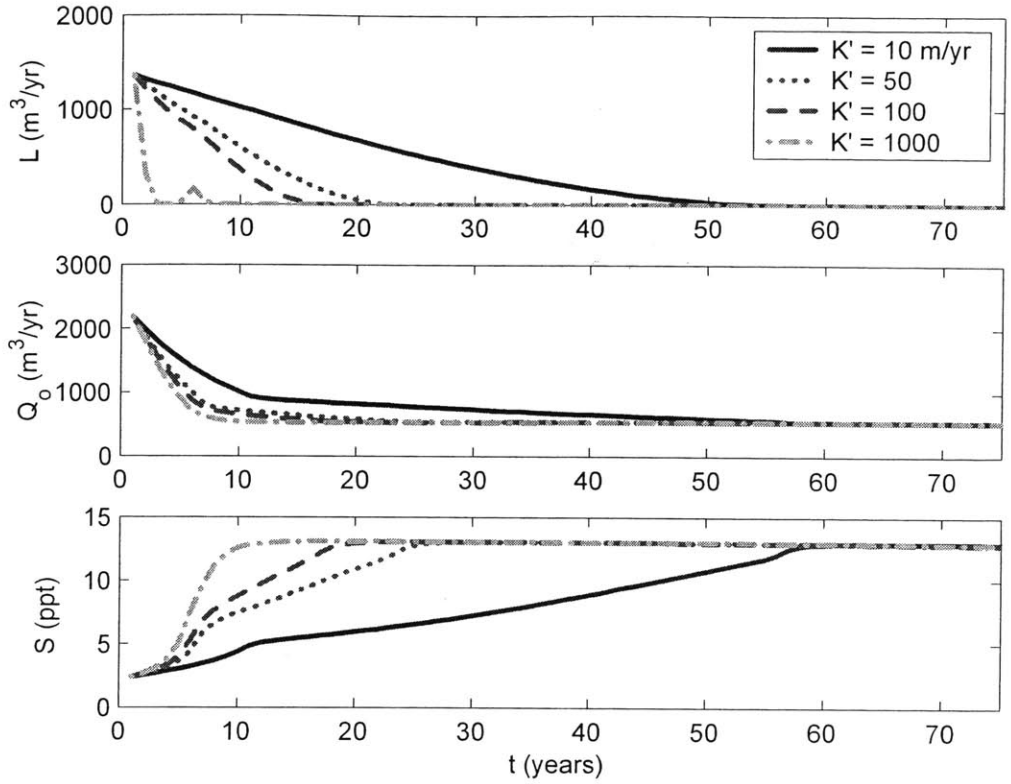

Figure 11-7: Optimal leakage, ocean discharge, and salinity results for the scenarios with K' varied.

blip at 6 years due to the inflection in high-level pumping. On the other hand, at increasingly low leakage factors the slopes of the leakage curves become much gentler and distribute the leakage of water over much longer times scales.

The discharge to the ocean is slightly higher for low K' values. The reason is that at early times the higher leakage is putting more water into the coastal aquifer than it can economically use, and so more is discharged to the ocean.

Salinity levels are depressed for a much longer time for low K' factors since leakage is higher and it takes much longer for the system to reach the long-term equilibrium.

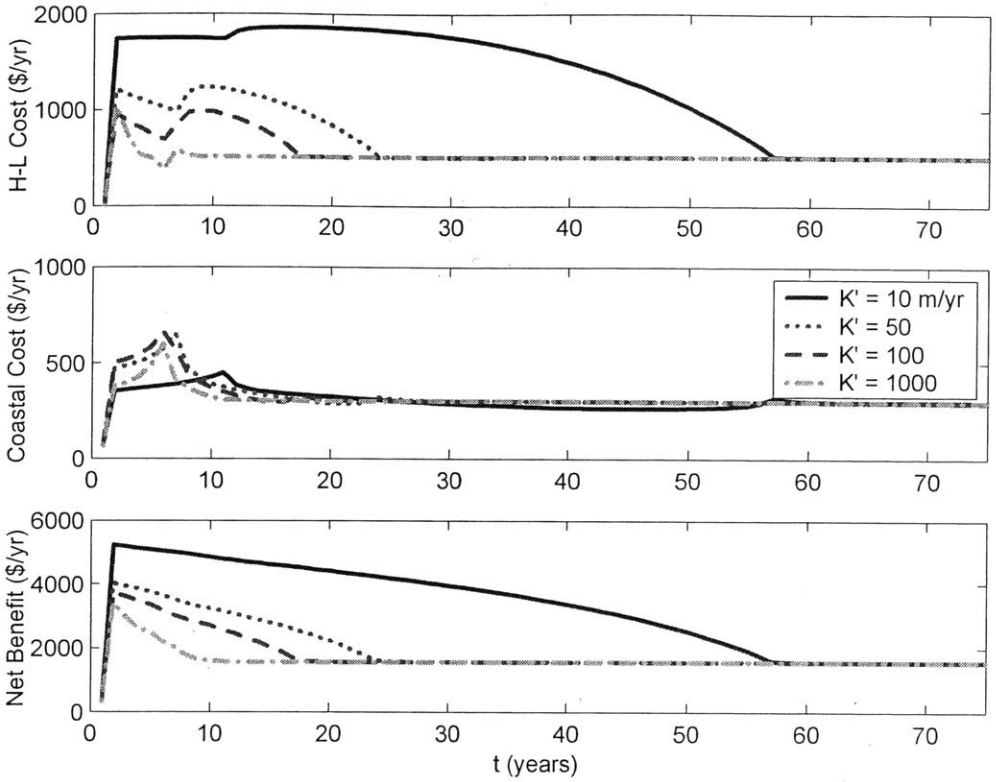

Figure 11-8: Cost and benefit trajectories for the scenarios with K' varied.

11.4.4 Economics

The economics are significantly affected by the the K' value. The high-level aquifer is deriving a lot more utility for low K'ca ses. Energy costs are higher of course, but the net benefit curve peaks at 5217 $/yr for K' = 10, as opposed to 3433 $/yr for K' = 1000. The long-term net benefit rate still levels out at a little less than 2000 $/yr, but that is not until over 55 years of highly profitable operation. Discounted net benefit over the 150 years is at $\$1.2\text{x}10^5$ for K' = 10; almost double the Control objective value of $\$6.34\text{x}10^4$.

Capital costs remain roughly the same because the transmission line is a fixed quantity and the coastal well optimal trajectories vary little. RO treatment costs vary at most by 30% over all the scenarios.

11.5 Sensitivity to Energy Costs

The model was tested for its sensitivity to energy rate by varying the amount paid per kilowatt-hour. Since the desalinization costs are directly related to head, which is then related to energy, all lift and desalinization costs are being affected when varying this one parameter. Four scenarios are run, \$0.09, \$0.15, \$0.30, and the base case of \$0.21. Results are summarized here, see Appendix B for complete plots of the results.

Pumping: Higher energy costs slightly depressed both coastal and high-level pumping rates, but the overall characteristics of the pumping trajectories changed very little. The only notable point is that higher energy rates extends the period of time until the high-level aquifer reaches its long-term equilibrium pumping rate. What is happening is that the higher energy prices translate to lower pumping rates and hence a longer period of time to mine the aquifer to the long-term optimal depth.

Heads: Heads in the two aquifers are slightly elevated for higher energy prices. This makes intuitive sense as higher heads mean lower lift costs, while the benefit of a unit of water lifted is still the same.

Leakage, Coastal Salinities, and Ocean Discharge: Leakage from the high-level aquifer to the coast is elevated and prolonged at higher energy prices since it takes longer to mine the high-level aquifer to its optimal depth. Leakage goes to zero in about 14 years for a price of \$0.09-\$0.21, and takes 20 years with a price of \$0.30. Ocean discharge rises slightly for higher energy prices due to higher equilibrium heads in the coastal aquifer and hence a higher gradient to the ocean. Coastal aquifer salinity values will obviously decrease in response to the higher coastal heads. It is worth noting that the highly non-linear salinity-head equation makes for fairly significant salinity changes with only modest heads changes. Heads change by only less than 25% over the range of energy prices, but salinity levels change by over 100%.

Economics: The effect of energy prices on the resultant economics and objective value are obvious. The high-level cost curve for the \$0.30 energy price is shifted up to almost double the \$0.09 scenario. The changes in the coastal cost curve are not quite as large due to the fact that the coastal well compensates by adjusting the coastal head slightly higher at higher energy prices and not pumping as much. Apparently it is optimal for the high-level aquifer to empty with time no matter the energy price, hence the relatively higher changes in high-level

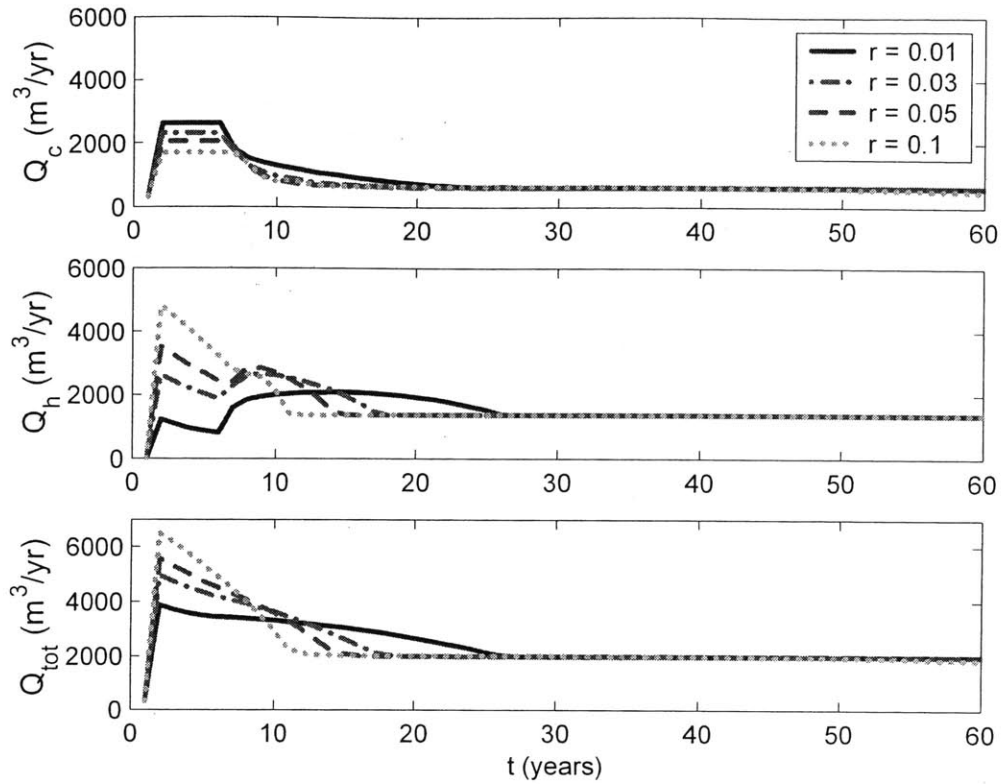

Figure 11-9: Pumping trajectories for scenarios with discount rate varied.

versus coastal costs. Yearly net benefits change by at most about 30% and the objective value varies from \$5.03x10^4 for a price of \$0.30, to \$8.33x10^4 for a price of \$0.09. That's about a 40% decrease in net discounted benefit for a 300% increase in energy price.

11.6 Sensitivity to Discount Rate

Four discount rates were tested with the model, r = 0.01, 0.03, 0.05, and 0.1. Only the pumping plot is shown here, all other plots may be found in Appendix C.

Pumping: A higher discount rate devalues the future more so there is more initial total pumping demand and the high-level aquifer pumps more at early times; Figure 11-9. Interestingly, since it is more economical for the high-level aquifer to meet this higher demand, the coastal well actually pumps less for higher discount rates.

Heads: High-level heads are higher for lower discount rates due to the lower peaks in

pumping spread out over more time. At early time, t < 6 years, coastal heads are higher for higher discount rates due to less pumpage. However, between years 6 and 25 high discount rates lead to lower coastal heads since the high-level aquifer has been mined faster and leakage correspondingly reduced.

Leakage, Coastal Salinities, and Ocean Discharge: Leakage is higher and spread over more years for lower discount rates. The higher high-level heads under low r conditions allows for more gradient between the aquifers. It takes about 10 years longer for leakage to empty the high-level aquifer for r = 0.01 as opposed to r = 0.1. Ocean discharge changes very little with discount rate. Coastal salinities are higher for lower discount rates at early times (1 < t < 8 years) due to more coastal pumping. However, at all later times salinity is elevated for higher discount rates since the buffering effect of the high-level aquifer is reduced with time as it is mined harder.

Economics: High-level costs increase significantly with discount rate, rising by a factor of 3.5 when r increase from 0.01 to 0.1. Coastal costs change very little with discount rate. There is more initial net benefit for higher discount rates, but not by more than 25% over the range. The objective function value varies from $\$1.36\text{x}10^5$ for r = 0.01 to $\$2.29\text{x}10^4$ for r = 0.1.

11.7 Sensitivity to Slope of Linear Demand Curve

11.7.1 Pumping

The optimal solutions are very sensitive to slope of the demand curve, Figure 11-10. Most notable is that for the steepest demand curve, slope of -0.001, the high-level well will never turn on. There simply is no economic demand for more water than the coastal aquifer can already supply. For a slightly shallower slope of -0.0005 the high-level well starts pumping at year 10, and gradually ramps up over time to equal high-level recharge. For a slope gentler than the base case, slope = -0.00001, there is much more high-level pumping and this pumping is initiated earlier.

The coastal well response depends on whether or not the steepness of the slope does or doesn't necessitate the need for high-level pumping. Like the base case, with a gentle slope of

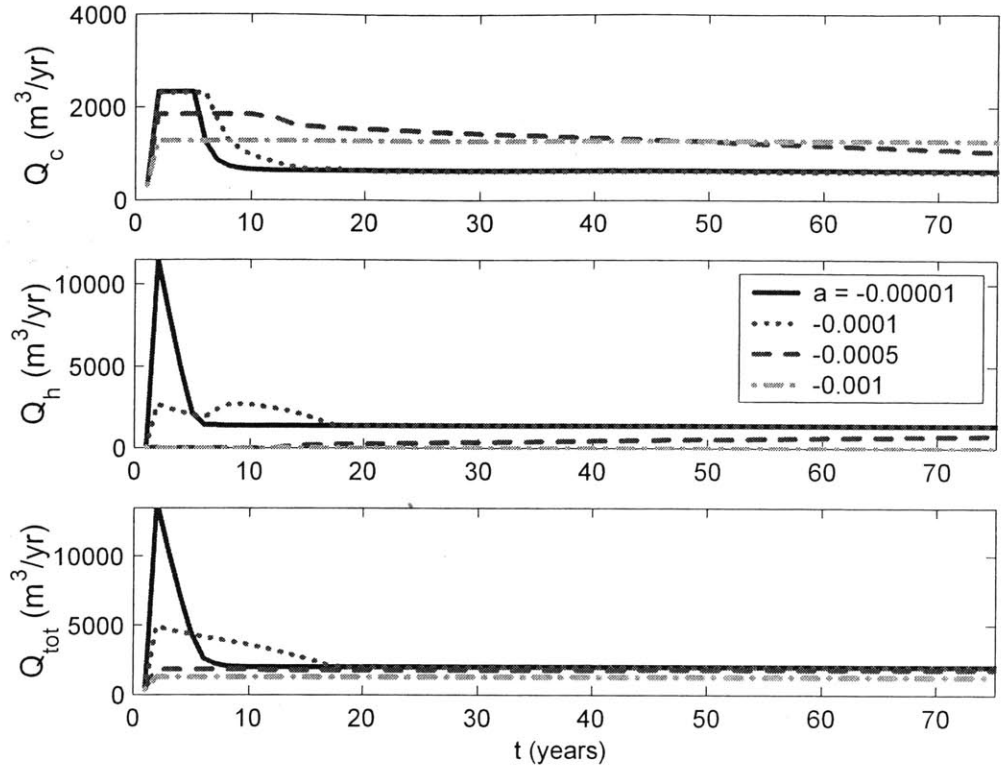

Figure 11-10: Optimal pumping strategies for scenarios with the demand curve slope varied.

-0.00001 the coastal well plateaus at early times and then drops to a new equilibrium pumping level. For the two steepest demand curves there is effectively a cap on pumping due to the lack of benefit of high volumes of water. Therefore, the coastal aquifer only peaks slightly at early times. For a = -0.0005 the coastal pumping well will gradually decline over time to the base case long-term rate. For a = -0.001, since the coastal well is supplying all demand, the initial peak is very small, but the long-term equilibrium rate is double the base case rate.

11.7.2 Heads

The lack of pumping in the high-level aquifer for a = -0.001 means that the high-level head remains at initial conditions; Figure 11-11.. For a = -0.0005 the high-level head very slowly declines with time; h_h is still at 7.71 m at year 75.

Though only the coastal well pumps for the steepest demand curve, coastal heads are higher.

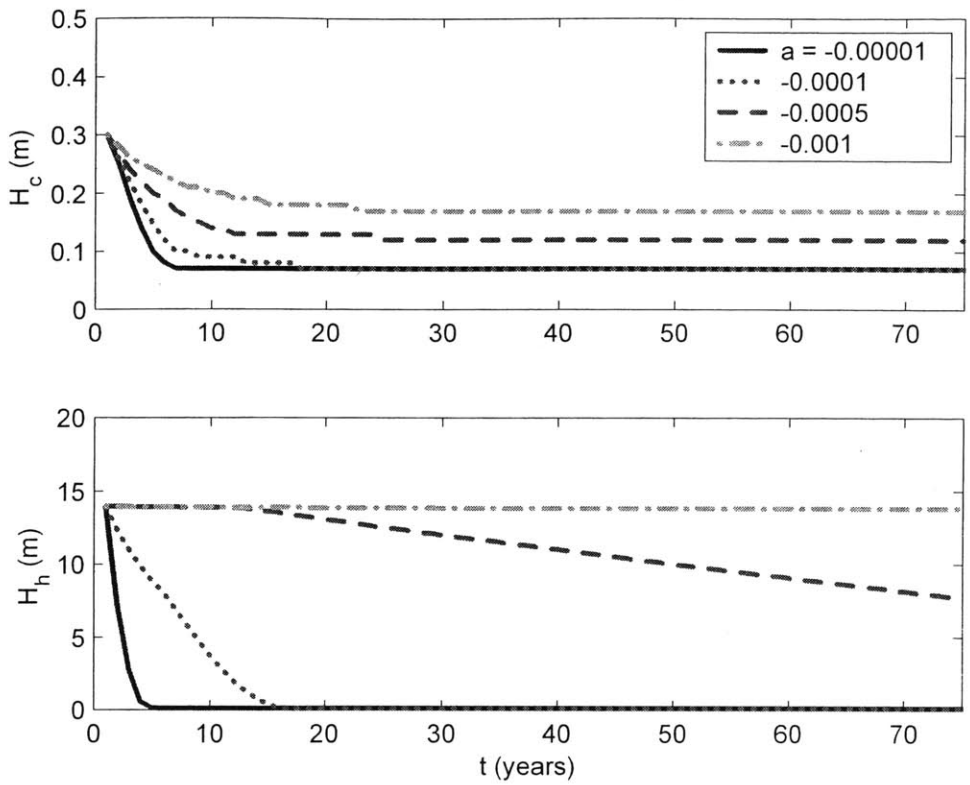

Figure 11-11: Head trajectories for scenarios with demand curve slope varied.

Equilibrium coastal heads more than double from 0.08 to 0.2 m when the demand slope is changed from -0.0001 to -0.001. Less demand for water causes the coastal well to implement a more moderate pumping trajectory which doesn't bring heads down radically initially, but rather brings it down to a modest level slowly.

11.7.3 Leakage, Coastal Salinities, and Ocean Discharge

Leakage from the high-level aquifer is sustained and fairly high for steep demand curves, Figure 11-12. Leakage equals incoming recharge for all time for the steepest slope. For a = -0.0005 leakage declines slowly to zero; at 75 years leakage is still at 760 m^3/yr.

Ocean discharge rises for the steep slope scenarios as less water is being taken out of the system.

Important for quality reasons, salinities are radically effected by the slope of the demand

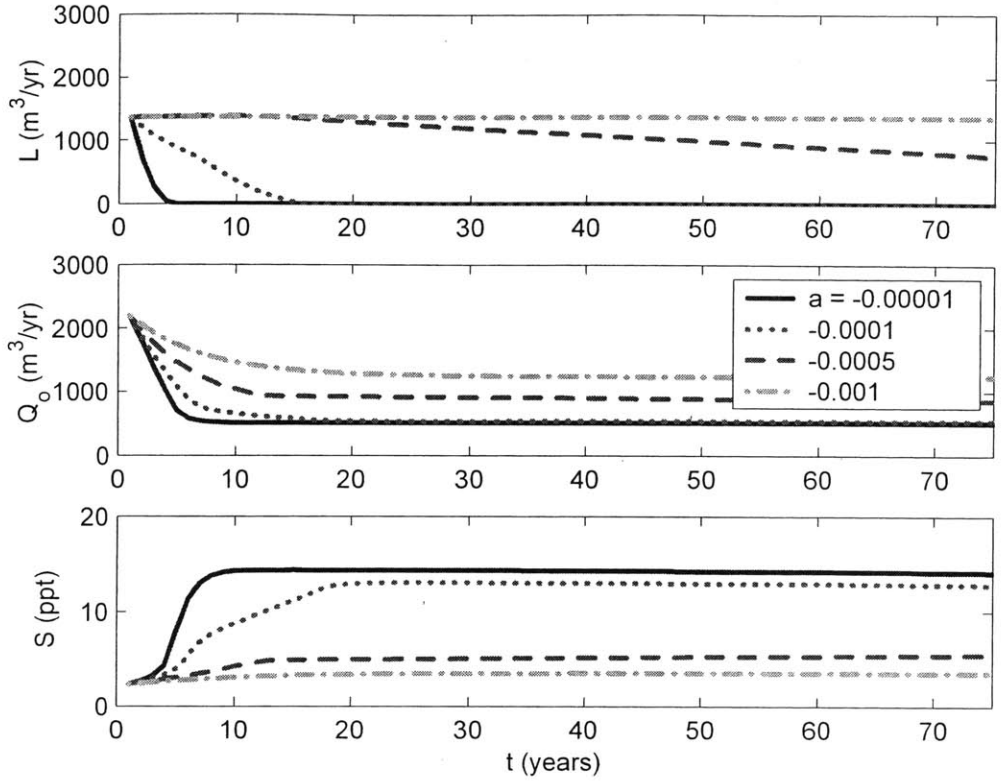

Figure 11-12: Leakage, ocean discharge, and salinities for scenarios with demand curve slope varied.

curve. The higher coastal heads due to steep demand curve slopes lead to significantly reduced chlorides from the Control. Salinities are only about 3.5 ppt as opposed to 13 ppt.

11.7.4 Economics

High-level costs obviously go to zero for the steepest demand curve modeled since there's no high-level pumping. Coastal cost changes resemble coastal pumping changes with slope. Gentler demand slopes lead to steeper inital cost curves, while steep demand slopes correspond to much flatter coastal cost curves, Figure 11-13.

Net benefits are reduced for steeper demand curves. Short term net benefits change radically, varying from 928 \$/yr to 11,941 \$/yr. Total net discounted benefit for the 150 years is \$7.47x10^4 for -0.00001 and \$2.73x10^4 for -0.001. Obviously the high-level capital costs need

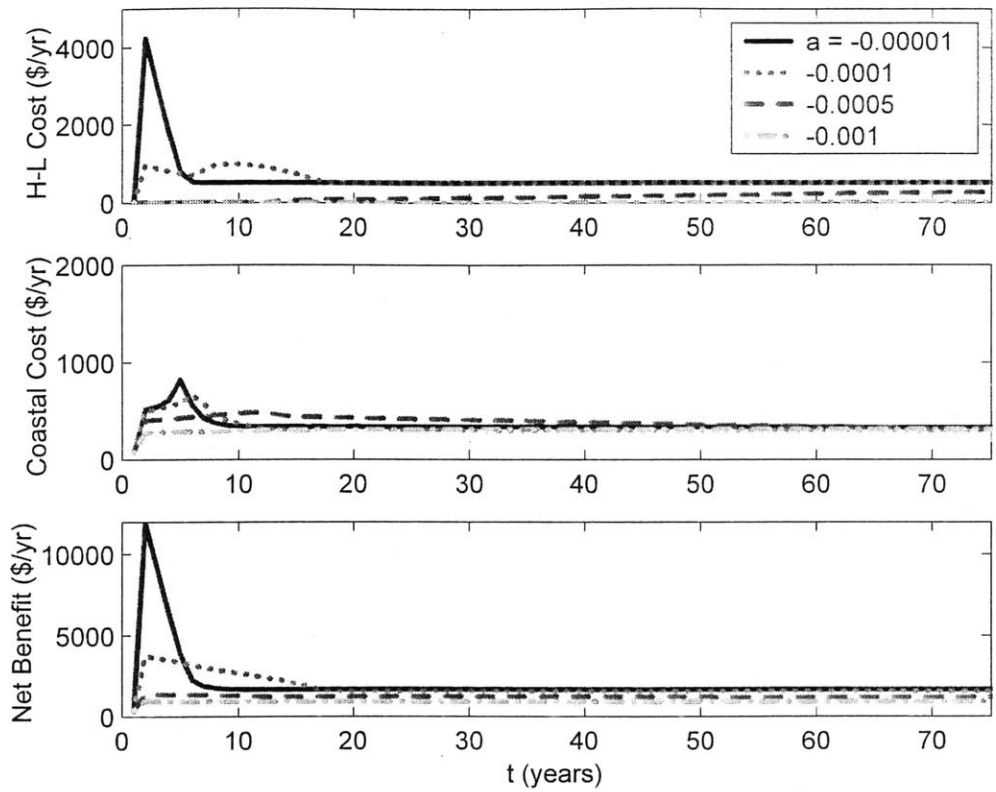

Figure 11-13: Economic results for the scenarios with demand curve slope varied.

to be subtracted from the total discounted benefit in the scenario where no high-level pumping occurs.

11.8 Constant Elasticity Demand Curve

Constant elasticity demand curves are tested to see how much the optimal solution trajectories vary from the linear demand curve trajectories. The constant elasticity curves shown in Figure 10-4 are used for the four scenarios run.

11.8.1 Pumping

The optimal coastal pumping solutions bear close resemblence to solutions with a linear demand curve, Figure 11-14. For the inelastic consumer, $\eta = -0.4$, pumping is low at only about 615

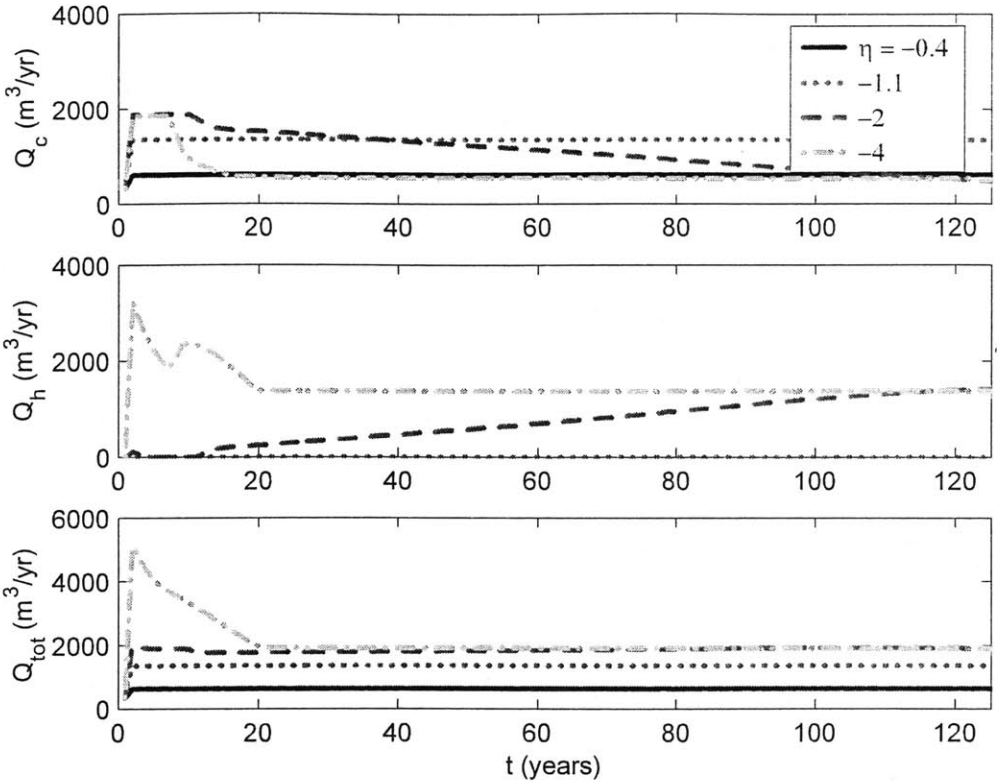

Figure 11-14: Optimal pumping for constant elasticity scenarios.

m^3/yr since the demand curve asymptotically approaches zero price very quickly; which is similar to the cases with a steep linear demand slope. With higher elasticities the coastal well pumps more and at magnitudes similar to the linear demand curve with gentler slope.

Only the two most elastic scenarios, $\eta = -2$ and -4, have any high-level pumping occuring. The demand price drops too much in the other cases to justify the costs of high-level pumping. The high prices at low quantities of water make pumping only the coastal aquifer much more attractive than pumping high volumes using the high-level aquifer except for the most elastic consumers.

11.8.2 Heads

Heads in the high-level aquifer only decline with time for the two high elasticity cases, Figure 11-15. The coastal heads are highest for the lower elasticities where little pumping is happening.

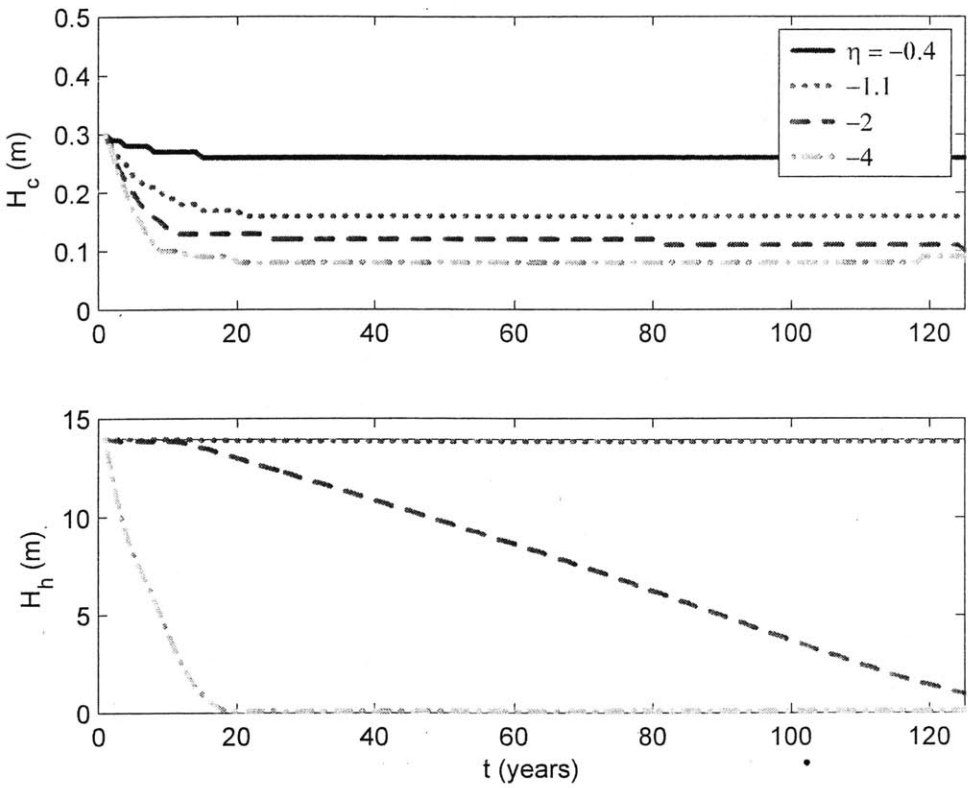

Figure 11-15: Optimal heads for constant elasticity scenarios.

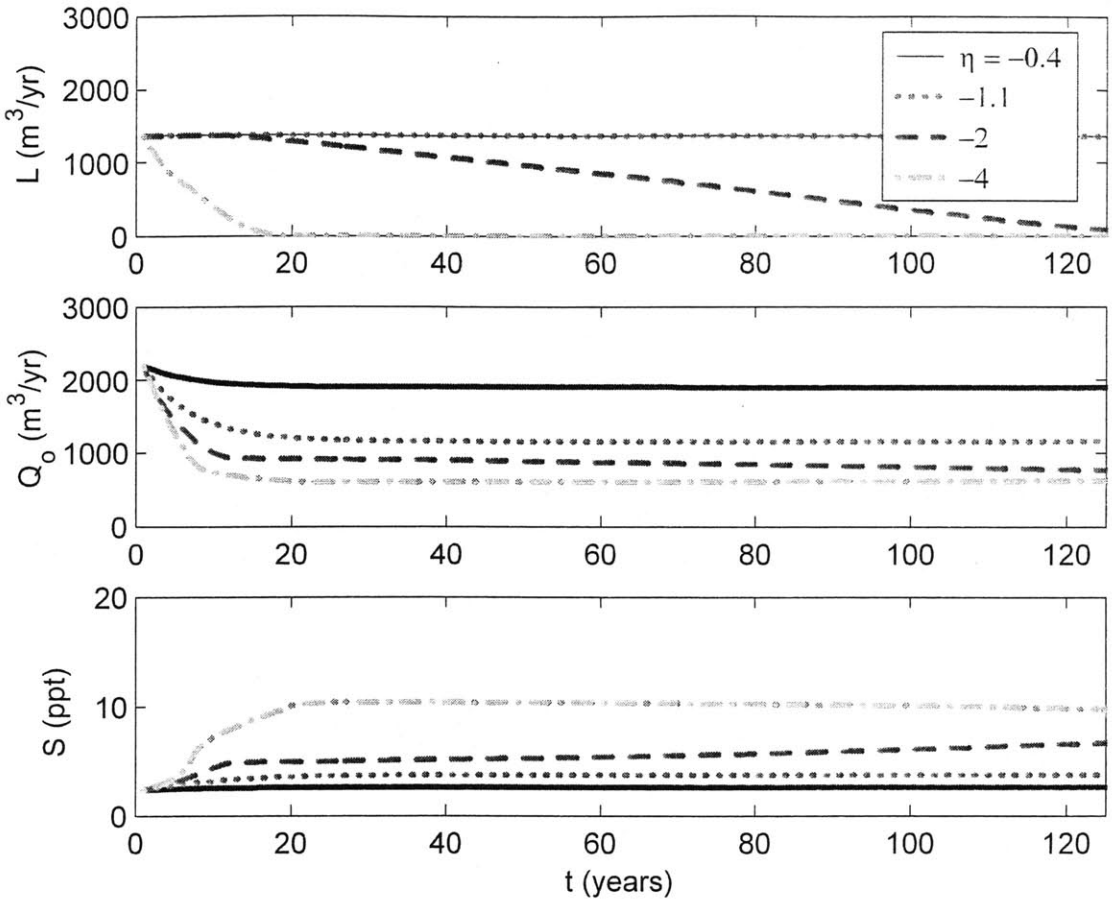

Figure 11-16: Leakage, ocean discharge, and coastal salinities for the constant elasticity scenarios.

11.8.3 Leakage, Coastal Salinities, and Ocean Discharge

Leakage does not change for the low elasticity cases where no high-level pumping occurs, Figure 11-16. Leakage declines much slower for $\eta = -2$ than for $\eta = -4$.

Ocean discharge decreases with increasing elasticity since there is increasing pumpage.

Salinity is just the opposite. Salinities drop significantly depending on the coastal aquifer head and pumpage. Salinity is lowest for the inelastic cases due to low pumpage. It changes by over 300% over the range of elasticities tested here.

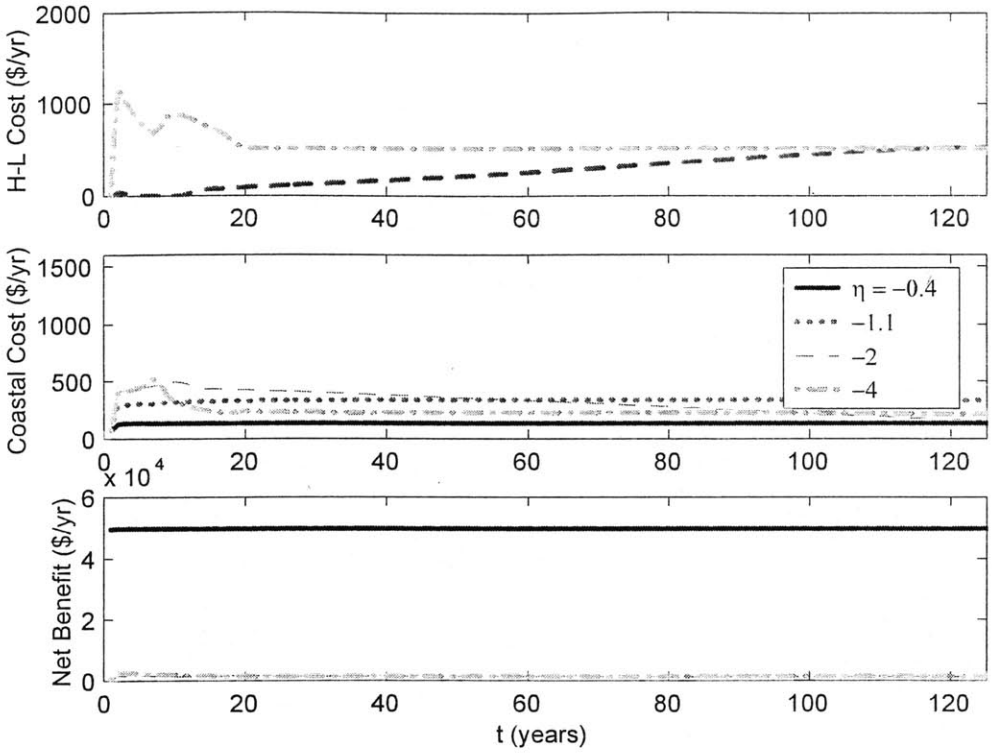

Figure 11-17: Economics for the constant elasticity scenarios.

11.8.4 Economics

The interesting economic result here is that even though there is no high-level benefit for the inelastic solution, $\eta = -0.4$, this one has the highest net yearly benefits. The very high (probably unrealistic) prices for low quantities of water for this low elasticity results in exhorbitant benefits at lower pumping rates. The objective value for $\eta = -0.4$ is $\$1.83\text{x}10^7$, while all the other scenarios are on the order of $\$10^4$.

11.9 Changing the Discounting Formulation

Now the whole discounting formulation, not just discount rate, is varied within the model. These scenarios investigate how hyperbolic discounting affects the optimal management strategies. The discounting factor implemented is that discussed in Part I of this dissertation, namely,

$$D^t = \frac{1}{(1+rt)^2}.$$

The hyperbolic discounting function is compared to the exponential base case, and both discounting factors are also applied to the scenario with K' = 10 m/yr. *All scenarios in this section are with r = 0.1 for both discounting formulations.*

11.9.1 Pumping

At early times the effect of the leakage factor dominates the results and the exponential and hyperbolic coastal trajectories are similar for each of the two leakage factor scenarios tested, with the hyperbolic solutions pumping less than the exponential solutions. At late times (t > 50 years) the discount factor begins to affect the solutions in a more significant way; Figure 11-18. Coastal pumping begins to decline for both of the exponential solutions, while the two hyperbolic scenarios continue to pump coastal water since the future is valued more.

High-level pumping trajectories do not change that dramatically. For the scenarios with K' =10, the hyperbolic solution starts off slightly higher than the exponential solution but is lower for years 5 - 35. After that the hyperbolic pumping solution is again higher than the exponential solution because it has been mining the high-level aquifer at a reduced rate. For K' = 100, the hyperbolic solution is lower than the exponential solution until year 8, and then it is lower for a few years until both high-level pumping solutions go to the same long-term equilibrium.

11.9.2 Heads

As with coastal pumping, at early times coastal heads are most influenced by the leakage factor but later dominated by the discount factor, Figure 11-19. It is interesting how the curves split at about 45 years. The two low K' curves were side by side all the way to year 40, then the exponential curve "jumps track" to follow the high K' exponential solution from that time on. From year 45 on the coastal heads recover for the exponential solutions, but continue to decline for the hyperbolic solutions.

The high-level heads are always dominated by the leakage factor, with the hyperbolic solu-

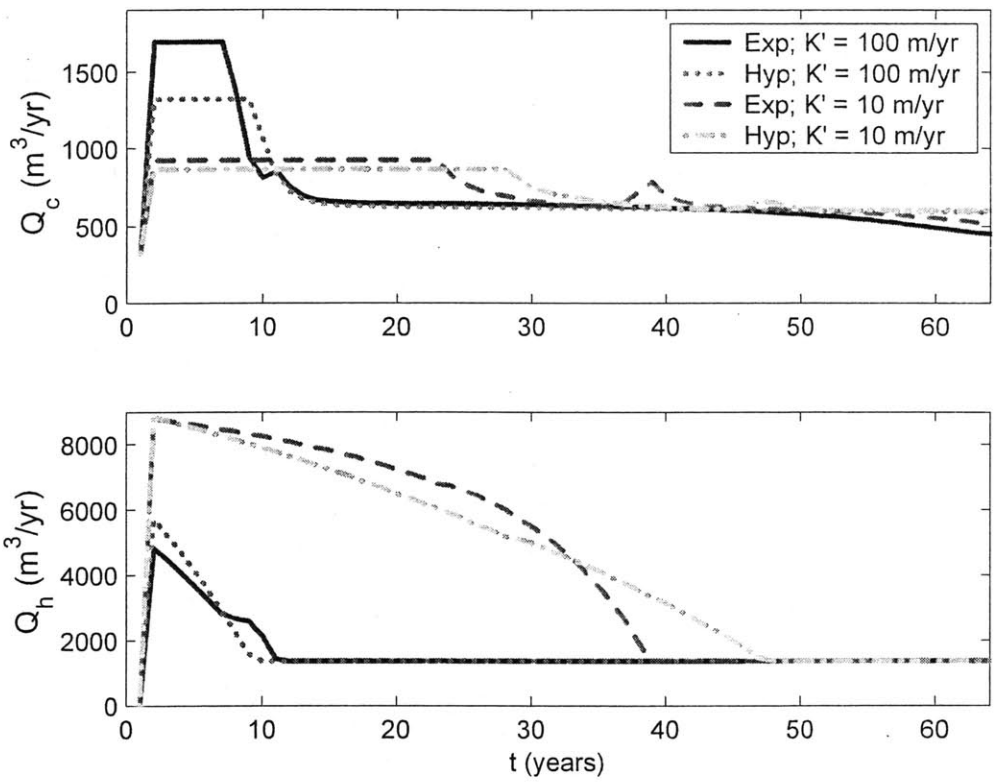

Figure 11-18: Pumping trajectories for hyperbolic and exponential scenarios with K' = 10, 100.

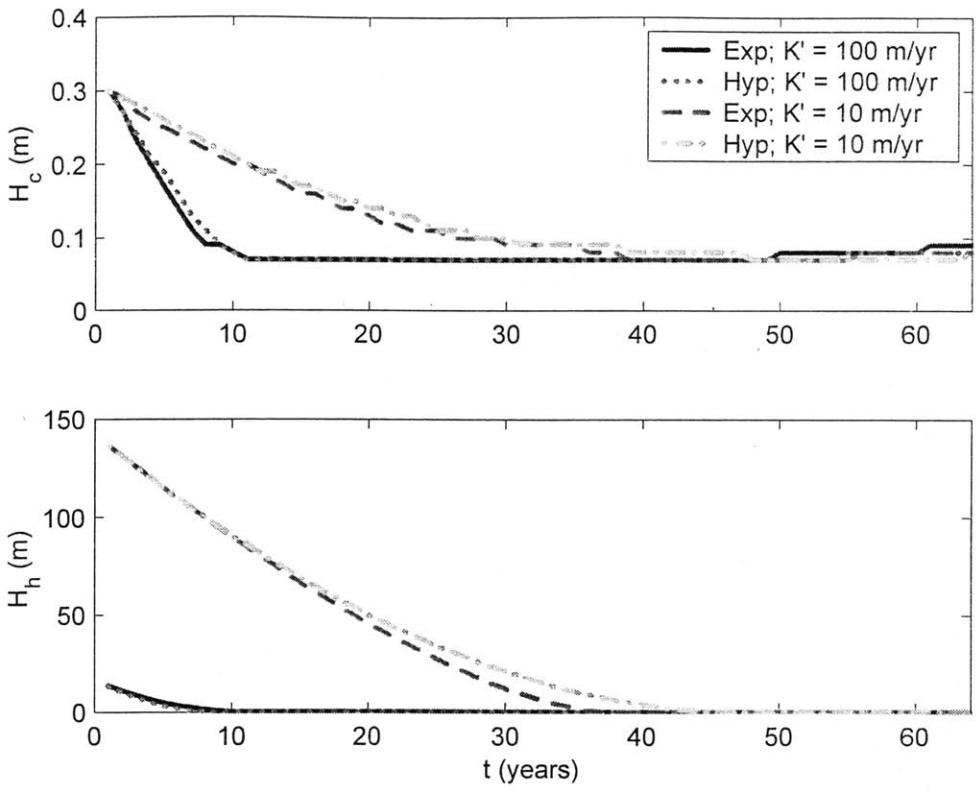

Figure 11-19: Head trajectories for hyperbolic and exponential scenarios with K' = 10, 100.

tion being more conservative (i.e. keeping the high-level head higher) for K' = 10, but slightly reducing heads for K' = 100.

11.9.3 Leakage, Coastal Salinities, and Ocean Discharge

Since leakage is directly related to K', it's not surprising that the leakage curves are always dominated by the leakage factor, Figure 11-20. The discount factor has little affect, but for K' = 100 the hyperbolic solution does lead to slightly lower leakage values compared to the exponential solutions. For K' = 10 leakage is higher for the hyperbolic case.

The ocean discharge, being a coastal aquifer "connection", is dominated by the leakage factor at early times and by the discount factor at late times.

The coastal salinities, exhibiting very unusual salinization and rebound periods, is leakage factor dominated at early times and discount factor dominated at late times. The hyperbolic

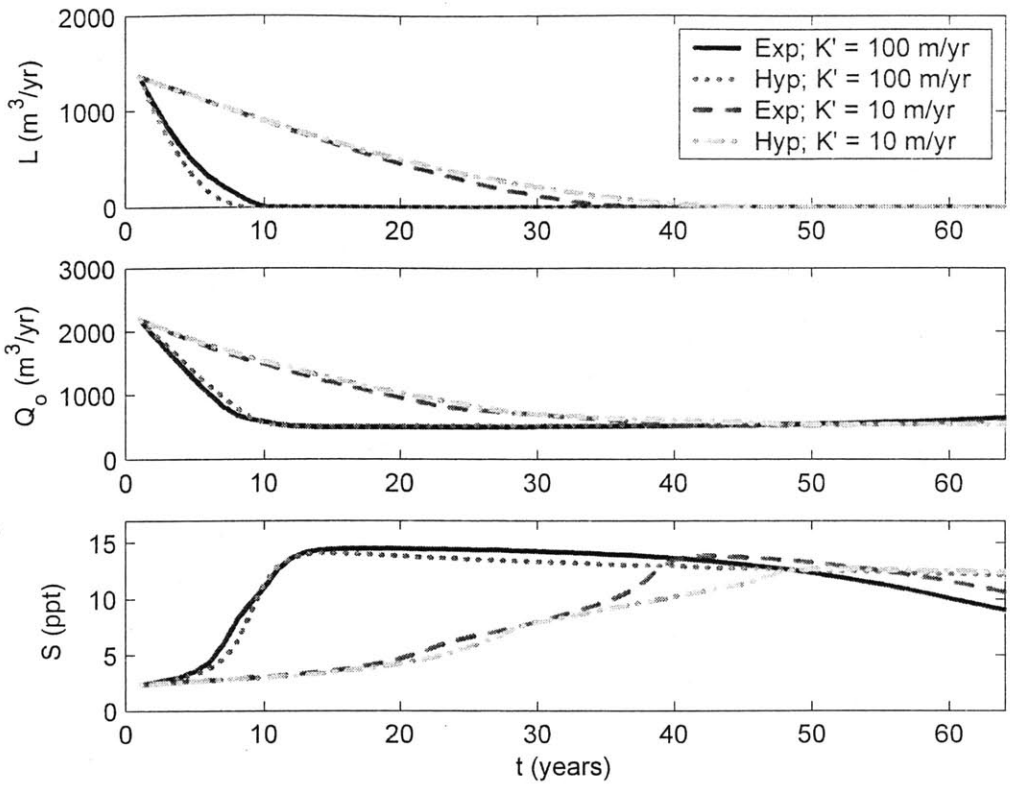

Figure 11-20: Leakage, ocean discharge and coastal salinity trajectories for exponential and hyperbolic scenarios with K' = 10, 100.

solutions are generally lower than the exponential solutions for t < 50 years. At times later than 50 years the two exponential curves begin declining to the equilibrium value while the hyperbolic trajectories decline more slowly since coastal pumping is still occurring.

11.9.4 Economics

The high-level costs are all leakage factor dominated, while coastal costs are discount factor dominated at late times, Figure 11-21. Since both aquifers are leakage factor dominated at early times, yearly net benefits are dominated by the leakage factor effects at early times. At late times it appears that the discount factor dominates. The reason is that at late times all the high-level solutions go to the same equilibrium pumping rate, while the coastal pumping rates diverge along discount function lines; hence the discount factor influence is more important for

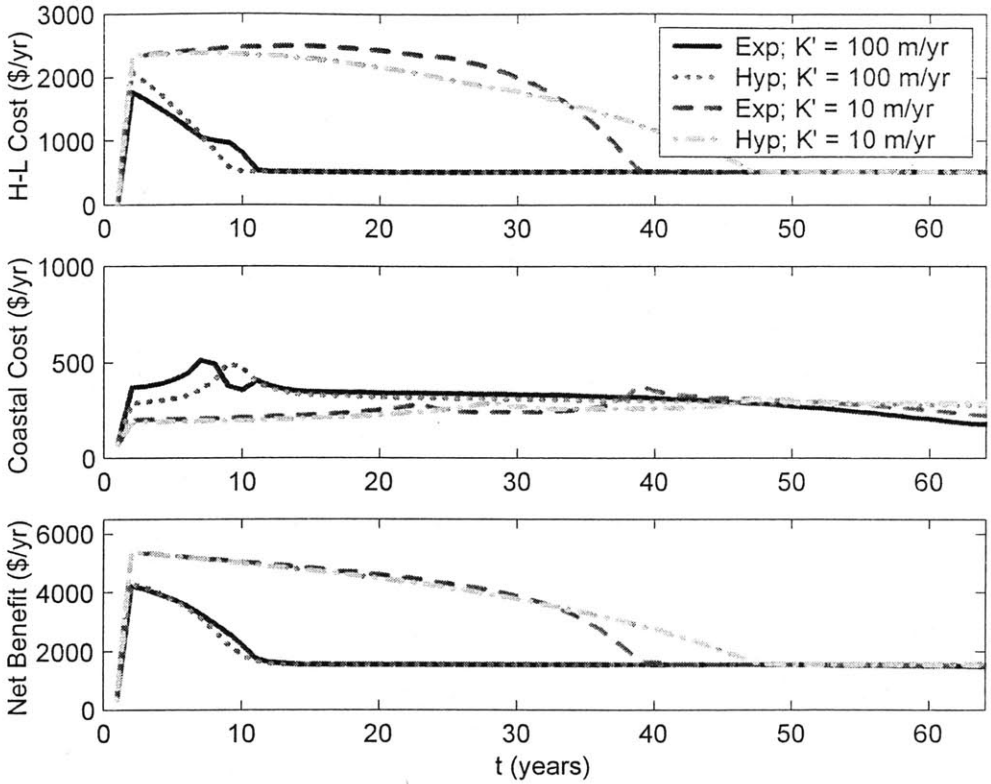

Figure 11-21: Economic solutions for exponential and hyperbolic scenarios with K' = 10, 100.

the long-term.

In summary, the hyperbolic discounting function is more conservative with coastal pumping at early times, but sustains pumping further into the future; thus sustaining more profit from the coastal aquifer into the future. The high-level results are dependent on the leakage factor. For K' = 10 the hyperbolic function produces a more conservative formulation that sustains high-level pumping further into the future. However, for K' = 100, the hyperbolic formulation leads to less conservative pumping for the groundwater mining portion of the high-level pumping curve.

11.9.5 Comments on the Discounting Factor Results

Using one or the other discounting functions will produce optimal system trajectories that may be very different, and it is a policy decision to decide if one scenario is more favorable

than another. It is recommended that a management model such as this one be run with both discounting formulations to give a range of possible solutions from which decisions may be made. For instance, for the Kuki'o case with K' = 10, the higher long-term benefits and slightly lower middle-term coastal salinities may warrant use of a hyperbolic formulation. On the other hand, the higher long-term salinities this course of action would cause may be a reason not to use it. The decision depends on the management time horizon and sustainability goals.

However, it could also be argued to first determine the way the population values the future through studies/surveys, then implement the discounting formulation those studies suggest.

11.10 The Value of Drilling a High-Level Well

Though the dual-aquifer model assumes high-level conditions in the uplands of Ka'upulehu, no high-level well has been drilled yet, and what level of water to expect is unknown. Deciding whether or not to invest the considerable capital for a high-level well and transmisson pipeline is a serious issue facing landowners in the Kuki'o-Ka'upulehu area. In this section we estimate the probable value of sinking a well in the uplands of Kuki'o.

What is needed is a probability distribution for drilling and hitting water of a given head. Once this is found we use these probabilities to weight the range of possible benefits. The sensitivity analysis done for various K' values conveniently provides us with high-level benefits for different high-level head conditions.

The benefits of pumping high-level water given K' are[2]:

	K' = 10 m/yr	K' = 50	K' = 100	K' = 1000
Pumping High-Level Aquifer	$1.26x10^5	$6.42x10^4	$5.43x10^4	$4.68x10^4

Determining the probability that drilling will discover water of a given K' is proportional to determining the probability of hitting initial high-level heads corresponding to initial conditions with that K' value. We may determine from the model what the inital head is for each of the leakage factors tested. This turns out to be h = 137 m, h = 27.6 m, h = 13.96 m, and h = 1.67 m for K' = 10, 50, 100, and 1000 m/yr respectively. Taking the average between each of these heads, we may define a set of four probabilities:

[2]This is net discounted benefit over 150 years for the high-level well only.

$P[(h > 82.3\ m)]$

$P[(h > 20.78) \cap (h < 82.3)]$

$P[(h > 7.82) \cap (h < 20.78)]$

$P[(h > 0) \cap (h < 7.82)]$

These probabilities may be determined using head data from other wells in West Hawai'i. It would be erroneous to use all the West Hawai'i well data since the majority are in the basal lens and would weight the results too heavily towards a non-related phenomenom. Instead, we use the head data from 24 wells north and south of Kuki'o that are drilled at an elevation of 305 m or higher. This is a reasonable elevation to possibly hit high-level water. The resultant discrete probability distribution is,

$P[(h > 82.3\ m)] = 6/24 = 0.25$

$P[(h > 20.78) \cap (h < 82.3)] = 3/24 = 0.125$

$P[(h > 7.82) \cap (h < 20.78)] = 1/24 = 0.042$

$P[(h > 0) \cap (h < 7.82)] = 14/25 = 0.583$

Now it is simple to compute an expected benefit from drilling and pumping a yet-unexplored Kuki'o mauka (for a unit width):

Benefit $= 0.25(\$1.26\text{x}10^5) + 0.125(\$6.42\text{x}10^4) + 0.042(\$5.43\text{x}10^4) + 0.583(\$4.68\text{x}10^4) =$ \$69,090

The total capital investment for a high-level well is \$4,920,000, but such a well would not only service a unit width. We need to now determine how many wells would be needed to support the resultant high-level pumping trajectory. Using an average yearly pumped quantity from the model results, and dividing that by the capacity of a typical in-hole pump (550GPM), we determine that about 30 wells would need to be drilled. So each well would service 6000/30 = 200 m of width; which means per unit drilling and set-up costs of \$920,000/200m = \$4,600. In addition, we assume that only one transmission pipeline need be built to service the region; \$4,000,000/6000 = \$667. Subtracting these costs from the expected benefit we now have an idea of the value of drilling the high-level well:

Expected value of high-level well = \$69,090 - \$4,600 - \$667 = \$63,823

Obviously it is economically desirable to drill a high-level well.

11.11 Comments on Discharge to the Ocean

It is worth noting the importance of the flux of basal water to the ocean. This discharge is a much studied topic that scientists are still at a loss to confidently model and characterize. Effectively doing so is paramount to environmental issues concerned with the near-shore marine environment and coral reefs in particular. It is almost certainly true that the significant amount of basal discharge is a key component in maintaining the temperature, chemical, and biological balance for the near-shore environment. How much and how so is unclear.

In sustainability studies which are sensitive to the reef environment it would make sense to include Q_o as a fixed constraint rather than as a decision variable. This would necessitate the need for input from marine biologists to better constrain a critical level of ocean discharge necessary for a healthy reef. The dual-aquifer model developed here would be a good "first-order" method to test how such constraints would then affect inland water management strategies. The economic value of preserving the reef environment could then be assessed by comparing net benefits with and without a fixed ocean discharge constraint.

Chapter 12

Conclusions

Kuki'o sustainable supply conclusions

The developers of Kuki'o have indicated a near-future demand of roughly 3.8×10^6 m^3/yr (2.75 MGD) of mixed potable and non-potable water. The base case results indicate that initially the two aquifers could supply the area with around 30×10^6 m^3/yr. For the first 10 years or so the optimal solution pumps more than the total recharge to both aquifers of 15×10^6 m^3/yr since water is being mined from storage. With time the total yield decreases from these storage reducing pumping levels, and pumping rates eventually reach the long-term sustainable rate of 12×10^6 m^3/yr.

Therefore, given our model assumptions, about three times the expected demand of Kuki'o could be met. However, these numbers may be high if (1) it is found that the ocean discharge must be near current levels to support the near-shore marine environment, or (2) future field and numerical work indicate that lowering the coastal aquifer heads will elevate salinities more severely and for a longer period of time than projected in our model.

Obtaining a long-term pumping rate of 12×10^6 m^3/yr will have its consequences. High-level heads fall to almost zero, leakage shuts off between the aquifers, ocean discharge decreases by 75%, and the coastal aquifer is salinized to 1/3 that of seawater. In addition, an $11 million dollar RO plant capable of treating 37,800 m^3/day (10 MGD) would need to be built.

For the Ka'upulehu region in general a number in the range of 12×10^6 m^3/yr amounts

to being able to support about 50,000 people[1]; neglecting golf course and landscaping needs. Again, it is important to note that this is taxing the resources to their limits with the high-level aquifer effectively emptying and the coastal well becoming very salty. Any changes in recharge patterns, a breakdown of the RO plant, or water capture by neighboring regions would be disastrous for such a high population.

General conclusions on a dual-aquifer hydrologic-economic model

Results indicate that the dual-aquifer model developed here is useful as a management tool to guide the development of dual-aquifer groundwater regimes. The framework is flexible and once a base case has been set-up it is easy to vary system parameters and constraints. Depending on the project goals for sustainability the model can be modified to focus on particular variables while constraining others. One example would be that of constraining the ocean discharge for an economic assessment of benefit loss for conservation of a near-shore environment.

A general feature of all the dual-aquifer scenarios is the interesting initial pumping curves. Before a long-term sustainable equilibrium is reached the high-level and coastal wells mine water from storage in a complicated fashion which is rooted in the trade-offs between treating salty coastal water and accessing deep high-level water. The coastal well will be pumped first since the water table is shallower and the initial water quality is fairly good. The high-level well will turn on only if the coastal well cannot meet demand, and how much it pumps to contribute to total pumping will depend on how salty the coastal well becomes and how deep the high-level water table is.

Though this case study is not focused on discounting, some comparisons to Part I of this dissertation may be made. For instance, as in Part I, initial aquifer conditions and the discount rate do not significantly affect the long-term sustainable pumping strategies. Initial conditions in the aquifers only matter for near to mid-future benefits due to mining water in storage, and the discount rate affects the rate and duration of pumping during this storage reduction phase.

Implementing a hyperbolic discount function sustains more profit in the far-future by sustaining pumping in the coastal aquifer. In contrast, after about 50 years coastal pumping rates

[1]This is using a number of 240 m^3/yr person. American Water Works Association Research Foundation (www.awwa.org).

for the exponential solutions are declining much faster. The effect of hyperbolic discounting on high-level pumping depends on the leakage factor. For high K' values the hyperbolic function leads to a faster rate of initial groundwater mining than the exponential solution. For low K' values the hyperbolic solution leads to a more conservative high-level groundwater mining strategy.

It was found that the dual-aquifer model is particularly sensitive to leakage between the two aquifers and to the shape of the demand curve. While other model inputs do affect the results, these two can radically change the nature of the optimal solution. For steep linear demand curves or low elasticity constant elasticity curves the high-level aquifer is not even used and the coastal well meets all demand.

It is notable that both the physics and economics can affect the solution severely and both need to be taken into careful consideration. This is an important realization for any future sustainability models that may try to only focus on either the physics or economics of a large-scale, long-term project.

Finally, we would like to again note that the methods developed here are merely as good as the model assumptions and inputs. Furthermore, the results should only serve as a general guide for developing sustainable stategies for a water resource. It is recommended that, if at all possible, a number of experts on the physical, economical, and socio-cultural aspects of the study area be involved in model formulation.

Models such as this can be constructive or destructive to sustainable management projects. The integrity of the user is paramount.

12.1 Summary of original contributions

1. Coastal well experiments at the Kuki'o irrigation well field. Effective methods were developed to measure salinity and head changes in the coastal well. Besides answering a number of important questions concerning coastal well response, the data set generated should prove useful for verification of numerical models and for generation of an optimal control model for a coastal well or well field.

2. Development of a dual-aquifer hydrologic-economic model to investigate the long-term

physical and economic characteristics of this unique water system. A general framework was developed that can be easily applied to other aquifer systems of this type.

3. We develop simple empirical equations to account for the physical and economic effects of coastal well salinization; thereby eliminating the need for complicated and ill-defiined numerical models.

4. The effects of alternative discount functions and discount rates were investigated for a real hydrologic system.

12.2 Recommendations for future research

- Long-term monitoring of coastal wells. Head, salinity, and pumping rate measurements should be continuously taken at Kuki'o and at other wells along the North Kona – South Kohala coastline. Such data will be essential to future long-term management model calibration and also for numerical modeling efforts.

- Full density-dependent numerical modeling of the coastal aquifer. This model should include pumping wells at various distances from the shoreline, tidal influences, and attempt to account for the structure of the layered volcanic subsurface. Various permutations on some basic model will be necessary to provide a range of possible solutions for an area with physical parameters which are so ill-defined. A 2-D cross-sectional model is probably sufficient for understanding the groundwater dynamics, but a 3-D model may desirable if large-scale water budgets and inter-well interactions are to be explored.

- Optimal control model for a coastal brackish well using the Kuki'o field experiment pumping and rebound curves. Though not appropriate for the long-term model, the results from the coastal experiment could be used to develop a short time scale model of coastal well pumping. This model would need to be of the mixed integer type to allow for the coastal well being turned off and on, and to effectively use the field curves. An optimal pumping schedule to a well-defined coastal well model would be extremely valuable to water managers in Hawai'i and elsewhere.

- Economic studies on consumer demand for water in Hawai'i. The dual-aquifer model results exhibit great variability with the demand curve, so it behooves us to better constrain this crucial economic input. Demand curves should be constructed for both the general populace and for any important sub-populations in the area of concern. For instance, it is likely that the demand curve for Hawaiian residents is different than for recent, wealthy immigrants to Hawai'i for whom projects such as Kuki'o are being built.

- Research on the importance of ocean discharge needs to be done to better constrain this important model boundary condition.

- More work studying high-level wells to determine their characteristics and possibly K' values. The dual-aquifer model could be applied to this end in an area where coastal and high-level well heads are available.

Appendix A

Kuki'o Irrigation Well Schematic and Water Demand Data

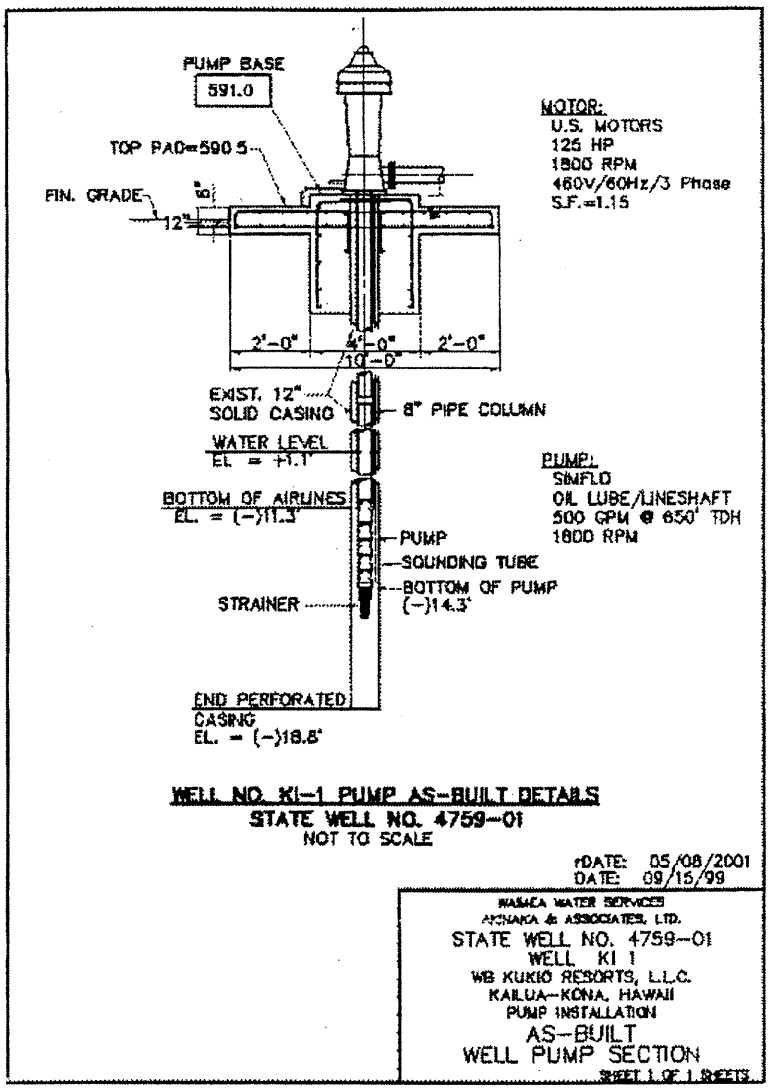

Figure A-1: Well schematic for KI1

3/13/02

KŪKI'O/MANINI'ŌWALI
Non-Potable Irrigation Water Budget

Phase	Project Area	Irrigated Area (acres)	Ave. Day Use Rate (GPD/Acre)	Ave. Day Estimated Water Demand (GPD)
1A	Roadways	14.75	6,000	88,500
1A	Assoc. Easements	16.68	6,000	100,080
1A	Kikaua Point Park	1.50	6,000	9,000
1A	Shoreline Zone	2.00	6,000	12,000
1A	Project Entry	0.13	6,000	780
1A	South Buffer (Public Access Road)	0.75	6,000	4,500
1A	Makai Golf Course Turf (10-Holes) [1]	34.00 [2]	6,000	204,000
1A	Makai Golf Course Landscaping	26.00	3,000	78,000
3	Roadways/Misc. Landscaping	6.67	6,000	40,000
4	Manini'ōwali Development Area (Refer Table C)	44.06	6,000	265,000
	Makai Subtotal:			**801,860**
2	Mauka Facilities and Road R [3]	10.40	6,000	62,400
4	Mauka - Future Development Roadways [3]	5.00	6,000	30,000
2	Mauka Golf Course Turf (18-Holes) [3]	110 [2]	6,000)	660,000 [4]
2	Mauka Golf Course Landscaping	60	3,000	180,000
1A	580' Reservoir Water Loss (Evaporation)	---	---	30,000
	Mauka Subtotal:			**962,400**
	Total:			**1,764,260**
	KI Wells Average Day Sustainable Yield:			1,300,000 [5]
	Manini'ōwali Average Day Sustainable Yield (Untested):			500,000 - 1,000,000
	Water Treatment Plant Reject Water (from HR Wells):			268,600
	Total Sustainable Yield:			**2,068,600 - 2,568,600**
	Non-Potable Average Day Surplus:			**304,340 - 804,340** [6] (15% to 31% of Estimated Sustainable Yield)

O:\JOB07\783.07\BM-72a.wpd

[1] Determined by WBK utilizing preliminary calculations from Fazio and ECDG that illustrated a range of water usage based on varying assumptions.

[2] Turf has been specified as Seashore Paspalum.

[3] Estimate only. Conceptual budge only for mauka facilities. Includes Resort Operations Center, Maintenance Center, WWTP, and related roadway landscaping.

[4] Water budget established by WB Kukio.

[5] Does not include volume of re-use water that would be available from WWTP.

Figure A-2: Non-potable water demand.

3/13/02

KÛKI'O/MANINI'OWALI
POTABLE WATER BUDGET SUMMARY

Product Type/Use	No. of Units[1]	Ave. Day Allocation (GPD/Unit)		Total Ave. Day Allocation (GPD)	
Estate Lots	43	3,000	2	129,000	
Estate Lots (Additional)[3]	-	-		50,250	3
Hale Lots	23	1,600		36,800	
Villa Lots	32	1,500		48,000	
Cottages	41	1,100		45,100	
Beach Club	-	17,500		17,550	
Beach Club (Potable Irrigation)	-	13,000	4	13,000	
Kikaua Point Park	-	5,000		5,000	
Wastewater Treatment Facility	-	3,000		3,000	
Golf Maintenance Facility	-	7,500		7,500	
		Phase 1A Subtotal:		**361,050**	
Phase 3 (Upper Makai)	46	3,000	5	138,000	
Golf Clubhouse	-	13,500		13,500	
Phase 4 (Mauka Lots - Estimated)	15	4,000	5	60,000	
Mauka Golf Course - Potable Irrigation for Greens	-	-		(Not Included)	
Manini'owali Development (Refer to Table C)	140	-		420,000	
		Balance Subtotal:		**631,500**	
		PROJECTED POTABLE WATER USE TOTALS:		**992,550**	
AVAILABLE POTABLE WATER RESOURCE HR WELLS: Ave. Day Sustainable Yield (16 hr. pumping) Capacity of HR-1, HR-2, HR-3, HR-4, HR-5, with planned HR-6 and another well between HR-2, HR-3, and HR-4 used as a stand-by (two stand-by wells required)[7]				**1,956,000**	7
Less Makalei/Other Water Commitments:			6	(687,400)	
Less Water Treatment Plan Reject Water:				(268,600)	
		Net Available Potable Water:		**1,000,000**	
		Potable Water Surplus or (Shortage):		**(7,450)**	

Figure A-3: Potable demand for Kuki'o

Appendix B

Results for Energy Cost Sensitivity Analysis

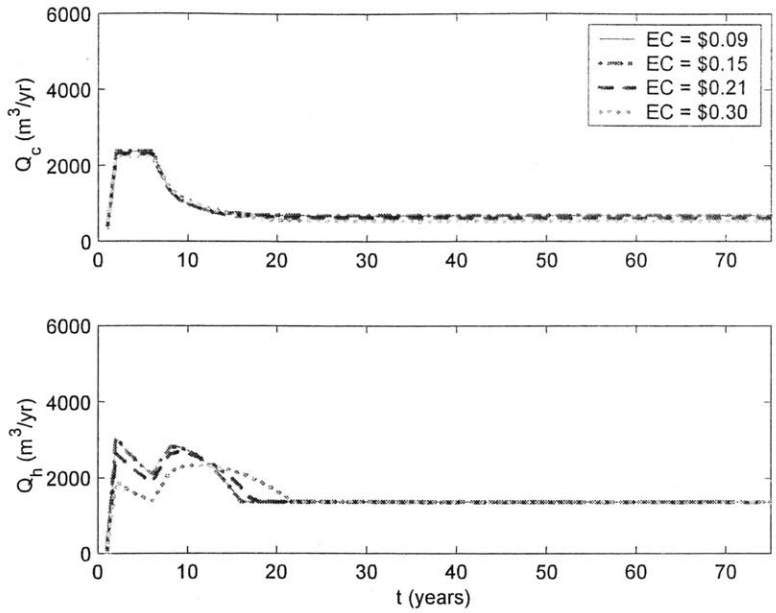

Figure B-1: Optimal pumping trajectories for scenarios with energy price varied.

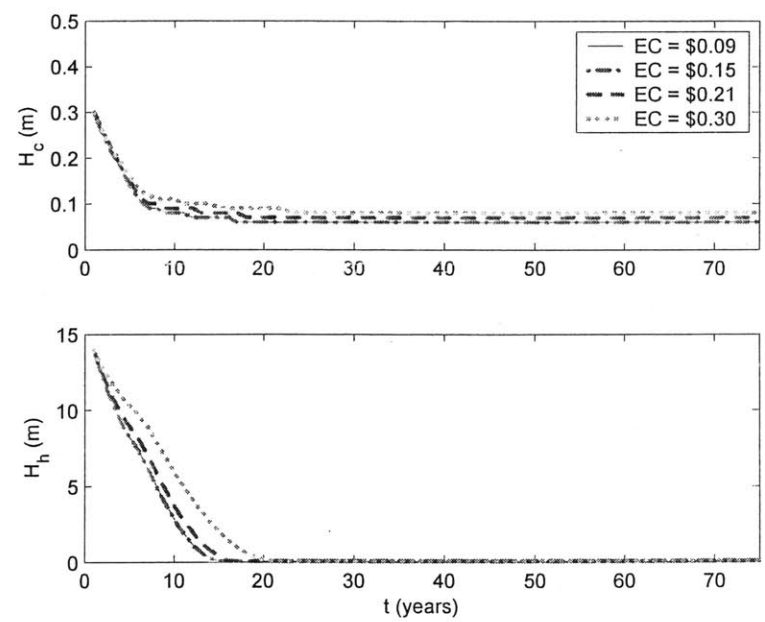

Figure B-2: Optimal head trajectories for scenarios with energy price varied.

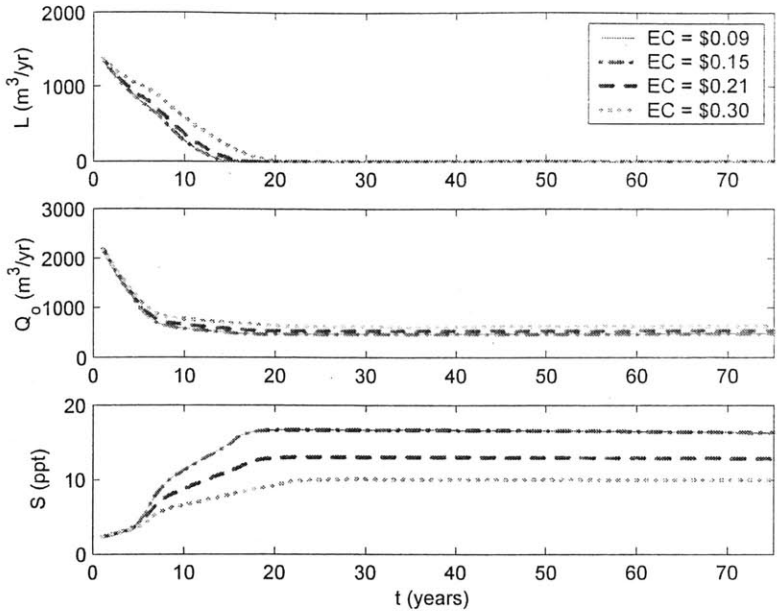

Figure B-3: Optimal leakage, ocean discharge, and salinity trajectories for the scenarios with energy price varied.

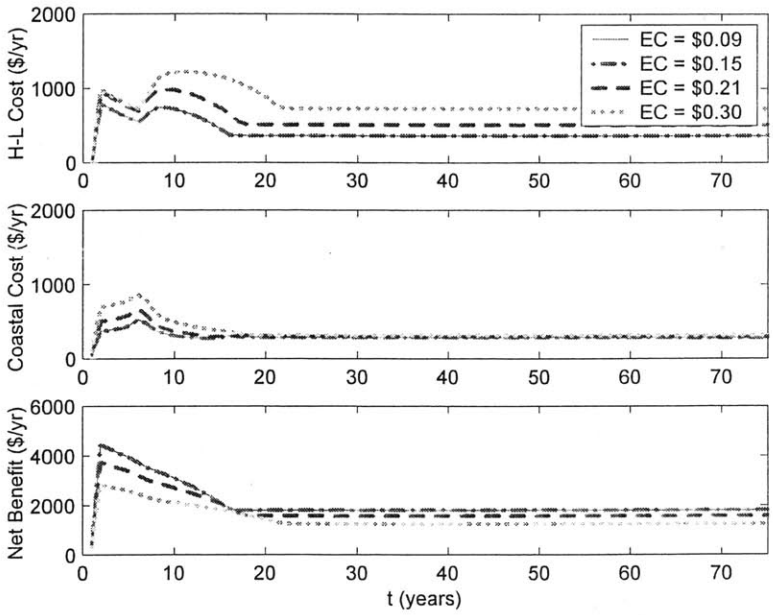

Figure B-4: Optimal cost and benefit trajectories for the scenarios with energy price varied.

Appendix C

Results for Discount Rate Sensitivity Analysis

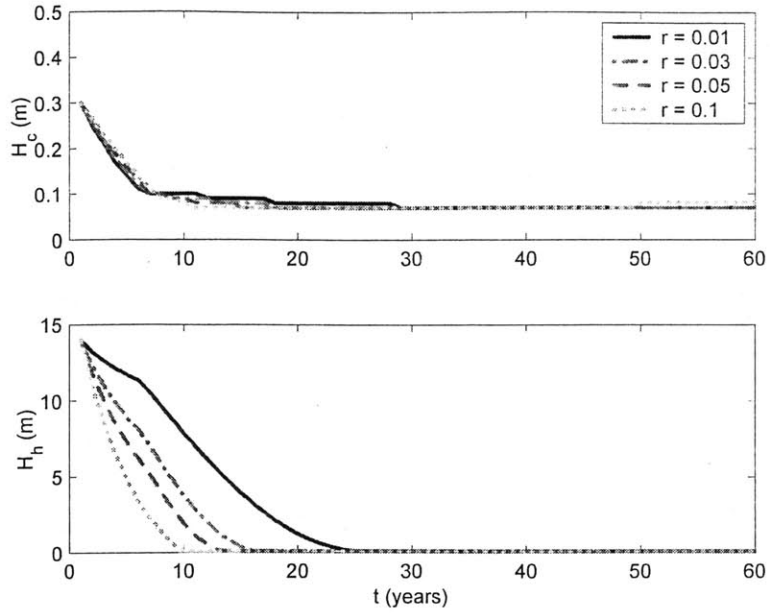

Figure C-1: Optimal head trajectories for scenarios with discount rate varied.

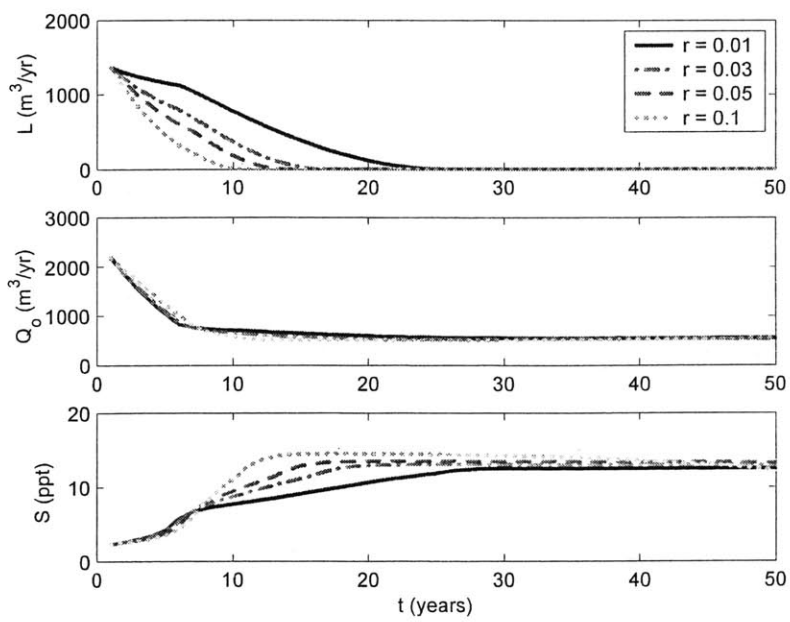

Figure C-2: Leakage, ocean discharge, and salinity values for scenarios with discount rate varied.

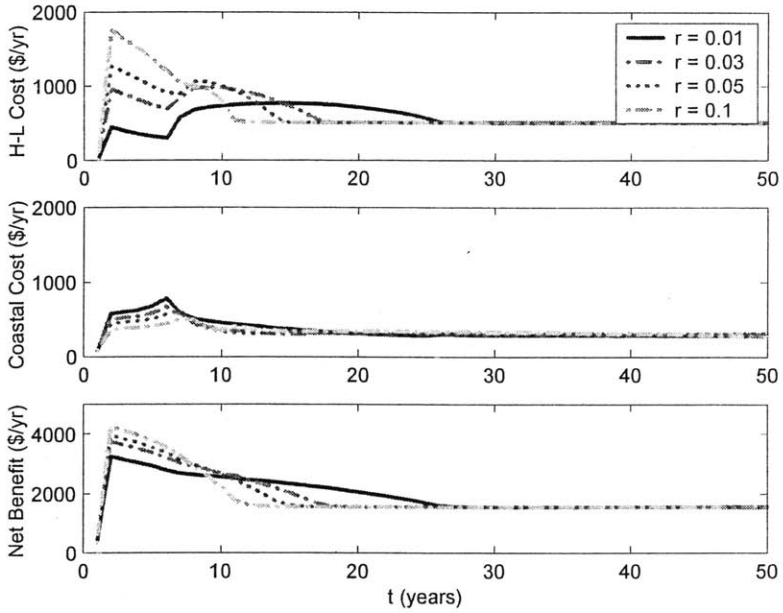

Figure C-3: Cost and benefit curves for scenarios with discount rate varied.

Bibliography

[1] Azfar, Omar. "Rationalizing Hyperbolic Discounting," *Journal of Economic Behavior and Organization*, *38*(2):245–252 (1999).

[2] Bear, Jacob. *Hydraulics of Groundwater*. New York: McGraw-Hill, 1979.

[3] Bear, Jacob, et al. "Pumping from the interface zone of a coastal aquifer," *forthcoming*

[4] Bohm-Bawerk, E.v. *Capital and Interest*. Illinois: Libertarian Press, 1970.

[5] Brooke, et al. *GAMS: a users guide*. Washington, D.C.: GAMS development corporation, 1998.

[6] Broome, J. *Counting the Cost of Global Warming*. London: White Horse Press, 1992.

[7] Chichilnisky, G., et al. "The green golden rule," *Economics Letters*, *49*:175–179 (1995).

[8] Chichilnisky, Graciela. "An axiomatic approach to sustainable development," *Social Choice and Welfare*, *13*(2):219–248 (1996).

[9] Cline, W.R. *The Economics of Global Warming*. Washington D.C.: Institute for International Economics, 1992.

[10] Cropper, M.L., et al. "Preference for life-saving programs: how the public discounts time and age," *Journal of Risk and Uncertainty*, *8*:243–265 (1994).

[11] Dagan, G. and J. Bear. "Solving the problem of local interface upcoming in a coastal aquifer by the method of small perturbations," *J. Hydraulic Res.*, *6*(1):15–44 (1968).

[12] Daley, H.E. *Steady State Economics: Second Edition with New Essay* (Second Edition). Washington D.C.: Island Press, 1991.

[13] DasGupta, P.S. and G.M. Heal. *Economic Theory and Exhaustible Resources*. Cambridge, England: Cambridge University Press, 1979.

[14] Fisher, F.M., et al. "Optimal water management and conflict resolution: Middle East water project," *Water Resources Research forthcoming* (2002).

[15] Fisher, I. *The Theory of Interest*. New York: MacMillan, 1930.

[16] Harrod, R. *Towards a Dynamic Economics*. London: MacMillan, 1948.

[17] Harvey, Charles. "The reasonableness of non-constant discounting," *Journal of Public Economics*, *53*:31–51 (1994).

[18] Harvey, Charles. "Proportional discounting of future bosts and benefits," *Mathematics of Operations Research*, *20*(2):381–399 (1995).

[19] Heal, G.M. "Depletion and discounting: a classical issue in resource economics." *Proc. of Symposia in Applied Mathematics*, number 32, edited by R. McElvey. 33–43. 1985.

[20] Heal, G.M. *Valuing the very long-run*. 1993. Working Paper.

[21] Heal, G.M. *Valuing the Future: cost-benefit analysis and sustainability*, *3*. UNDP/ODS: Discussion Paper Series. 1997.

[22] Heal, G.M. *Valuing the Future: Economic Theory and Sustainability*. New York: Columbia University Press, 1998.

[23] Ho, M.-Y., et al. "Theory and method in the quantitative analysis of "impulsive choice" behavior: implications for psychopharmacology," *Psychopharmacology*, *146*:362–372 (1999).

[24] Hunt, C.D., et al. "Region 27, Hawaiian Islands." *Hydrogeology*. Number 27. 255–262. 1988.

[25] J. Cairns, M. Van der Pol. "Constant and decreasing timing aversion for saving lives," *Social science and medicine*, *45*(11):1653–1659 (1997).

[26] Jevons, W.S. *Theory of Political Economy*. London: MacMillan, 1871.

[27] Kamien, M. and N. Schwartz. *Dynamic Optimization*. Amsterdam: North Holland, 1991.

[28] Kaneshiro, B.Y. and F.L. Peterson. "Groundwater recharge and coastal discharge for the northwest coast of the island of Hawaii: a computerized water budget approack," *WRRC Technical Report*, (110):1–73 (1977).

[29] Kirby, K.N. and R.J. Herrnstein. "Preference reversals due to myopic discounting of delayed reward," *Psychological science*, *6*(2):83–89 (1995).

[30] Knapp, K.C. and L.J. Olson. "The economics of conjuctive groundwater management with stochastic surface supplies," *J. of Envir. Econ. and Mngmt.*, *28*:340–356 (1995).

[31] Koopmans, T.C. "Stationary Ordinal Utility and Impatience," *Econometrica*, *28*:387–309 (1960).

[32] Lin, Lung-Chuan, et al. "Saltwate upcoming due to freshwater pumping," *Proc. Natl. Sci. Counc. ROC*, *23*(2):248–258 (1999).

[33] Loewenstein, G. and D. Prelec. *Anomalies in intertemporal choice: evidence and interpretation*. Choice Over Time, New York: Russel Sage Foundation, 1992.

[34] Lumley, Sarah. "The environment and the ethics of discounting: An empirical analysis," *Ecological Economics*, *20*:71–82 (1997).

[35] Negri, D.H. "The common property aquifer as a differential game," *W ater Resources Research*, *25*(1):9–15 (1989).

[36] of, Hawaii State. "Median Rainfall Map," *Circular C88*, (88) (1982).

[37] Pollak, R. "Additive van Neumann-Morgenstern Utility Functions," *Econometrica* (1967).

[38] Portney, Paul R. and John P. Weyant. *Discounting and Intergenerational Equity*. Washington D.C.: Resources for the Future, 1999.

[39] Postel, Sandra. *Pillar of Sand: Can the irrigation miracle last?*. New York: W.W. Norton and Company, Inc., 1999.

[40] Poulos, C. and D. Whittington. "Time preferences for life-saving programs: evidence from six less developed countries," *Environmental Science and Technology*, *34*:1445–1455 (2000).

[41] Rabl, Ari. "Discounting of long-term costs: What would future generations prefer us to do?," *Ecological Economics*, *17*:137–145 (1996).

[42] Rae, John. *The Sociological Theory of Capital*. London: MacMillan, 1905.

[43] Ramsey, F. "A mathematical theory of saving," *Economic Journal*, *38*:543–559 (1928).

[44] Raucher, L.R. "A conceptual framework for measuring the benefits of groundwater protection," *Water Resources Research*, *19*(2):320–326 (1983).

[45] Reilly, T.E. and A.S. Goodman. "Quantitative analysis of saltwater-freshwater relationships in groundwater systems - a historical perspective," *Journal of Hydrology*, *80*(12):125–160 (1985).

[46] Samuelson, P. "A note on measurement of utility," *Review of Economic Studies*, *4*:155–161 (1937).

[47] Schmorak, S. and A. Mercado. "Upconing of freshwater-seawater interface below pumping wells, field study," *Water Resources Research*, *5*(6):1290–1311 (1969).

[48] Senior, N.W. *An Outline of the Science of Political Economy*. London: Clowes and Sons, 1836.

[49] Simpson, C.A. and R.E. Vuchinich. "Reliability of a measure of temporal discounting," *Psychological Reward*, *50*(1):3–16 (2000).

[50] Sozou, Peter D. "On hyperbolic discounting and uncertain hazard rates," *Proc. R. Soc. Lond. B*, *265*:2015–2020 (1998).

[51] Thaler, R. "Some empirical evidence on dynamic inconsistency," *Economic Letters*, *8*:201–207 (1981).

[52] Tsur, Y. and T. Graham-Tomasi. "The buffer value of groundwater with stochastic surface water supplies," *J. of Envir. Econ. and Mngmt.*, *21*:201–224 (1991).

[53] UNDP. *Our Common Future*. New York: Oxford University Press, 1987. Brutland Report.

[54] Varian, H.R. *Intermediate Economics: A modern approach*. New York: W.W. Norton and Co., 1987. First Edition.

[55] Weitzman, Martin L. "Why the far-distant future should be discounted at its lowest possible rate," *Journal of Environmental Economics and Management*, *36*:201–208 (1998).

[56] Weitzman, Martin L. "Gamma Discounting," *American Economic Review*, *91*(1):260–271 (2001).

[57] Wilf, Mark and Kenneth Klinko. "Optimization of seawater RO systems design," *Hydranautics Technical Reports* (2001).

[58] Winter-Nelson, Alex. "Discount rates, natural resources, and the measurement of aggregate economics growth in Africa," *Ecological Economics*, *17*:21–32 (1996).

[59] Wirojanagud, J. and R.J. Charbeneau. "Saltwater upconing in unconfined aquifers," *J. Hyrdaulic Eng., ASCE*, *111*(3):417–434 (1985).

[60] Young, Reginald, et al. "Hydrologic and ecologic inventories of the coastal waters of West Hawaii," *Sea Grant Cooperative Technical Report*, (105) (1977).